DEVELOPMENT AND ACCURACY IMPROVEMENT OF EVALUATION METHODS FOR DEW CONDENSATION IN STEEL BRIDGES

(鋼橋における結露評価方法の開発と精度向上に関する研究)

Zabihullah Rasoli

January 2021

DEVELOPMENT AND ACCURACY IMPROVEMENT OF EVALUATION METHODS FOR DEW CONDENSATION IN STEEL BRIDGES

（鋼橋における結露評価方法の開発と精度向上に関する研究）

A thesis submitted to the Faculty of Engineering of
Nagoya Institute of Technology
in partial fulfillment of the requirements for the
Degree of Doctor of Engineering

by
Zabihullah Rasoli

January 2021

Abstract

In Japan, the development of steel bridges peaked during the period of high economic growth of the 1960s. The country is now facing the challenges of aging infrastructure. Additionally, large bridges are rather costly to design, construct, maintain, and rehabilitate. Therefore, preventive maintenance and management has been introduce to address this issue. For effective maintenance and management of environmental corrosion of steel bridges, an initial inspection and survey must be conducted. As individual investigation of the corrosive environment for each single steel structure using field measurements is not just complicated but time-consuming and costly as well, therefore, it is important to evaluate the corrosive environment prior to the commencement of the maintenance and management. Corrosion is a major problem that causes the deterioration of steel infrastructure and affects its long term mechanical performance and durability. Principally, various factor can cause corrosion. Among them, dew condensation is an important factor in the occurrence of bridge corrosion and contributor to the deterioration of the protective coating. In the last couple of years, an evaluation method of the dew condensation due to atmospheric temperature and relative humidity was developed using a weather research and forecasting (WRF) numerical weather prediction and inverse distance weighting (IDW) techniques. In the present study, the accuracy enhancement of the method was investigated.

First, an accuracy enhancement of IDW for different land topographies and its employment was investigated to achieve more accurate results. Additionally, appropriate adaption points selection of IDW was discussed, as a results the optimum number of interpolation points for evaluation of corrosion environment was proposed. In this study, the temperature and relative humidity of three meteorological observatories were used such as; Osaka, Suwa and Shizuoka to compare the results obtained from IDW. Here, Osaka represent flat land, Suwa mountainous area and Shizuoka an area relatively close to sea, to reflect the influence of water. Subsequently, a quantitative investigation of the IDW was carried out for the above mentioned meteorological observatories from four, three, and two of their own local surrounding meteorological observatories. The outcome of the present investigation revealed that a higher accuracy of temperature and humidity were obtained for flat land compare to mountainous and oceanic areas. The errors in temperature and humidity are smaller at 0.8 °C and 6 % for flat land, respectively, but higher at 1.3 °C and 12 % in the case of mountainous and oceanic areas. That is, the accuracy of IDW for flat land is two times higher compared to mountainous areas. Moreover, A quantitative investigation using IDW when applying four, three and two points revealed that the accuracy of the calculations can be enhanced to certain extend using three points for flat land and two points for mountainous areas.

Additionally, the field observation was carried out for the Ooeyousui and Sanbonmatsu bridges in the northeast and northwest of the Aichi prefecture for the flat and mountainous areas as a case study. The temperature and humidity of both bridges were measured using sensor, subsequently, their results were compared with Nagoya meteorological observatory (NMO) to examine the weather situation in the prefecture. The comparison results shows that the changes in temperature and humidity at both bridges are

extremely linked with the changing rate at Nagoya meteorological observatory, but the value of temperature and humidity of these three points (Ooeyousui, Sanbonmatsu, and NMO) are not quite the same. The difference in temperature is about 1ºC, and humidity 9% at Ooeyousui compare to NMO, and it was almost two-times higher for Sanbonmatsu. Therefore, evaluation of dew condensation of the entire prefecture only from the NMO is not suitable, and it is essential to evaluate the characteristics of corrosion environment owing to temperature and humidity for each single point using IDW technique. Moreover, the evaluation of dew condensation was conducted for the both bridges using ACM sensors to examine the occurrence of dew through field observation and confirms the occurrence of dew. The investigation revealed that dew can easily occur in the bridges, the tendency dew occurrence at Sanbonmatsu bridge is higher as compared to Ooeyousui. Also, the evaluation of dew condensation was performed at Ooeyousui bridge using IDW technique, and their results were compared with field observation to see the validity of the IDW method. The evaluation outcome of dew condensation owing to temperature and humidity when using IDW technique and field observation were quite similar, and both confirmed the dew occurrence at bridge. This shows the usefulness and effectiveness of the IDW.

Secondly, an improvement of accuracy for the evaluation of corrosion environment was discussed using WRF technique. By default, the WRF uses land-use data based on the United States Geological Survey (USGS), which may not represent the real land situation in Japan, and might yields inaccurate results to a certain extent. Currently, reliable land use data is provided by the Geospatial Information Authority of Japan (GSI), and can be integrated into the WRF simulation to improve the calculation accuracy. Principally, the land use is a very important parameter that describes the land surface properties, it regulates the exchange of heat and momentum between soil and air, which in numerical model determine the meteorological magnitude near the surface. The urbanization increases the temperature due to change in land surface characteristics, and deforestation can affect the evapotranspiration. As, this study is focused on the evaluation of dew condensation due temperature and humidity, it is necessary to examine the effect of land use in the WRF model. In this study, a comparative investigation between USGS and GSI land use data was conducted for Aichi prefecture, as a results, the USGS land use data classified most of the entire analysis domain as cropland/Grassland Mosaic, and Mixed Shrubland/ Grassland, which is outdated, and does not take into account urbanization over the recent decades. Whereas, the wider urban area has been accurately identified along with, industrial area including well distribution of irrigated cropland and forest when the GSI land use data integrated into the WRF model. Further, the evaluation of dew condensation was conducted for Aichi and Gifu prefecture based on the USGS and GSI land use data. The outcome of present investigation revealed that the accuracy of WRF improved when the GSI land use employed into the model for flat area, however, for mountainous area both USGS and GSI can be used, and has similar results.

Thirdly, the girder temperature is assumed to be equal to the atmospheric temperature. Based on this, the evaluation of dew condensation was performed. However, in reality, there is a minor difference between the atmospheric temperature and girder temperature. To equalize them, a modification factor is

proposed. In the present study, the atmospheric temperature and girder temperature were obtained by field measurements and their relationship were investigate for a targeted bridge. The investigation results shows that the girder temperature is higher almost 1°C than atmospheric temperature and a mathematical relationship is proposed, which can be simply apply to obtain girder temperature form the atmospheric temperature. Finally, the dew condensation normally occur when the girder temperature is either equal or below the dew point temperature. However, the field observation results at Sanbonmatsu and Toyokuni bridges show, the dew can occur even when the girder temperature is higher than the dew point-temperature, this phenomena is thought to be due to fog, because the fog is forms when the difference between temperature and dew point temperature reach almost 2.5 ºC. Thus, an evaluation of dew condensation as a results of fog was proposed using WRF technique, and validity of the proposed method was confirmed by field measurements.

Lastly, a method for the evaluation of dew condensation already has been proposed using WRF and IDW technique. Through, the method the corrosion environment of bridges can be evaluated simply at global scale (around the bridge) not specifically on the bridge members. In the present study, a total evaluation system was proposed to evaluate the corrosion environment of bridges through WRF or IDW technique as large scale environmental information approach to proceed the investigation of corrosion environment in local scale on the bridge members using STAR-CCM+ program. The proposed method comprises of two major steps. Step_ 1 is used for the evaluation of corrosion environment at a global scale, and the procedure in this step is as follows: select the targeted bridge and determine the coordination points (latitude and longitude), use the WRF or IDW technique to calculate the atmospheric temperature, relative humidity, and wind speed, subsequently conduct the evaluation of dew condensation at global scale. Step_ 2 is employed when the corrosion environment of a bridge due to dew condensation is required for each structural members. In Step_ 2, the meteorological data such as; atmospheric temperature, relative humidity, and wind speed that are already obtained in Step_ 1 are used for the STAR_CCM+ software program, as input for proper boundary and initial conditions, and subsequently the evaluation is simply conducted.

Additionally, field measurements were carried out for the Ooeyousui bridge as case study, to confirm the validity of the proposed method. In this study, initially evaluation of dew condensation was carried out using field measurements, then the evaluation of dew condensation was conducted using WRF technique for dry and dew cased, and lastly the dew condensation was conducted on bridge girder using STAR_CCM+ Program. The results obtained through field observation are in a good agreement with the numerical evaluation results using STAR-CCM+ and confirmed the validity of the proposed method.

Acknowledgments

First and foremost, I want to offer this endeavor to our **God Almighty** for the wisdom he bestowed upon me, the strength, peace of my mind and good health in order to finish this research.

The author is deeply grateful and indebted to his academic advisor, Associate Professor Kazutoshi Nagata, Associate Professor of Structural Engineering, in the Department of Architecture, Civil Engineering and Industrial Management Engineering, Nagoya Institute of Technology, for his crucial guidance, encouragement and support throughout this study.

Special thanks goes to Professor Makoto Obata and Professor Tetsuya Nonaka of the Department of Architecture, Civil Engineering and Industrial Management Engineering, Nagoya Institute of Technology, and Professor Takeshi Kitahara of the Department of Civil Engineering, Kanto Gakuin University for their detailed review of this dissertation.

The author also wishes to express his grateful appreciation to Professor Kunitomo Sugiura of the Department of Civil and Earth Resource Engineering, Kyoto University for his valuable advice and continuous encouragement. Acknowledgment goes to Dr. Kyohei Noguchi from Kyoto University for providing valuable technical support.

The author is thankful for the perfect assistance of students Naoto Miwa and Mori Kohei, and also the former student's structural laboratory, Kimura Kento, Asada Satoru, and Matsuoka Yuka.

Finally, the author expresses his deepest appreciation to his wife, parents, and brothers, for their love, patience, encouragement and prayers throughout the Doctor Study program which helped the completion of this dissertation. This dissertation is dedicated to my family.

Table of Contents

Chapter 1

Introduction

1.1 Aging Problem of Bridges in Japan

The deterioration of modern road bridges in Japan has become an important subject in bridge management because many of them constructed during the rapid economic growth of the 1960s. The country is now experiencing the challenges of aging infrastructure (Noguchi et al., 2017; Sugimoto et al., 2006). It is estimated, in the near future, their service period will exceed their design life. More precisely, by 2023, the number of bridges 50 years age will be more than 43 % and will increase further to 67 % by 2033, as can be observed from Fig. 1.1 (Ministry of Land Infrastructure Transport and Tourism, 2016). The durability of these bridges has now become a major concerns. Furthermore, large steel bridges are costly to design, construct, maintain and rehabilitate (Appuhamy et al., 2012). Therefore, the aging problem of bridges gained a significant attention of the governments in Japan for proper managing. Mainly, one of the key problem of developed societies is that they had a construction in the period of high economic growth and they have the problem of aging society of people as well. Particularly, in the local areas it is considered a more serious problem. Although, the governments are facing the lack sufficient of public personnel, they have the responsibility to manage and maintain the existing bridges (Nakashima and Nagai. 2014).

As mentioned in above that the large road bridges are expensive and it not easy to replace or renew them immediately, it requires enough budget. In the current condition of finance, there is even more pressing to establish a sustainable method to maintaining and keep safe these bridges to increase their operational life rather than replacement. Therefore, to flatten the cost to the years, preventive maintenance and management have been introduced to address this challenging issue (Asao and Fujii. 2018).

1.2 General Remarks on Structural Corrosion

Steel has been accepted as best construction material due to the fact that opposing to concrete it has a better strength to weight relationship, least expensive, and has been used widely in the construction of many engineering systems since 20^{th} century, specially, the use of steel bridges goes back to almost 100 years (Sakthivel et al., 2015; Kreislova and Geiplova, 2012). However, the main disadvantage is the unprotected structural steel in the environmental conditions subjected to corrosion which leads to reduction of their load carrying capacity of a components either by reducing its size or by pitting (Gurrappa et al., 2008). Pitting not only reduces the effective cross section in the pitted region but also introduce the stress raiser, which create cracks. Thus, corrosion can be a serious threat to the long-term function and integrity of a

steel bridge. It is a time-based process that generally takes several years to developed deterioration significant enough to cause concern, for this reasons, corrosion is often considered a maintenance issue. Also, it has been shown that the corrosion played a significant role in the catastrophic collapse of both the Silver Bridge in 1967 and the Mianus River Bridge in 1983(USA Steel Bridge Design Handbook., 2012). Those collapse indicated remarkably the importance of attention to the condition of old bridges which leading to intensified inspection protocol and numerous eventual retrofits or replacements.

In Japan, there were approximately 102,300 railway bridges of at least 1 m in length in 2012. The steel plate girder bridges are the most oldest, and the amount of the corrosion damage due to age is becoming more pronounced. Generally, corrosion can be associated with the huge economic, social and environmental losses for steel constructions which should be investigated from all aspects. Specially, it is offered that the corrosion damage has led to the collapse of a bridge (Secer and Uzun, 2017; Shimozato et al., 2009). From this perspective of view, many of the bridges in Japan can be under risk of deterioration and it will further increased in subsequent decades. Therefore, a comprehensive assessment is required to determine the priority of the bridges for prevention of corrosion and maintenance.

1.3 Corrosion Environment of Bridge

The exposure of a steel structure to aggressive environmental conditions and its inadequate maintenance can results in corrosion, which is mainly responsible for the deterioration of existing steel structures, causing reduced long-term mechanical performance, usability, and durability as shown in photo.1.1 (Appuhamy et al., 2013; Sharifi and Rahgozar. 2010; Yasser, 2010). For effective maintenance and management of environmental corrosion of steel bridges, an initial inspection and survey must be performed. The investigation regarding the corrosive environment for each steel structure separately using field measurements is substantially complicated and requires a significant amount of time and cost. Therefore, it is important to evaluate the general characteristics of the corrosive environment for steel bridges prior to the commencement of maintenance and management programs.

Several studies have been conducted on the corrosion evaluation of steel bridges in the following. Iwasaki et al (2009, 2015) carried out a research to weathering steel bridges. The weathering steel bridges are widely used in Japan to reduce the life cycle cost. The author discussed that in marine areas with frequently high rainfall, high humidity or persistent fog, even the weathering steel cannot have sufficient corrosion resistance. Also, it is found that the rust progress is different in each part of the bridge. The numerical method to simulate the adhesion behavior of sea salt particles oriented from the ocean was developed by Obata et al (2011). According to this study, the temperature, humidity, and various dust on the surfaces of steel bridges are the critical factors of corrosion. Among them, the sea-salt particulate matter is the most important and must be consider for the bridge site in its design stage. A study was conducted to examine the corrosive environment of steel bridge constructed in mountainous area by Maruyama et al (2016, 2017). In the research, the temperature, humidity, wind conditions and amount of airborne salt have been measured. The results show that the temperature and humidity distribution were not uniform in the

cross section of the bridge. Further, the amount of airborne salt to each girder strongly can be influenced by anti-freezing agent, the more critical point where corrosion has a significant progresses due to deposits and water leakage is on the upper surface of the lower flange of girder. Noguchi et al (2017) investigated the airborne sea salt amount adhered to the structural members of bridge. Through accurately estimating airborne sea salt concentrations, and the salt amount adhering on the bridge members, a suitable prediction can be mad regarding structure deterioration. An investigation carried out to examine the environmental characteristics of the local region for construction of bridges by Ohya et al (2017). This study focused on determining the salt accumulation on the bridge as estimation of corrosion durability of bridge prior to its construction. The author, payed effort to propose a procedure for estimating the airborne salt amount based on available meteorological information, and their results were compared with measured airborne salt level to confirm the validity of the method. As a results, it is found that the wind direction and wind speed information is useful as a method for the estimating the airborne salt level.

In general, the maintenance and management of aging steel structure due to corrosion is currently a tough job in Japan. Principally various factors cause corrosion in steel structures. Among them, dew condensation due to atmospheric temperature and relative humidity, has received significant attention in the field of maintenance and management of bridge (Nagata et al, 2016; Imai et al., 2020). This study payed attention on the evaluation of corrosion environment of bridges by considering dew condensation owing to atmospheric temperature and relative humidity without field measurements.

1.4 Evaluation of Corrosion Environment

Steel structure corrosion is caused due to various factors, one of them being dew condensation as a results of temperature and relative humidity (Imai et al., 2020). In the last couple of years, a method for the evaluation of dew condensation due to atmospheric temperature and relative humidity was developed using inverse distance weighting (IDW) and a weather research and forecasting (WRF) numerical weather prediction technique (Nagata et al, 2016). The method is useful for the evaluation of dew condensation, and it can be simply applied for any arbitrary point or from small to excessively large area. However, studies on the improvement of accuracy for the evaluation of corrosion environment using IDW and WRF techniques has not been deeply investigated.

This study aims to investigate the improvement of accuracy for the evaluation of corrosion environment of steel bridges using IDW and WRF technique due to atmospheric temperature and relative humidity. Additionally, the relationship between girder temperature and atmospheric temperature were investigated, as a result a temperature modification factor was proposed to obtain the actual girder temperature from the atmospheric temperature. Moreover, a total evaluation system was proposed to evaluate the corrosion environment of bridges through WRF or IDW technique as large scale environmental information approach to proceed the investigation of corrosion environment in local scale on the bridge members using STAR-CCM+ program.

More precisely, this research aims to investigate the use and adaption of an IDW method to estimate the temperature and humidity for different land topographies, and propose the optimum number of interpolation points for the accurate evaluation of a corrosive environment. The IDW is the simplest interpolation technique available and can be applied to estimate the temperature and humidity using weights as a function of the distance between observation point and interpolation point at which the prediction has to be made, with IDW the rate of correlation and similarities between neighbors are proportional to the distance between them, and also it can be called as a distance reverse function. A closer point's has substantially more influence than those farther points (Chen et al., 2012; Setianto et al., 2013; Wong et al., 2004; Moeletsi et al., 2016). In the present study, the weather data of three meteorological observatories were used which consists of Osaka, Suwa and Shizuoka to compare the results obtained from IDW. Here, Osaka represent flat land, Suwa mountainous area and Shizuoka an area near to sea, to take into account the influence of water from the sea. A quantitative investigation of the IDW was conducted for the above mentioned meteorological observatories from the four, three, and two of their own local surrounding area, respectively. Moreover, an evaluation of dew condensation was carried out using IDW technique and their results were compared with field observation to confirm the validity of the IDW technique.

Next, the WRF model is a mesoscale numerical weather prediction system designed to serve both operational forecasting and atmospheric research needs. The temperature, humidity, and wind speed of any point can be easily obtained using WRF technique as well (Khandaka and Moritmi, 2013; Janjic et al., 2010; Skamarock et al., 2008). By default, the WRF use land-use data based on the United States Geological Survey (USGS), which may not represent the real land situation in Japan, and might yield inaccurate results to a certain extent. Currently, reliable land use data provided by the Geospatial Information Authority of Japan (GSI) is available, and can be integrated into the WRF simulation model to enhance the calculation accuracy (Anderson et al., 1976; Geographical Information System, 2019). Land use is a very important parameter that describes the land surfaces properties, it regulates the exchange of heat and momentum between air and soil that in numerical model determine the meteorological magnitude near the surface. Thus, the effect of land use data were examined in the WRF model to achieve more accurate results for the evaluation of dew condensation due to temperature and humidity. Additionally, a quantitative investigation of dew condensation were carried out for Aichi and Gifu prefecture using WRF technique. This numerical investigation was conducted based on the USGS and GSI land use data, respectively, and their results were compared.

In this study, the girder temperature is assumed to be equal to the atmospheric temperature. Based on this, the evaluation of dew condensation was done. Although, in reality, there is a minor difference between the atmospheric temperature and girder temperature between. Thus, a temperature modification factor is proposed to obtain the girder temperature from atmospheric temperature. Further, the dew normally occur when the girder temperature is either equal or below the dew point. The field observation shows that dew can occur even the girder temperature is higher than the dew point temperature, this

phenomena is thought to be owing to fog. As the fog forms when the difference between temperature and dew point is less than 2.5 ºC. Also, an evaluation of dew condensation as a results of fog was proposed using WRF technique, and the validity of the proposed method was confirmed through field observation.

Finally, the WRF/IDW method has the potential to evaluate dew condensation at global scale (around the bridge) not specifically on the bridge members. Thus, a total evaluation system was proposed to evaluate the corrosion environment of bridges through WRF/IDW technique as large scale environmental information approach to proceed the investigation of corrosion environment in local scale on the bridge members using STAR-CCM+ program. The proposed method comprises of two major steps. Step_ 1 is used for the evaluation of corrosion environment at a global scale, and the procedure in this step is as follows: select the targeted bridge and determine the coordination points (latitude and longitude), use the WRF or IDW technique to calculate the temperature, humidity, and wind speed, subsequently conduct the evaluation of dew at global scale. Step_ 2 is employed when the corrosion environment of a bridge due to dew condensation is required for each structural members. In Step_ 2, the meteorological data (temperature, humidity, and wind speed) that are already obtained in Step_ 1 are used for the STAR_CCM+ software program, as input for proper boundary and initial conditions, and subsequently the evaluation is simply conducted.

1.5 Objectives and Scope

Previously, a method for the evaluation of corrosion environment of bridges was proposed using a weather research and forecasting (WRF) numerical weather prediction technique, and inverse distance weighting (IDW) technique to simply evaluate the dew condensation without filed measurements. However, the studies on the accuracy enhancement of the proposed method has not been sufficiently discussed to achieve accurate result. This study aims to investigate the development and accuracy improvement of evaluation method for dew condensation in steel bridges. More specifically, this study deal with following issue:

(a) The use and adaption of an IDW method to estimate the temperature and humidity for different land topographies, and proposing optimum number of interpolation point for the accurate evaluation of corrosion environment.
(b) Evaluation of dew condensation using IDW technique and field measurements for a bridges as a case study to examine the validity of the method
(c) Improvement of accuracy for the evaluation of corrosion environment using WRF technique.
(d) Investigation of the relationship between girder temperature and atmospheric temperature, and also evaluation of dew condensation as results of fog.
(e) Investigation of dew condensation on structural members of bridge using STAR-CCM+ program at local scale.

In Chapter 1, the current and future challenges of aging infrastructure and their needs for the proper maintenance and management are described.

In Chapter 2, an accuracy improvement of IDW with considering different land topographies was discussed. The atmospheric temperature and relative humidity of the following three meteorological observatories were used; Osaka, Suwa and Shizuoka to compare the results obtained from IDW. Here, Osaka represent flat land, Suwa mountainous area and Shizuoka an area relatively near to sea, to reflect the influence of water. Additionally, appropriate adaption points selection of IDW was discussed, and the optimum number of interpolation points for evaluation of a corrosive environment was proposed.

In Chapter 3, the evaluation method for dew condensation due to atmospheric temperature and relative humidity was discussed, and its mathematical procedure were demonstrated in details. Furthermore, the evaluation of dew condensation was carried out using atmospheric corrosion monitoring (ACM) sensor for both the Ooeyousui and Sanbonmatsu bridge. Further, a comparative investigation was conducted between Ooeyousui, Sanbonmatsu, and Nagoya meteorological observatories to examine the difference in atmospheric temperature and relative humidity for each single point.

In Chapter 4, the accuracy improvement of WRF by considering the land use data was investigated. By default, the WRF model use land-use data based on United States Geological Survey (USGS), which may not represent the real land situation in Japan and yield into inaccurate results. Instead the land use data provided by the Geospatial Information Authority of Japan (GSI) was employed into the model. Subsequently, a comparative investigation was conducted based on USGS and GSI land use data, and their results were compared.

In Chapter 5, the evaluation of dew condensation was discussed using atmospheric corrosion monitoring (ACM) sensors. Additionally, the occurrence of dew condensation due to foggy weather condition was demonstrated, and its evaluation method was proposed using WRF technique. In this study, a temperature modification factor is also proposed to obtain the girder temperature from the atmospheric temperature.

In Chapter 6, a total evaluation system was proposed to evaluate the corrosion environment of bridges through WRF or IDW technique as large scale environmental information approach to proceed the investigation of corrosion environment in local scale on the bridge members using STAR-CCM+ program. Additionally, a field measurement was carried out at Ooeyousui bridge as a case study, to confirm the validity of the proposed method.

In Chapter 7, the conclusion made from this study are summarized and discussed.

References

Anderson, J.R., Hardy, E.E., Roach, J.T. and Witmer, R.E., (1976), "A land use and land cover classification system for use with remote sensor data", Geological Survey Professional Paper 964, U.S. Government Printing Office.

Appuhamy, J.M.R.S., Ohga, M., Chun, P. and Dissanayake, P.B.R., (2012), "Consequence of corrosion on dynamic behavior of steel bridge members", International Journal of Modern Engineering Research (IJMER), Vol.2, No.1, pp.281-288.

Appuhamy, J.M.R.S., Ohga, M., Chun, P. and Dissanayake, P.B.R., (2013), "Role of corrosion & eathquakes on degradation of dynamic behavior of steel bridge plates", Journal of Civil Engineering and Science, Vol.2, No.1, pp.7-14.

Asao, N. and Fujii, K., (2018), "Remaining strength evaluations of steel girder with corrosion near supports and their reinforcements", KSCE Journal of Civil Engineering, Vol.22, No.10, pp.4047-4055.

Chen, F. and Liu, C., (2012), "Estimation of the spatial rainfall distribution using inverse distance weighting (IDW) in the middle of Taiwan", Paddy Water Environ, pp. 209-222.

GSI, (2019), "Geospatial Information Authority of Japan", http://www.gsi.go.org.

Gurrappa, I. and Malakondaiah, (2008), "Effect of environment on corrosion characteristics of newly developed DMR-1700 structural steel", Science and Technology of Advanced Materials.

Imai, R., Miyasou, T. and Aso, T., (2020), "An evaluation of dew condensation on steel plate girder bridges", Journal of Structural Engineering, Vol. 66A, pp. 443-451 (in Japanese).

Iwasaki, E. and Kato, M., (2009), "Estimation of marine salt behavior around the bridge section", Challenge, Opportunities and Solutions in Structural Engineering and Construction, pp. 463-466.

Iwasaki, E., Kato, M., Nakanishi and Kage, I., (2015), "A feature of corrosion and its evaluation around the cross section of weathering steel bridge", IABSE-JSCE Joint Conference on Advances in Bridge Engineering-III, pp. 154-163.

Janjic, Z., Gall, R. and Pyle, M.E., (2010), "Scientific documentation for the NMM solve", National Center for Environmental Prediction Office, NCEP. NCAR Tech. Note NCAR/TN-475+SR, 54pp.

Khandar, M.H.A. and Moritomi, H., (2013), "Numerical simulation for regional ozone concentration: A case study by weather research and forecasting/ chemistry (WRF/Chem) model", International Journal of energy and environment, Vol.4, No.6, pp.933-954.

Kreislova, K. and Geiplova, H., (2012), "Evaluation of corrosion protection of steel bridges", Procedia Engineering, Vol. 40, p.229-234.

Maruyama, K. and Aso, T., (2016), "An investigation of corrosion environment of a bridge constructed in mountainous area", The third Australasia and south-east Asia Structural Engineering and Construction Conference.

Maruyama, K., Kamasaki, S., Tajima, K. and Aso, T., (2017), "Local corrosion environment around cross section of a plate girder bridge", ISEC PRESS.

Ministry of Land, Infrastructure, Transport and Tourism. (2016), "White Paper on Land, Infrastructure, Transport and Tourism in japan".

Moeletsi, M.E., Shabalala, Z.P., Nysschen, G.D. and Walker, S., (2016)," Evaluation of an inverse distance weighting method for patching daily and dekadal rainfall over the Free State Province, South Africa", Water SA, Vol.42, No.3. Pp.466-474.

Nagata, K., Naito, R., Yagi, C. and Kitahara, T., (2016), "Evaluation method of dew condensation of steel girders using weather data", Journal of Structural Engineering, Vol.62A, pp.796-803 (in Japanese).

Nakashima, M. and Nagai, K., (2014), “An investigation of road bridge maintenance systems in Japan in developed society”, Society for Social Management Systems Internet Journal, Vol. 09.

Noguchi, K., Shirato, H. and Yagi, T., (2017), “Numerical evaluation of sea salt amount deposit on bridge girder”, Journal of Bridge Engineering, Vol.22, No.7.

NSBA. (2006), “Corrosion protection of steel bridges”, Steel Bridge Design Handbook, Chapter 23, National Steel Bridge Alliance.

Obata, M., Watanabe, Y., Goto, G.T.LI., and Goto, Y., (2011), “Prediction of adhered behavior of sea-salt particles on bridge girder”, Procedia Engineering, Vol.14, pp.1043-1050.

Ohya, M., Takebe, M., Hirose, N., Ajiki, S. and Aso, T., (2017), “Estimation of airborne salt level for bridge construction”, ISEC PRESS.

Sakthivel, M., Chinitha. A., Umesha, .P.K., Paradeep Kumard, D. and Vikraman, R., (2015), “Numerical investigation on remaining capacity of corroded steel tubular members”, Proceeding of International Conference on Advances in Materials, Manufacturing and Applications (AMMA 2015).

Sece, M. and Uzun, E.T., (2017), “Corrosion damage analysis of steel frames considering lateral torsional buckling”, Procedia Engineering, Vol.171, pp. 1234-1241.

Setianto, A. and Triandini. (2013), “Comparison of kriging and inverse distance weighting (IDW) interpolation method in Lineament extraction and analysis”, Journal of Southeast Asian Applied Geology, Vol.5, No.1, pp. 21-29.

Sharifi, Y. and Rahgozar, R., (2010), “Simple assessment method to estimate the remaining moment capacity of corroded I-Beam section”, International Journal of Science and Technology, Vol.17, No. 2, pp. 161-167.

Shimozato, T., Murakoshi, J., Tamaki, Y. and Takahashi, M., (2009), “Real time monitoring of bridge collapse due to intense corrosion”, Bridge and Foundation Engineering, Vol.64, No.1, pp.55-60.

Skamarock, C.W., Klemp, J.B., Dudhia, J., Gill, D.O., Barker, D.M., Duda, M.G., Huang, X.Y. Wang, W. and Powers, J.G., (2008), “A description of the advance research WRF version 3”, NCAR Tech. Note NCAR/TN-475+STR, 13pp.

Sugimoto, I., Kobayashi, Y. and Ichikawa, A., (2006), “Durability evaluation based on buckling characteristics of corroded steel deck girder”, QRT of RTRI, Vol.47, No.3, pp. 150-155.

Wong, D.W., Yuan, L. and Perlin, A.S.A., (2004), “Comparison of spatial interpolation methods for the estimation of air quality data”, Journal of Exposure Analysis and Environmental Epidemiology, Vol.14, pp. 404-415.

Yasser, S., (2011), “Reliability of deteriorating steel box-girder bridges under pitting corrosion”, Advanced Steel Construction, Vol.7, No.3, pp. 220-238.

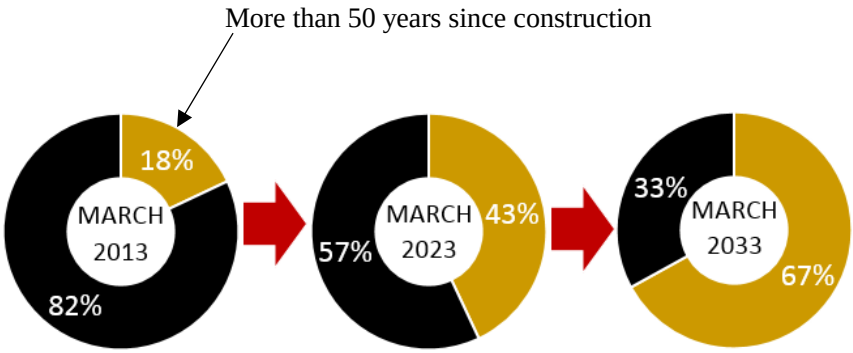

Fig.1.1 Change in the ratio of bridges of over 50 years in age

Photo 1.1 Corrosion of bridge and deterioration of protective coating

Chapter 2

Investigation of the Use and Adaption of an IDW Method to Estimate the Temperature and Humidity

2.1 Introduction

Accurate evaluation of corrosion environment of bridges for corrosion prevention and maintenance is very important. To perform efficient and effective maintenance management for the bridge due to environmental corrosion, an initial inspection and survey need to be conducted with simple possible technique without field observation to reduce the cost. As individual investigation of the corrosive environment for each single steel structure is not only complicated but it is time-consuming and costly as well, therefore, it is essential to evaluate the corrosive environment of steel bridges prior to the commencement of the actual maintenance and management program (Obata et al., 2011; Nagata et al.,2016).

The corrosion of steel structure is caused by various factors such as dust, adhering sea salt particles, and dew condensation. Among them, dew condensation as a results of atmospheric temperature and relative humidity, has received a significant attention in the field of maintenance and managements of bridges (Imai et al., 2020; Rasoli et al., 2018). In the last couple of years, an evaluation of dew condensation as results of atmospheric temperature and relative humidity was carried out using inverse distance weighting (IDW) technique, it was found that dew can easily occur in Aichi prefecture (Nagata et al., 2016). The study revealed that the IDW method has the potential for more easily estimating atmospheric temperature and relative humidity for any arbitrary point as compared that of other techniques (Field measurements or WRF technique).

However, studies on the utilization of IDW for the evaluation of corrosive environment and an appropriate point's selection for different land topographies have not been deeply conducted yet. This chapter describes the use and adaption of an IDW method to estimate the atmospheric temperature and relative humidity for different land topographies, and also propose the optimum number of interpolation points for the accurate evaluation of a corrosive environment.

2.2 Inverse Distance Weighting Method

The IDW is based on the concept of Tobler`s first law (the first law of geography) from 1970. As it was stated everything is related to everything else, but near things are more related than distant things (Chen and Liu, 2012; Garnero and Godone, 2013). The first law is the foundation of the fundamental definition

of spatial dependence and spatial autocorrelation which utilized widely for IDW (Tobler. 1970). The IDW was developed by the U.S National Weather Service in 1972 and is classified as a deterministic method. This is owing to absences of requirement in the calculation to meet specific statistical assumptions, hence, the IDW is different from the stochastic methods (e.g., Kriging and TRA). The multivariate interpolation also can be conducted by the IDW method. The general idea of IDW is originated, according to the assumption that the attribute value of an unsampled point is the weighted average of known values within the neighborhood (Lu and Wong, 2008; Mitas and Mitasova, 1999). This comprises the process of assigning values to unknown points by using values from a scattered set of known points. More precisely, the IDW assumes that each measured point has a local influence that diminish with distance and weights change according to the linear distance of the samples from the unsampled point (Li and Revesz, 2004; Moeletsi et al., 2016). The spatial arrangement of the samples does not affect the weights (Collins and Bolstad, 1996).

In this study, the IDW is employed to predicting the atmospheric temperature and relative humidity using weights as a function of the distance between observation point and the interpolation point at which the prediction has to be made as shown in Fig. 2.1, with IDW it is substantially assumed that the rate of correlation and similarities between neighbors are inversely proportional to the distance between them, which can be defined as a distance reverse function as well (Setianto and Triandini., 2013; Chen and Liu, 2012; Wong et al., 2004). The atmospheric temperature and relative humidity at any arbitrary point were obtained from Japan meteorological observatory (JMA, 2018), using equation of IDW and given by Eq. (2.1). The Japan meteorological data used in this study is freely available.

$$z(x, y) = \sum_{i=1}^{N} w_i z_i \tag{2.1}$$

$$w_i = \frac{\left(\frac{1}{d_i}\right)^n}{\sum_{i=1}^{N}\left(\frac{1}{d_i}\right)^n}$$

In the equation, *z(x, y)* is the predicted value at location *(x, y)*, *N* is the number of nearest known points surrounding *(x, y)*, w_i is the weights assigned to each known points value z_i at location (x_i, y_i), d_i is the distance between each (x_i, y_i) and *(x, y)*, and *n* is the exponent such that; an increase in the distance would cause an exponential decrease in the weighting, it is a control parameter which is generally assumed as two (Chen and liu, 2012). In the present study a power of 2 was employed in the IDW.

The statistical measures used to assess the IDW performance for the atmospheric temperature and relative humidity is the mean error (ME), which is the mean of all differences between the weather prediction data (P_i) and the observed value (O_i). These differences can be averaged over a particular time

period at a single point as well as over different points. Here, N_0 is the total number of values that are used to calculate the ME using Eq. (2.2).

$$ME = \frac{1}{N_0}\sum_i (P_i - O_i) \tag{2.2}$$

The ME gives an indication of the general deviation of the prediction. When the ME is zero, the prediction is neither positive nor negative, and if the ME is positive the prediction tends to be overestimated, whereas if the ME is negative, it underestimates the values.

Similarly, the root mean squared error (RMSE) was adopted to further examine the IDW model performances. The RMSE is also called root-mean deviation (RMSD), it is a measure frequently used on the differences between values predicted by a model or an estimator and the values actually observed from the thing being modeled or estimated. The RMSE is a robust measure of accuracy. These individual differences are also called residuals, and the RMSE is served to aggregate them into a single measure of predictive power. The RMSE is applied widely in various field as follows: in hydrology, RMSE is used to evaluate the calibration of a groundwater; in meteorology, to see the how effectively a mathematical model predicts the behavior of the atmosphere; in GIS, the RMSE is one of the measures used to assess the accuracy of spatial analysis and remote sensing. The root mean squared error (RMSE) mathematically, defined using Eq. (2.3), it gives us an idea of the absolute deviation (Chai and Draxler. 2014).

$$RMSE = \left[\frac{1}{N_0}\sum_i (P_i - O_i)^2\right]^{\frac{1}{2}} \tag{2.3}$$

2.3 Inverse Distance Weighting Setting

In this study, the use and adaption of an IDW for different land topographies, and the optimum number of interpolation points for accurate prediction of corrosive environment due to dew condensation will be demonstrate in detailed.

2.3.1 Determination the Optimum Number of Interpolation Point for IDW

It is necessary to describes how to determine the optimum number of observatory points from an unmeasured point where the prediction has to be performed (targeted point) for establishing the proper setting and achieving more accurate results when using equation (2.1). Mainly, the IDW results is dependent to the suitable setting and adaption, however, there is no specific rule for determining or selection of the points and utilization of IDW to lead for reliable and accurate results. In addition for only two near meteorological observatories, the third meteorological data from farther distance need to be used, which will significantly change the atmospheric temperature and relative humidity results of IDW. Fig.2.2 demonstrates, a comprehensive information about the weather stations in Japan. According to the figure,

the third meteorological stations are too far away in the case of Hokkaido and Tohoku which can influence the results of temperature and humidity when using IDW interpolation technique.

2.3.2 The Use and Adaption of IDW for Different Land Topographies

The inverse distance weighting method is intended to be used for the planar space and does not take into account the influence of terrain by altitude, river, and ocean. Mainly, the atmospheric temperature is lower in the higher elevation compare to ground surface. In other word, the temperature decreases as the elevation increases from the earth surface, the air temperature decrease by 6.5 °C degree for every 1000 meters (Keith Montgomery, 2006). The major part of Japan is covered with mountains, about three-fourth of land surface is mountainous (Land and geography of Japan). Therefore, the land topographies can influence the results of IDW. In the present study a quantitative investigations of the temperature and humidity using IDW were carried out for different land topographies, and their results were compared.

2.4 Description of Investigated Area

In the present study, the atmospheric temperature and relative humidity data of three target meteorological observatories, Osaka, Suwa and Shizuoka were used to compare the results obtained from the IDW. We assumed Osaka to represent flat land, Suwa to demonstrate the mountainous area, and Shizuoka an area relatively close to the sea or ocean, to reflect the influence of water. A quantitative investigation of the temperature and humidity using IDW were carried out for the above mentioned meteorological stations from four, three, and two of their own local surrounding meteorological observatories, respectively. The details of the surrounding meteorological observatories and their distance from the targeted point, elevation, elevation differences are provided in Table 2.1.

In this investigation, the meteorological observatory data of Japan meteorological agency (JMA) are used to obtain the atmospheric temperature and relative humidity, and the quantitative measurement was conducted for the months of January 2018. In the study, the equal distance between observation points and prediction were tried to choose for minimizing the radial influence in IDW, but the same distance meteorological observatories (MO) from the prediction point could not be selected exactly. Because it is difficult to find the equal distance meteorological observatories from the existing MO points.

2.4.1 Overview of Temperature and Humidity of Meteorological Observatories

This section describes, the monthly measured atmospheric temperature and relative humidity of three targeted meteorological observatories (MO) of Osaka, Suwa and Shizuoka with their own local surrounding MO prior to the commencement of IDW investigation. The main purpose of this comparison is to clearly describe the rate of difference in temperature and relative humidity between the existing meteorological observatories. In addition, the minimum (Min), average (Ave) and maximum (Max) value of temperature

and relative humidity of each meteorological observatory point will be demonstrated for the month of January 2018.

(a) Osaka Meteorological Observatory

Fig. 2.3 shows the location of Osaka and its surrounding meteorological observatory. The Osaka MO stations is located in the flat area, and we used four surrounding meteorological stations of Kyoto, Kobe, Wakayama, and Nara. The distance, elevation and difference in the elevation for each meteorological stations compare to Osaka MO are presented in Table 2.1. For this case, the difference in elevation between Osaka and its surrounding meteorological is less than 18 m, which is made small difference. The comparison results of atmospheric temperature and relative humidity of Osaka and its four own local surrounding MO are presented in Figs. 2.4(a) and 2.4(b) respectively.

The monthly temperature (RMSE) is about 1.5 °C at Kyoto, 1°C at Kobe. 1.3 °C at Wakayama and 2°C at Nara MO, as compare to Osaka meteorological observatory in the month of January 2018. Similarly, the humidity is 11% at Kyoto, 7 % at Kobe, 12.5 % at Wakayama and 11.5 % at Nara as shown in Table 2.2. The comparative investigation results revealed that the difference in temperature between Osaka and its surrounding MO being within the range of 1 °C to 2 °C in this month, the higher difference in temperature is obtained from Nara, and the lower difference in temperature is obtained from Kobe compare to Osaka. Regarding relative humidity the higher difference is obtained at Wakayama, and lower difference obtained at Kobe compare that of with Osaka MO, the difference is being ranged between 7 % - 12.5 %.

(b) Suwa Meteorological Observatory

The Suwa meteorological observatory was located in mountainous area, and it is adopted to represent the influence of mountain in the investigation. Fig. 2.5 shows, the location of Suwa and its four surrounding meteorological observatory which consist of Iida, Nagano, Takayama, and Chichibu, respectively. For this particular case the difference in elevation between Suwa and its surrounding MO exceeds 200 m as shown in Table 2.1. The comparison results of atmospheric temperature and relative humidity were illustrated in Figs. 2.6 (a) - 2.6 (b) respectively.

According to Table 2.3, the monthly temperature RMSE is 2.1 °C at Iida, 1.7 °C at Nagano, 1.6 °C at Takayama and 4 °C at Chichibu compare to observation value of Suwa. Also, the monthly relative humidity is about 11.4 % at Iida, 19.30 % at Nagano, 12.50 % at Takayama and 18.2 % at Chichibu MO. In this case, the differences in temperature were ranged from 1.6 °C to 4 °C, the larger difference was obtained 4 °C from Chichibu and the small difference was obtained 1.6 °C from Takayama meteorological observatory compare to Suwa. The higher difference in relative humidity was obtained from 19.30 % from Nagano and the lower difference was 11.4 % at Iida. The difference in humidity were ranged between 11.4% - 19.30 %. Hence, the difference in temperature and relative humidity of Suwa MO is larger than, the difference in temperature and relative humidity of Osaka which is obtained from its surround MO.

(c) Shizuoka Meteorological Observatory

The location of Shizuoka and its surrounding meteorological observatories is shown in Fig. 2.7. Shizuoka is used to take into account the influence water due to ocean, the four its own local surrounding meteorological are Hamamatsu, Mishima, Ajior and Omaezake. The detail information about the elevation, difference in elevation and distance from targeted station to surrounding are presented in Table 2.1. In this study, the observation value of temperature and relative humidity of Shizuoka were compared with its surrounding meteorological observatories in the month of January 2018 and their results are presented in Figs. 2.8 (a) and 2.8(b).

According to Table 2.4, the temperature RMSE is about 1.7 °C at Hamamatsu, 1.8 °C at Mishima, 2 °C at Ajiro and 1.8 °C at Omaezaki meteorological observatories respectively. Also, the RMSE of relative humidity is about 16.6 % at Hamamatsu, 12.5 % at Mishima, 15.4 % at Ajiro and 16.6 % at Omaezaki. The comparative investigation revealed that the higher difference in temperature is obtained at Ajiro and the lower difference is obtained from Hamamatsu in comparison to Shizouka, in this case the temperature difference is ranged between 1.7 °C to 2 °C. Regarding, humidity the larger difference were observed at Hamamatsu and the small difference was obtained at Ajiro, the difference of humidity was being ranged between 12.4 to 16.6 %.

2.4.2 Comparison of IDW by Applying Four Interpolation Points

This section demonstrates, the comparative investigation of inverse distance weighting technique for three different cases of flat land, mountainous and the area close to the ocean as following: Table 2.5 shows the monthly comparison results of IDW technique for three independent cases of Osaka, Suwa and Shizuoka. In case 1, the temperature RMSE is about 1°C and the relative humidity 6.5 % which results in a small error that be due to inclusion of Nara, which has a difference in elevation. In this case the temperature obtained lower when using IDW compare to Osaka because the mean error is (ME) is negative. Regarding the relative humidity, the IDW results is higher compare to Osaka because the ME has positive value.

In case 2, the atmospheric temperature RMSE is about 1.7 °C, and relative humidity is about 12%, both which have the errors, the errors attributed to the significant differences in elevation, which varies from 200 m to 500 m. For case 2, the temperature ME was positive, it means that IDW predicted higher than Suwa. The ME was positive for the relative humidity as well, which implies the higher prediction.

Finally, the RMSE of case 3 shows a smaller temperature error of almost 1.3 °C and a relative humidity of 14 %. In case 3, the error in temperature is smaller compared to case 2, but the humidity to be increased owing to influence of the water from the ocean. Moreover, for case 3 the lower temperature and higher relative humidity obtained by employment of IDW compare to Shizuoka, because the ME is negative and positive for temperature and relative humidity, respectively. Also, the minimum, average, and maximum value of temperature and relative humidity for the month of January are present in the Table for more detail explanation.

2.4.3 Comparison of IDW by Considering Three Interpolation Points

A quantitative comparison of the atmospheric temperature and relative humidity were carried out for Osaka, Suwa, and Shizuoka by selecting three of their four sounding meteorological observatories (MO) eliminating one of them in turn. Table 2.6 shows the monthly comparison results of the inverse distance weighting (IDW) for the different combinations and herein the accurate cases are discussed in more detailed, as the shading in the Table indicates.

In case 4, the RMSE was obtained as 0.76 °C for the temperature, and 5.6 % for the relative humidity when Nara was not included in the calculation. In this case, the accuracy of the calculation improved by removing Nara; because the elevation of Nara is almost 81 m higher compared to that of Osaka. For this particular case, the temperature was underestimate when using IDW compared that of observation temperature from Osaka, this is due to negative value of ME which is -0.15. The relative humidity was overestimated when using IDW, as the ME is positive.

In case 5 two results were obtained, the higher accuracy of which was obtained for the temperature when Chichibu, which is located 528 m lower than Suwa, was not included in the calculation, the RMSE was almost 1.3 °C, but followed by low accuracy of the relative humidity compare to four interpolation points, and a high accuracy of humidity obtained when Takayama was omitted from the calculation, 10.870%. The ME was obtained positive for temperature in case 5, which means the temperature was higher when using IDW compare to observation temperature from the Suwa, and the ME was positive that indicate the higher relative humidity of IDW compared that of the Suwa. Finally, in case 6, the accuracy of the temperature was improved when the Omaezaki was not included in the calculation, in which the temperature was almost 1.25 °C but a low accuracy of humidity of 14.45 % as compared to four interpolation points. For this case, as the ME is positive for the relative humidity, it means that IDW overestimate compared that of Shizuoka and the ME is negative for temperature which indicate the lower prediction of IDW.

That is to say, in this particular month the temperature of Hamamatsu, Omaezaki and Mishima is lower compare to Shizuoka and the temperature of Ajiro is higher as can be seen from Table 2.4. Therefore, the combination of Hamamatsu, Mishima and Ajiro was able to obtain accurate results. Furthermore, Shizuoka is located almost exactly in the middle of Hamamatsu and Ajiro in the same direction with Mishima which is an appropriate interpolation point, and Omaezaki is quite in the edge of ocean and away from the straight direction. Hence, this situation caused that the accuracy of temperature improved when the Omaezaki was not included in the calculation.

2.4.4 Comparison of IDW by Considering Two Interpolation Points

The number of meteorological observatories were reduced from accurate cases from three interpolation points to two, the monthly results of which can be seen in Table 2.7. In case 7, the results of both temperature and relative humidity have low accuracy compared to the use of three interpolation points. In case 8, also the results of temperature has received the low accuracy compared to use of three interpolation

points. However, the accuracy of humidity improved compared to the use of three points when Takayama was removed from the calculation (this was compared with Iida, Nagano, and Takayama in case 5 shown in Table 2.6). This was due to the use of Suwa, which is located in the middle Iida and Nagano.

Finally, in case 9, the accuracy of the humidity improved by employment of two interpolation points compared to three points when removing Mishima. However, the temperature has low accuracy for two interpolation point as compare using three interpolation points.

2.4.5 Comparative Study Results of Four, Three, and Two Interpolation Points

A quantitative comparison of the inverse distance weighting method when applying four, three, and two points clearly shows that the accuracy of the IDW can be improved to a certain extend by using three interpolation points for both atmospheric temperature and relative humidity, rather than four or two interpolation points for flat land. The higher accuracy of the IDW was achieved from two interpolation points for mountainous and oceanic areas. Which is due to the increased climate similarities when removing the points which have significant difference in elevation. If we see in Table 2.1, Nara is close to the Osaka as compared to Wakayama, but the difference in elevation is significant high compared to Wakayama, that is why the accuracy of IDW improved when Nara was not included in calculation.

Additionally, the investigation revealed that although a slight difference was shown, almost the same precision was achieved for both three and two interpolation points. Therefore, it is possible to evaluate the corrosion environment of any arbitrary point using the IDW technique from two interpolation points, this can be useful particularly when we have originally only two meteorological observatory or a combination of both flat and mountainous points, by eliminating the points from three point that has a remarkable differences in elevation, using only two instead.

Regarding the land topography, the highest accuracy was obtained for both atmospheric temperature and relative humidity for flat land as compared to mountainous and oceanic areas. The monthly RMSE was smaller at 0.8 °C for temperature, and 12 % for humidity in the case of mountainous and oceanic areas. The outcome of the present investigation showed that the accuracy of IDW for flat land is almost two-times higher compare to mountainous areas.

2.5 Concluding Remarks

An inverse distance weighting (IDW) method has the potential for easily predicting the atmospheric temperature and relative humidity at an arbitrary point. This chapter aimed to evaluate the use and adaption of the IDW method for different land topographies, and the optimum number of interpolation points for an accurate evaluation of a corrosive environment was proposed. The following summery can be made:

1) The present investigation revealed that a more accurate results of IDW for atmospheric temperature and relative humidity were achieved from three interpolation points in the case of flat land and two interpolation points in the case of mountainous and oceanic area.

2) The outcome of present study clearly showed that although, slight difference exist between the results of three and two interpolation points but the same level of precision were obtained. Hence, it is possible to obtain the temperature and relative humidity a similar climate from two-point weather station using IDW.
3) Regarding land topographies, a higher accuracy of the temperature and humidity were achieved for flat land compare to mountainous or oceanic areas. That is, the accuracy of IDW for flat land is two-times higher in comparison to oceanic and mountainous areas.

References

Chai, T. and Draxler, R.R., (2014), " Root mean square error (RMSE) or mean absolute error (MAE)-Arguments against avoiding RMSE in the literature", Geoscientific Model Development, pp. 1247-1250.

Chen, F. and Liu, C., (2012), "Estimation of the spatial rainfall distribution using inverse distance weighting (IDW) in the middle of Taiwan", Paddy Water Environ, pp. 209-222.

Collins, FC. and Bolstad, PV., (1996), " Comparison of spatial interpolation techniques in temperature estimation", Proceedings of the Third International Conference.

Garnero, G and Godone, D.,(2013), " Comparisons between difference interpolation techniques", The international Archives of the Photogrammetry, Remote Sensing and Spatial Information Sciences, Vol. XL-5/W3, pp.139-144.

Imai, R., Miyasou, T. and Aso, T., (2020), "An evaluation of dew condensation on steel plate girder bridges", Journal of Structural Engineering, Vol. 66A, pp. 443-451 (in Japanese).

JMA, (2018), "Japan Meteorological Agency", https://www.data.jma.go.jp/gmd/risk/obsdl/index.php.

Keith Montgomery. (2006), "Variation in temperature with altitude and latitude", Journal of Geography, Vol.105, No.3, pp.133-135.

Land and geography of Japan: http://factsanddetails.com/japan/cat26/sub160/item860.html#chapter-5.

Li, L. and Revesz, P., (2004), "Interpolation methods for spatio-temporal geographic data", Journal of Computers, Environment and Urban Systems, Vol. 28, No. 3, pp. 201-227.

Lu, GY. and Wong, DV., (2008), " An adaptive inverse-distance weighting spatial interpolation technique", Computer and Geoscience, pp. 1044-1055.

Mitas, L., Mitasova, H., (1999), "Spatial Interpolation", In: P.Longley, M.F. Goodchild, D.J. Maguire, D.W.Rhind (Eds.), Geographical Information Systems: Principles, Techniques, Management and Applications, Wiley.

Moeletsi, M.E., Shabalala, Z.P., Nysschen, G.D. and Walker, S., (2016)," Evaluation of an inverse distance weighting method for patching daily and dekadal rainfall over the Free State Province, South Africa", Water SA, Vol.42, No.3. Pp.466-474.

Nagata, K., Naito, R., Yagi, C. and Kitahara, T., (2016), “Evaluation method of dew condensation of steel girders using weather data”, Journal of Structural Engineering, Vol.62A, pp.796-803 (in Japanese).

Obata, M., Watanabe, Y., Goto, G.T.LI., and Goto, Y., (2011), “Prediction of adhered behavior of sea-salt particles on bridge girder”, Procedia Engineering, Vol.14, pp.1043-1050.

Rasoli, Z., Nagata, K. and Kitahara, T., (2018), “Monitoring of corrosive environment focusing on dew condensation in steel bridges”, Proceeding of the Sixth International Symposium on Life-Cycle Civil Engineering (IALCCE2018), pp.1175-1182.

Setianto, A. and Triandini. (2013), “Comparison of kriging and inverse distance weighting (IDW) interpolation method in Lineament extraction and analysis”, Journal of Southeast Asian Applied Geology, Vol.5, No.1, pp. 21-29.

Tobler, W.R., (1970), “A computer movie simulating urban growth in the Detroit region”, Proceeding of International Geographical, pp. 234-240.

Wong, D.W., Yuan, L. and Perlin, A.S.A., (2004), “Comparison of spatial interpolation methods for the estimation of air quality data”, Journal of Exposure Analysis and Environmental Epidemiology, Vol.14, pp. 404-415.

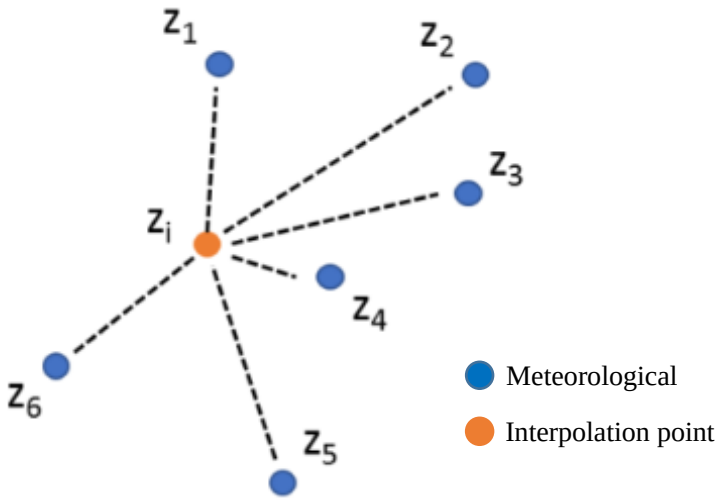

Fig. 2.1 Interpolation point from surrounding meteorological observatories

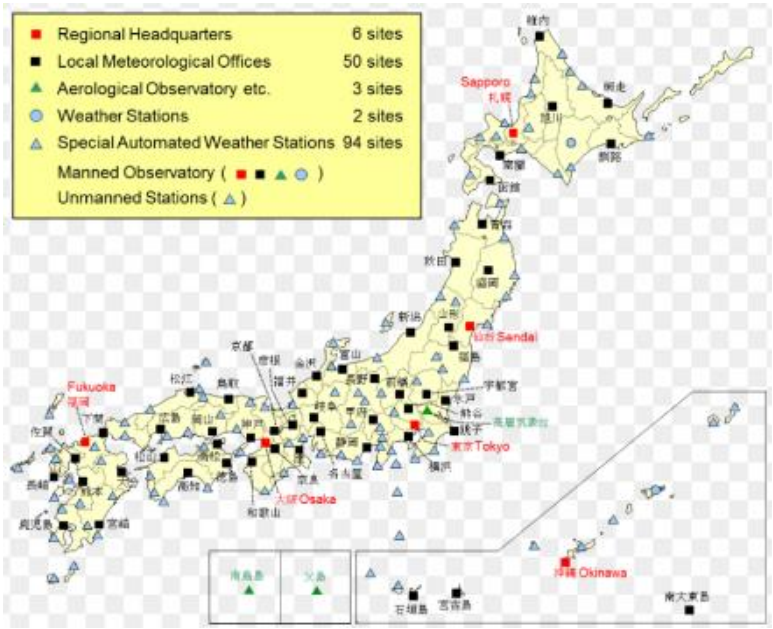

Fig. 2.2 Location of weather stations

Table 2.1 Distances, elevations and differences in elevation from targeted weather stations to the neighboring stations

	A	B	C	D	E	F
No	Targeted weather stations	Elevation of Column (A) (m)	Surrounding meteorological observatories	Distance (km)	Elevation of Column (C) (m)	Elevation difference Column (E)-Column(B) (m)
1	Osaka	23.00	Kyoto	42.02	40.80	17.80
			Kobe	28.01	5.30	-17.70
			Wakayama	58.78	13.90	-9.10
			Nara	28.39	104.40	81.40
2	Suwa	760.00	Iida	64.06	516.20	-243.80
			Nagano	69.02	418.20	-341.80
			Takayama	77.89	560.00	-200.00
			Chichibu	87.05	232.10	-527.90
3	Shizuoka	14.10	Hamamatsu	67.80	45.90	31.80
			Mishima	49.96	20.50	6.40
			Ajiro	63.25	66.90	52.80
			Omaezaki	44.85	44.70	30.60

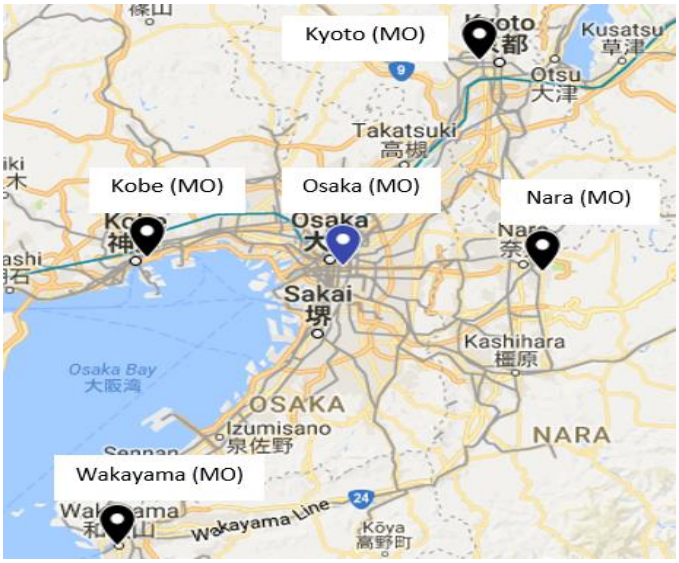

Fig. 2.3 Location of Osaka and its surrounding meteorological observatories (image generated using Google Maps)

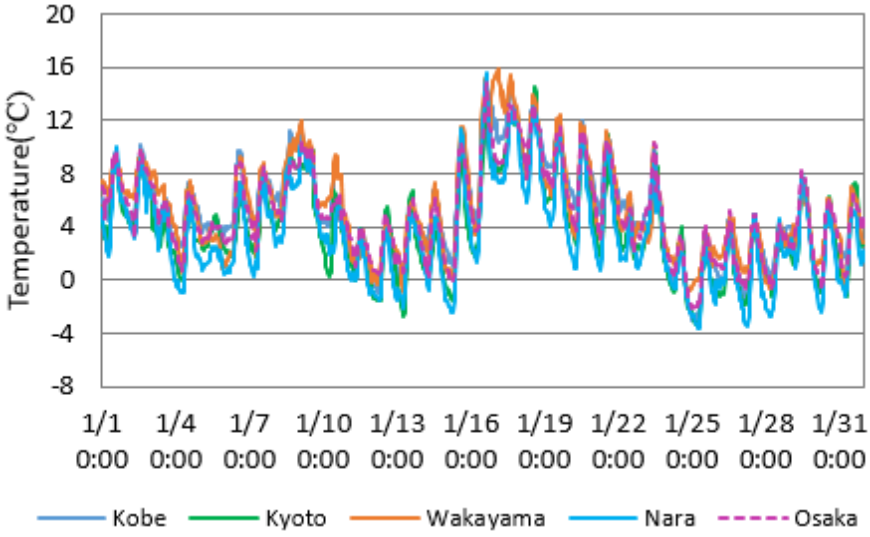

(a) Temperatures of Kobe, Kyoto, Wakayama, Nara, and Oska

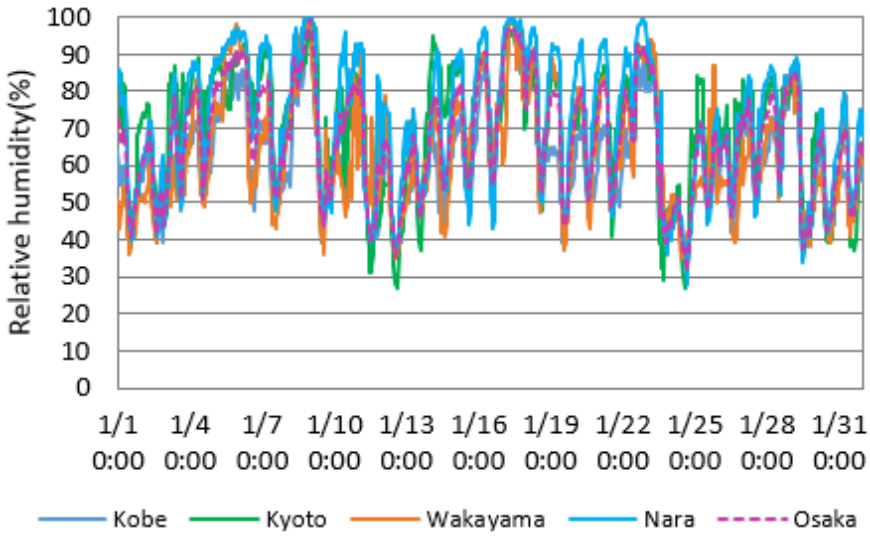

(b) Relative humidity of Kobe, Kyoto, Wakayama, Nara, and Osaka

Fig. 2.4 shows the comparison results of temperature and relative humidity Osaka and its surrounding meteorological observatories.

Table 2.2 Min, Ave, Max, ME and RMSE of temperature and relative humidity of Osaka with its surrounding meteorological observatories in January 2018

	Temperature (℃)					Relative humidity (%)				
Meteorological Observatories	Min	Ave	Max	ME	RMSE	Min	Ave	Max	ME	RMSE
Kyoto	-3.30	3.91	14.60	-1.10	1.50	27.00	69.71	98.00	6.40	11.00
Kobe	-3.10	5.19	14.40	0.20	1.00	33.00	62.60	100.00	-0.70	6.90
Wakayama	-1.00	5.44	15.90	0.40	1.30	34.00	63.84	100.00	0.50	12.50
Nara	-3.70	3.46	15.60	-1.60	1.90	28.00	71.33	100.00	8.00	11.50
Osaka	-2.10	5.04	14.80	0.00	0.00	29.00	63.33	99.00	0.00	0.00

Fig. 2.5 Location of Suwa and its surrounding meteorological observatories (image generated using Google Maps)

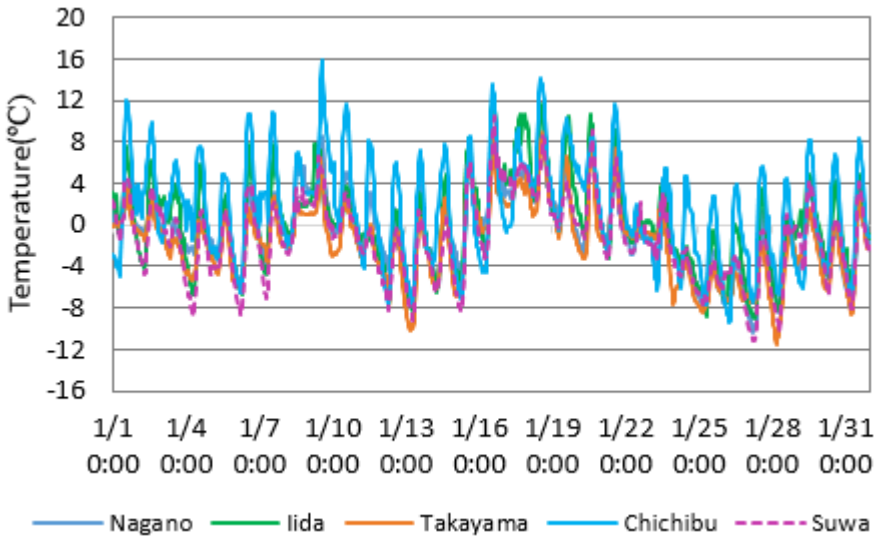

(a) Temperatures of Nagano, Iida, Takayama, Chichibu, and Suwa

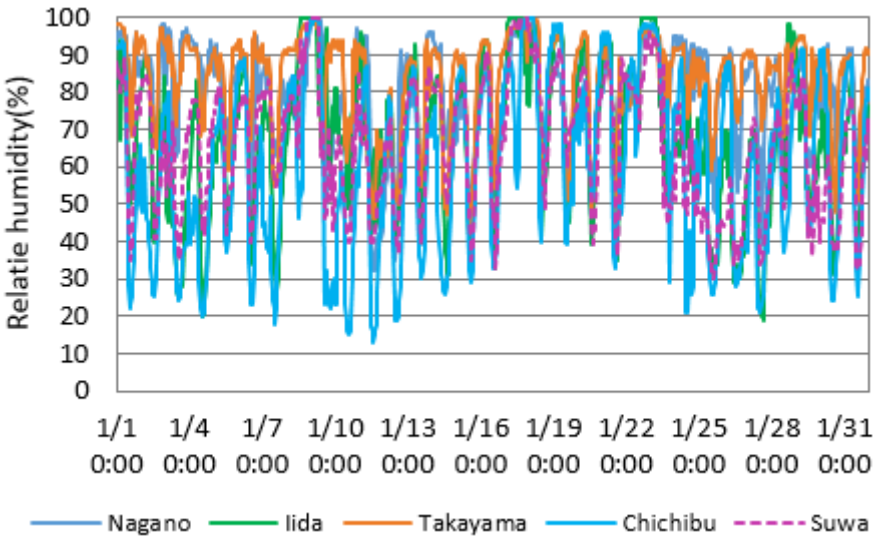

(b) Relative humidity of Nagano, Iida, Takayama, Chichibu, and Suwa

Fig. 2.6 shows the comparison results of at temperature and relative humidity Suwa and its surrounding meteorological observatories.

Table 2.3 Min, Ave, Max, ME and RMSE of temperature and relative humidity of Suwa with its surrounding meteorological observatories in January 2018

	Temperature (℃)					Relative humidity (%)				
Meteorological Observatories	Min	Ave	Max	ME	RMSE	Min	Ave	Max	ME	RMSE
Iida	-9.10	0.24	11.70	1.50	2.10	19.00	67.33	100.00	0.80	11.40
Nagano	-10.40	-0.67	9.30	0.60	1.70	32.00	78.89	99.00	12.50	19.30
Takayama	-11.50	-1.67	8.90	-0.40	1.60	44.00	82.81	99.00	16.40	12.50
Chichibu	-9.40	1.58	15.80	2.90	4.30	13.00	60.81	100.00	-5.60	18.20
Suwa	-11.20	-1.30	10.40	0.00	0.00	30.00	66.41	100.00	0.00	0.00

Fig. 2.7 Location of Shizuoka and its surrounding meteorological observatories (image generated using Google Maps)

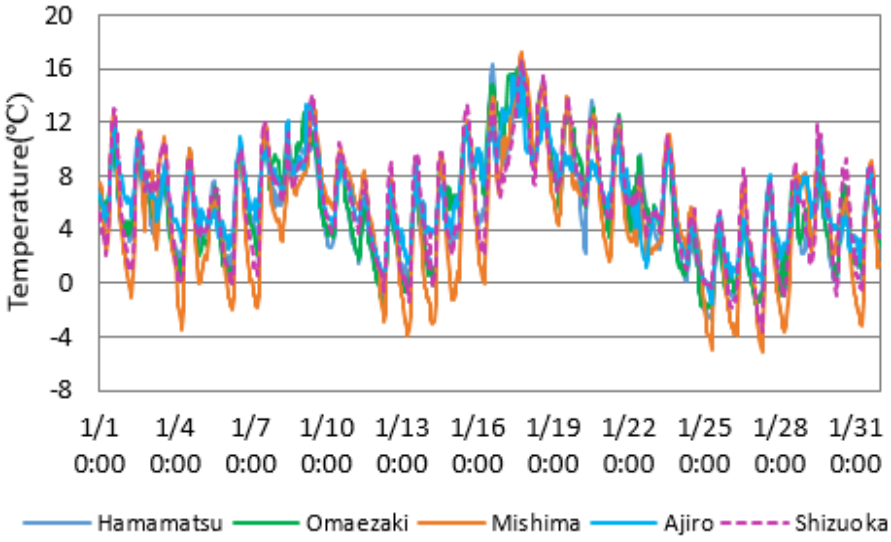

(a) Temperatures of Hamamatsu, Omaezaki, Mishima, Ajiro, and Shizuoka

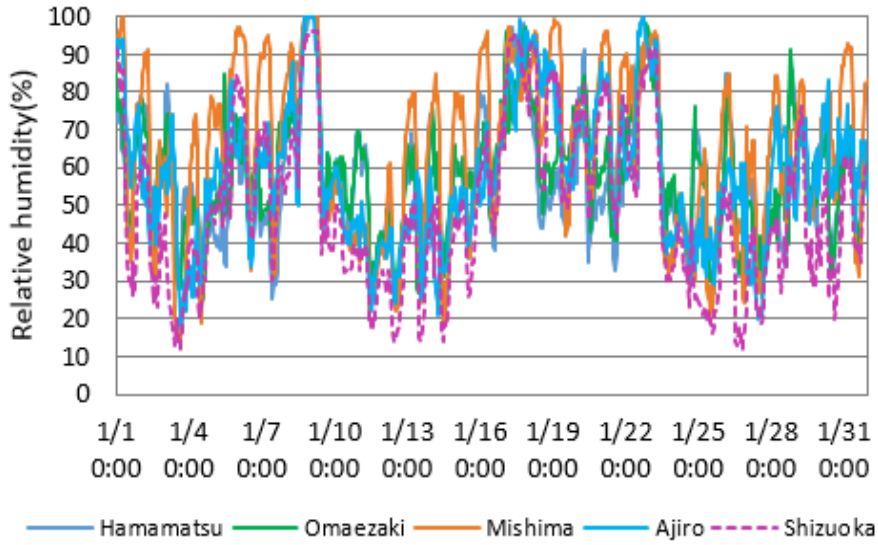

(b) Relative humidity of Hamamatsu, Omaezaki, Mishima, Ajiro, and Shizuoka

Fig. 2.8 shows the comparison results of at temperature and relative humidity Shizuoka and its surrounding meteorological observatories.

Table 2.4 Min, Ave, Max, ME and RMSE of temperature and relative humidity of Shizuoka with its surrounding meteorological observatories in January 2018

	Temperature (℃)					Relative humidity (%)				
Meteorological Observatories	Min	Ave	Max	ME	RMSE	Min	Ave	Max	ME	RMSE
Hamamatsu	-2.70	5.46	16.40	-0.60	1.70	22.00	56.27	100.00	6.50	16.60
Mishima	-5.20	5.24	17.30	-0.80	1.80	14.00	63.82	100.00	14.10	12.50
Ajiro	-1.60	6.40	16.50	0.30	2.10	18.00	58.16	100.00	8.40	15.40
Omaezaki	-1.90	5.91	16.40	-0.20	1.80	25.00	58.75	100.00	9.00	16.30
Shizuoka	-3.60	6.08	16.70	0.00	0.00	12.00	49.74	96.00	0.00	0.00

Table 2.5 Comparison results of inverse distance weighting (IDW) by applying four interpolation points

(a) Min, Ave, Max, ME and RMSE of temperature in January 2018

			Temperature (℃)				
No	Type of land/ area	Four points considered	Min	Ave	Max	ME	RMSE
Case. 1	Flat area	Kyoto, Kobe, Wakayama, Nara	-2.91	4.36	13.74	-0.68	0.93
Case. 2	Mountainous area	Iida, Nagano, Takayama, Chichibu	-8.71	-0.20	10.43	1.08	1.68
Case. 3	Oceanic/Coastal area	Hamamatsu, Mishima, Ajiro, Omaezaki	-2.81	5.73	16.60	-0.36	1.300

(b) Min, Ave, Max, ME and RMSE of relative humidity in January 2018

			Relative humidity (%)				
No	Type of land/ area	Four points considered	Min	Ave	Max	ME	RMSE
Case. 1	Flat area	Kyoto, Kobe, Wakayama, Nara	31.12	67.12	99.50	3.79	6.46
Case. 2	Mountainous area	Iida, Nagano, Takayama, Chichibu	37.05	72.79	99.11	6.38	11.96
Case. 3	Oceanic/Coastal area	Hamamatsu, Mishima, Ajiro, Omaezaki	23.57	59.74	100.00	9.99	14.29

Table 2.6 Comparison results of inverse distance weighting (IDW) by considering three interpolation points

(a) Min, Ave, ME and RMSE of temperature in January 2018

			Temperature (℃)				
No	Type of land/area	Three points considered	Min	Ave	Max	ME	RMSE
Case. 4	Flat area	Kyoto, Kobe, wakayma	-2.71	4.88	13.91	-0.15	0.76
		Kobe, wakayma, Nara	-2.86	4.45	14.02	-0.58	0.88
		wakayma, Nara, Kyoto	-3.08	3.86	14.89	-1.17	1.41
		Nara, Kobe, Kyoto	-3.20	4.26	13.66	-0.77	1.01
Case. 5	Mountainous area	Iida, Nagano, Takayama	-8.97	-0.58	9.95	0.70	1.32
		Nagano, Takayama, Chichibu	-8.67	-0.41	9.86	-4.32	6.31
		Takayama, Chichibu, Iida	-8.62	-0.01	11.10	1.26	1.88
		Chichibu, Iida, Nagano	-9.00	0.29	11.35	1.57	2.13
Case. 6	Oceanic/Coastal area	Hamamatsu, Mishima, Ajiro	-3.44	5.63	16.72	-0.46	1.25
		Mishima, Ajiro, Omaezaki	-2.83	5.78	16.74	-0.30	1.30
		Ajiro, Omaezaki, Hamamatsu	-1.90	5.93	16.31	-0.15	1.64
		Omaezaki, Hamamatsu, Mishima	-3.08	5.58	16.63	-0.51	1.32

(b) Min, Ave, Max, ME, and RMSE of relative humidity in January 2018

			Relative humidity (%)				
No	Type of land/area	Three points considered	Min	Ave	Max	ME	RMSE
Case. 4	Flat area	Kyoto, Kobe, wakayma	32.94	64.66	99.20	1.31	5.64
		Kobe, wakayma, Nara	31.35	66.59	100.00	3.22	6.26
		wakayma, Nara, Kyoto	29.37	69.86	99.19	6.44	9.28
		Nara, Kobe, Kyoto	30.85	67.42	99.45	4.04	6.69
Case. 5	Mountainous area	Iida, Nagano, Takayama	39.27	75.35	99.13	8.94	13.60
		Nagano, Takayama, Chichibu	32.13	75.46	98.67	2.44	17.31
		Takayama, Chichibu, Iida	27.94	70.42	99.15	3.90	11.25
		Chichibu, Iida, Nagano	27.25	69.48	99.39	2.97	10.87
Case. 6	Oceanic/Coastal area	Hamamatsu, Mishima, Ajiro	21.03	60.30	100.00	10.55	14.45
		Mishima, Ajiro, Omaezaki	21.59	60.39	100.00	10.65	14.49
		Ajiro, Omaezaki, Hamamatsu	24.51	58.04	100.00	8.32	14.63
		Omaezaki, Hamamatsu, Mishima	23.75	60.09	100.00	10.35	14.96

Table 2.7 Comparison results of inverse distance weighting (IDW) by considering two interpolation points

(a) Min, Ave, ME and RMSE of temperature in January 2018

			Temperature (℃)				
No	Type of land/area	Three points considered	Min	Ave	Max	ME	RMSE
Case. 7	Flat area	Kyoto, Kobe	-3.10	4.80	13.69	-0.24	0.82
		Kobe, wakayma	-2.56	5.24	14.53	0.27	0.90
		wakayma, Kyoto	-2.19	4.43	14.30	-0.60	1.02
Case. 8	Mountainous area	Iida, Nagano	-9.54	-0.18	10.54	1.10	1.57
		Nagano, Takayama	-9.32	-1.11	8.88	0.16	1.43
		Takayama, Iida	-9.25	-0.53	10.39	0.75	1.41
Case. 9	Oceanic/Coastal area	Hamamatsu, Mishima	-4.19	5.31	16.81	-0.77	1.41
		Mishima, Ajiro	-3.69	5.68	16.99	-0.40	1.35
		Ajiro, Hamamatsu	-2.11	5.96	16.22	-0.13	1.66

(b) Min, Ave, Max, ME, and RMSE of relative humidity in January 2018

			Relative humidity (%)				
No	Type of land/area	Three points considered	Min	Ave	Max	ME	RMSE
Case. 7	Flat area	Kyoto, Kobe	32.46	64.79	99.08	1.44	5.98
		Kobe, wakayma	34.00	62.83	100.00	-0.11	6.31
		wakayma, Kyoto	30.04	67.73	98.01	4.34	8.16
Case. 8	Mountainous area	Iida, Nagano	28.79	72.64	99.54	6.23	11.61
		Nagano, Takayama	38.16	80.62	98.56	14.21	19.68
		Takayama, Iida	25.02	73.52	99.19	7.12	12.39
Case. 9	Oceanic/Coastal area	Hamamatsu, Mishima	20.33	61.16	100.00	11.41	15.71
		Mishima, Ajiro	16.69	61.65	100.00	11.89	15.73
		Ajiro, Hamamatsu	22.93	57.28	100.00	7.55	13.88

Chapter 3

Evaluation of Dew Condensation by Field Measurements

3.1 Introduction

The field observation was conducted for two bridges in the northeast and northwest of Aichi prefecture, for Ooeyousui and Sanbonmatsu bridge, respectively. First the atmospheric temperature and relative humidity of Ooeyousui and Sanbonmatsu were measured by using sensor in the two different regions such as flat area and mountainous area, subsequently their results were compared with Nagoya meteorological observatory to examine the weather situation in Aichi prefecture. The comparison results shows the temperature and humidity are not quite the same in the entire prefecture. Therefore it is difficult to evaluate the corrosion environment of steel bridge in the whole prefecture from only Nagoya meteorological observatory, and it is essential to use IDW technique for calculation of temperature and humidity to evaluate dew for each single point.

Secondly, the evaluation of dew condensation (Nagata et al., 2016; Imai et al., 2020) was carried out using the atmospheric corrosion monitoring sensor (ACM) for both Ooeyousui and Sanbonmatsu bridges to examine the actual occurrence of dew condensation in the prefecture. The investigation outcomes revealed that dew condensation tend to occur in the bridges but the occurrence of dew were not quite the same in the both bridges, the occurrence of dew for each bridge were different and could be depend on the environment where the bridge located in. Further, the tendency occurrence of dew condensation in the bridge increased from midnight to morning compare to that of whole day. Finally, the evaluation of dew condensation was carried out for a bridge as case study using IDW technique, and their results were compared with field observation. The outcome of the present investigation shows that there is a good agreement between field observation and IDW technique. However, the use and adaption of IDW for accurate prediction of temperature and humidity was already discussed in the previous chapter and detailed description are provided.

Thirdly, the relation between girder temperature and atmospheric temperature already has been investigated via using field measurement (Nagata et al., 2016). The investigation revealed that in the morning when the dew condensation tends to occur, the girder temperature and atmospheric temperature are almost the same. Hence, it is acceptable to assume the girder temperature equal to as atmospheric temperature, and based on this as assumption the evaluation of dew condensation will be carried out in the present study as well. In the next section, the evaluation method of dew condensation and its mathematical procedures are described in details.

3.2 Evaluation Method for Dew Condensation

In this study, the dew point temperature ((T_{DEW}) was required for each single point to evaluate the dew condensation. The dew point temperature can be calculated as follows:
The atmospheric temperature and relative humidity are obtained using the inverse distance weighting (IDW) technique. Then, the saturated vapor pressure at certain atmospheric temperature *T* is calculated from Eq. (3.1) (Diaiichi-kagaku.co.jp: Humidity calculation 1).

$$\ln(e_w) = -6096.9385 \times T^{-1} + 21.2409642 - 2.711193 \times 10^{-2} \times T + 1.673952 \times 10^{-5} T^2 + 2.433502 \times \ln(T) \quad (3.1)$$

If the atmospheric temperature is calculated in Celsius t (°C), it should be converted into the Kelvin using the given Eq. (3.2)

$$T = t + 273.15 \quad (3.2)$$

The relation of water vapor pressure which is obtained based on relative humidity and saturated vapor pressure is calculated by the given Eq. (3.3).

$$e = e_w \times \frac{U}{100} \quad (3.3)$$

Finally, the dew-point temperature is calculated based on the atmospheric temperature and relative humidity at saturated vapor pressure using Sonntag's equation (Diaiichi-kagaku.co.jp: Humidity calculation 1) either from the given Eq. (3.4) or Eq. (3.5). Here, y = ln (e/611.213).

In the case of $y \geqq 0$;

$$T_{DEW} = 13.715 \times y + 8.4262 \times 10^{-1} \times y^2 + 1.9048 \times 10^{-2} \times y^3 + 7.8158 \times 10^{-3} \times y^4 \quad (3.4)$$

In the case of $y<0$;

$$T_{DEW} = 13.7204 \times y + 7.36631 \times 10^{-1} \times y^2 + 3.32136 \times 10^{-2} \times y^3 + 7.78591 \times 10^{-4} \times y^4 \quad (3.5)$$

The dew point can be evaluated by subtracting the girder temperature from the dew point temperature ($\Delta t = T_{Dew} - T_{Girder}$). The dew condensation occur when Δt is greater than zero.

In the equations *e* is the water vapor pressure, *U* is the relative humidity, e_w is the saturated water vapor pressure, *T* is absolute temperature and T_{Girder} is the girder temperature which assumed as equal to

atmospheric temperature, *y* is a parameter that can be calculated from the *e*, and the T_{DEW} is the dew point temperature.

3.3 Overview of Field Measurements

In this research, the field measurements were carried out for the bridges using sensors to evaluate dew condensation. Previously, investigation of dew condensation was conducted at Aichi prefecture by using WRF (Nagata et al., 2016). The investigation results revealed that dew condensation easily can occur in the entire prefecture, but it is remarkably higher at northeast and northwest of the prefecture. Based on the information obtained from the WRF, the field measurements were conducted in the northeast and northwest regions of the prefecture as well.

3.3.1 Measurement Instruments (Sensors)

The measurement instruments (sensor), type of sensor used in the present study, installation position of the sensors, and location of monitoring bridges were described in detailed as following:

(a) Atmospheric Corrosion Monitoring Sensor

The atmospheric corrosion monitoring (ACM) sensor is made of a base plate of carbon steel with size of (64mm×64mm) and a silver conductive paste (30-40μm thickness), is used over steel substrate (Shin-ichi et al., 1994). Both species of metal (Fe/Ag) are mutually insulted by (30-35μm thickness) as shown in Fig. 3.1. If they are exposed to the atmosphere, a thin water film will form on the surface due to rainfall and condensation, when the water film covers the entire surface of two metal, an electrical cell is formed and the current which passes between the electrodes are measured as the sensor output. Indeed, in this process Fe melts out due to corrosion and release electron e. the released electron e causes a chemical reaction on the surface of Ag and the chemical equations is as following:

$$2\mathrm{Fe} \rightarrow 2\mathrm{Fe}^{2+} + 4\mathrm{e}^{-} \tag{3.6}$$

$$2\mathrm{H_2O} + \mathrm{O_2} + 4\mathrm{e}^{-} \rightarrow 4\mathrm{OH}^{-} \tag{3.7}$$

OH is generated due to reaction and the amount of consumed electron is measured as a corrosion current. In this case, atmospheric corrosion is considered when the current is ranged between (0.1 ~1 mA). Also, the measurement interval of ACM sensor is 10 minutes (Shrinks Co., Ltd, Principle and outline of ACM sensor measurements).

(b) Thermocouple (Sensor)

Fig. 3. 2 shows the thermocouple that has been used in the field measurements. More precisely, (a) shows T-type thermocouples, and (b) shows its data logger EL-USB-TC. The measurements interval of this sensor

is 10 mint. The specification of thermocouples presented in Table 3.1, the red circled line shows the sensor units of this instrument.

(c) Atmospheric Temperature and Relative humidity Sensor

In this study, the atmospheric temperature and relative humidity that has been used in the field measurement is EL-USB-2. As shown Fig. 3.3, the circled on its head shows the sensor units of this instrument. The specification of this sensor is presented in Table 3.2.

3.3.2 Description of Investigated Bridges

In this section, the Ooeyousui and Sanbonmatsu bridges which is used as case study will be described as following.

(a) Ooeyousui Bridge

One-site, observation has been conducted at Ooeyousui bridge in the northwest (35.316° N, 136.814° E) of Aichi prefecture. Fig. 3.4 shows the monitoring location of the bridge (image generated using Google Map), and photo 3.1 shows an overview of the bridge, which was built in 1966. This bridge is located in Ichinomiya, Aichi prefecture, and this is steel girder bridge with length of 21.50 m.

(b) Set Position of Measurement Instruments

Fig. 3.5 shows the cross section and set position of measuring instruments in the bridge. In this study, totally eight ACM sensors were set on the web and bottom flange of the bridge girders for the exterior left, right, and middle to evaluate the dew condensation on the both web and flange of girder. Photo 3.2 and 3.4 shows the actual ACM on the web and flange of girder, respectively. Additionally, atmospheric temperature and relative humidity sensor were set for both exterior girder on the left, right and the middle girder to evaluate the atmospheric temperature and relative humidity around the girder. Photo 3.5 and 3.5 show the actual atmospheric temperature and relative humidity sensor after installation for exterior and middle girder respectively.

(c) Sanbonmatsu Bridge

An observation was also carried out at Sanbonmatsu, this bridge is located on the northeast of Aichi prefecture (35.135° N, 137.308° E). The monitoring location of this bridge has been shown in Fig 3.6 (image created using Google Map), and photo 3.7 shows an overview of the Sanbonmatsu bridge. This is a steel girder bridge of 142.60 m in length, and was built in 2007. This bridge is located in the Toyota city of the Aichi prefecture. Additionally, the cross section of the bridge and installation positions of the measuring sensors are shown in Fig. 3.7. The number of ACM and temperature and relative humidity sensor used in the bridge are quite similar to the Ooeyousui bridge as described in section (b). Photo 3.8 ~ 3. 9 shows the actual position of sensors after their installation in the bridge.

3.3.3 Field Measurement

The investigation results of atmospheric temperature, relative humidity, and evaluation of dew condensation using sensor are described in the following:

(a) Comparison of Nagoya Metrological Observatory with Field Measurement

Fig. 3.8 and 3.9 show the simultaneous comparison results of the atmospheric temperature and relative humidity of Ooeyousui bridge, Sanbonmatsu, and the Nagoya meteorological observatory (NMO) weather data, the measurement period is for the month of January 2018. The atmospheric temperature and relative humidity were obtained through field measurements using a temperature and relative humidity sensor. In this study, the temperature and humidity of outer girder from the right side of the bridges which is shown in a triangle shape were used, and the 8 ACM sensors for both bridges as shown in a circle shape. The main purpose of this comparison is to see and extensively examine the corrosive nature of both regions and confirm the mount of dew condensation.

As clearly shown in figures, the change in behavior of the temperature and relative humidity in both bridges are extremely linked with the rate of change in the NMO. The temperature RMSE is about 1 °C and the relative humidity is 9 % at Ooeyousui bridge compare to NMO. Similarly, the difference in temperature is 1.7 °C and relative humidity is 15 % at Sanbonmatsu. The comparison results demonstrate that the temperature and humidity of both bridges are not quite the same as NMO, but the results of Ooeyousui is approximately similar to NMO, because it is located near to NMO as compare to Sanbonmatsu. Thus, the difference in temperature and humidity at three points increased as a distances increased, and it is difficult to estimate the temperature and humidity of the entire prefecture only from NMO. In addition, the graph shows the low temperature and higher relative humidity at Sanbonmatsu bridge as compare to Ooeyousui.

(b) Evaluation of Dew Condensation using Atmospheric Temperature and Relative Humidity Sensor

An evaluation of dew condensation was carried out at both Ooeyousui and Sanbonmatsu bridges using atmospheric temperature and relative humidity sensor from the December 2017 to January 2018. First, the atmospheric temperature and relative humidity were obtained by field observation using sensor. Subsequently, the dew-point temperature was calculated at saturated vapor pressure as it was described in section 3.2. According to Fig. 3.10 and 3.11 the tendency of occurrence of dew condensation is increased when the difference between temperature and dew point temperature becomes significantly small and even at some instances they are the same which shows the high tendency of dew occurrence. The tendency of occurrence of dew condensation is higher in January 2018 as compare to December 2017 at Ooeyousui bridge. Thus, it is concluded from the field observation that dew can easily occur at Ooeyousui bridge.

Fig. 3.12 and 3.13 show the evaluation results of dew from December 2017 to January 2018 at Sanbonmatsu. According to the figures the difference between temperature and dew-point temperature are significantly small and in most instances they are same. The frequency of dew condensation was

determined from the sensor and it reached about 38 occurrences during January 2018. The field observation results completely show dew condensation at Sanbonmatsu, but the frequency of dew condensation was higher in January 2018 as compare to December 2017. It means, the occurrence of dew condensation due to temperature and humidity was remarkably higher in the month of January 2018, as it can be observed from the figures as well.

(c) Evaluation of Dew Condensation using ACM Sensor

The corrosion current results obtained by the atmospheric corrosion monitoring (ACM) sensor at Ooeyousui bridge can be seen in Fig. 3.14. As indicated by the graph, dew occurred in the ACM1, ACM2, ACM4, ACM7, and ACM8 because the corrosion current value was within the range of 0.01 to 0.1mA (National institute for materials science, 2004). This is a significant state of dew condensation which is highlighted by a red-colored rectangle, whereas ACM3, ACM5 and ACM6 showed dry condition.

An evaluation of dew condensation was carried out at Sanbonmatsu bridge using atmospheric corrosion monitoring (ACM) sensor. The results obtained by the ACM clearly show dew condensation in this bridge. Because the corrosion current value being within the range of 0.01 -0.1 mA. This range is remarkably accurate indication of dew condensation as shown in the red-colored rectangle in the Fig. 3.15. Hence, the evaluation results obtained by the ACM sensor during the field measurement also confirm the dew condensation. Further, an evaluation of dew condensation from the temperature and humidity sensor was conducted with regard to current amount of corrosion by ACM sensor at the Sanbonmatsu bridge, and the results from both sensors were plotted simultaneously as shown in Fig. 3.16. The differences between temperature and dew-point became small and continuously increased the tendency occurrence of dew condensation. In addition, as is clearly demonstrated, the ACM sensor also shows the occurrence of dew condensation during the same period of time and the values of which are shown on the left-hand side of this graph. Finally, from the field measurement results, we clearly see that the dew occurred in the both bridges, and that the environment caused corrosion in steel bridge.

(d) Comparative Study Results of Field Measurements

Fig. 3.8 and 3.9 obviously demonstrate that the changes in temperature and relative humidity at Ooeyousui and Sanbonmatsu are extremely linked with the changing rates of temperature and relative humidity at the NMO. The differences in temperature was about 1 °C, and relative humidity 9 % at Ooeyousui compare to NMO, and it was almost two times higher for Sanbonmatsu (because Ooeyousui is located near to NMO compare to Sanbonmatsu), it can be seen that the difference in atmospheric temperature and relative humidity at three points (Ooeyousui, Sanbonmatsu, and NMO) increased as distance increased. Therefore, it is difficult to evaluate the corrosive environment of bridges as a results of dew condensation in the entire prefecture from the NMO. Moreover, the results demonstrate a lower temperature and higher relative humidity at Sanbonmatsu as compared to Ooeyousui as shown in the figures, it means the more dew

condensation likely to occur at Sanbonmatsu, although both regions show similar corrosiveness environment.

The comparison results of dew condensation in both bridge shows that dew can occur in the bridges as shown in Fig. 3.10 and 3.11 for Ooeyousui corresponding with in Fig 3.12 and 3.13 for Sanbonmatsu bridge. According to the figures, although the condensation tends to occur in both bridges but the amount of dew condensation is not exactly the same, the tendency occurrence of dew is remarkably higher at Sanbonmatsu compare to Ooeyousui, this might be due to Sanbonmatsu is located at mountainous area, where the low temperature and high relative humidity were observed. From the evaluation results at both bridges, it is concluded that dew condensation is not quite the same for every single bridge. On the other hand, evaluation of dew condensation for every bridge using field measurement might be expensive and time-consuming. Thus, it important to evaluate dew condensation using IDW technique as it was discussed in previous chapter or other technique without field observations.

Regarding ACM sensors, the results obtained by the ACM also demonstrate dew condensation in the both bridges because the corrosion current value being within the range of 0.01 to 0.1 mA as shown by the red-colored rectangle in Fig. 3.14 and 3.15 for both Ooeyousui and Sanbonmatsu respectively. Although, both graphs confirm dew but it is significantly higher for Sanbonmatsu compare to Ooeyousui bridge. Thus, the evaluation results of dew obtained by atmospheric temperature and relative humidity sensors, and ACM sensors show higher tendency occurrence of dew at Sanbonmatsu.

3.4 Evaluation of Dew Condensation using IDW

In the previous section, the atmospheric temperature and relative humidity measured by using sensor for the two bridges, and their results were compared with NMO observatory. Additionally, the evaluation of dew condensation was carried out for the bridges, and the results of dew condensation were compared. The investigation by field measurements revealed that the weather data (temperature and relative humidity) for the three points such as Ooeyousui, Sanbonmatsu, and NMO were different as it was discussed in section 3.3.3. Thus, it is not possible to evaluate the dew condensation as results of temperature and relative humidity from only NMO, it is essential to use IDW or WRF technique to simply obtain the weather data of any arbitrary points.

This section, demonstrates the use and employment of the IDW for the evaluation of dew condensation due to atmospheric temperature and relative humidity.

3.4.1 Comparison of Nagoya Meteorological Observatory with IDW

This section describes, a comparative investigation into the inverse distance weighting (IDW) technique using Nagoya meteorological observatory by applying three points at the Gifu, Tsu, and Hamamatsu meteorological observatories as shown in Fig. 3.17. In this study, the meteorological observatories are used from Japan meteorological agency (JMA). The comparison was conducted for the month of January 2018, the distances of each meteorological observatory and weight factor (w_i) from Nagoya are given in Table

3.3. The main purpose of this comparative study was to confirm the accuracy and certainty of the IDW prior to the commencement of the actual dew condensation evaluation.

The differences in temperature and relative humidity were obtained through a subtraction of the NMO from the IDW data. Subsequently, the mean error and root mean square error of temperature and relative humidity were calculated. As a result, the ME was positive for both temperature and humidity, which means that IDW data for both temperature and humidity are higher compared to the NMO. This occurred because the lower value of temperature and humidity of the NMO were lower in the morning compare to the IDW. The results of the temperature and relative humidity can be seen in Figs. 3.18 and 3.19. The ME and RMSE of the temperature and humidity are listed in Table 3.4. According to the table, the temperature error is almost 0.7 ℃ and the humidity is 6 %, which are nearly the same for flat land as it was discussed in the chapter 2 of the present study. That is, this comparison results fully confirms the accuracy of the IDW. Finally, to summarize the present comparison, it can be stated that, although slight differences exist between the IDW and NMO data their results are quite similar and that the method can be effective.

3.4.2 Observation Value of Temperature and Humidity of Three Interpolation Points of Gifu, Nagoya, and Tsu

This section demonstrates, a quantitative investigation of temperature and relative humidity of three interpolation points of Gifu, Nagoya and Tus meteorological observatories (OM), prior to evaluate the dew condensation of Ooeyousui bridge from these three points as shown in the Fig. 3.20. The main purpose of investigation is to demonstrate the observation values of this three points relatively to each other's. The observation period is January 2018, the geographical information of the points are given in the Table 3.5.

The temperature RMSE is about 0.8 ℃ and the relative humidity is 8 % at Nagoya as compare to Gifu. Similarly, the temperature RMSE is about 1.72 ℃ and the relative humidity is 19 % at Tsu as compare to Gifu. The quantitative investigation clearly revealed that the observation value of temperature and the relative humidity of Gifu and Nagoya MO are significantly similar as compare to Tsu, the reason could be due to similar environment. As it was discussed in section 3.3.3, that value of temperature and relative humidity of each single points are not quite the same, however, the difference in temperature and relative humidity between two observation points can be minimized when the climate similarities increased by proper selection points. In this particular case, Nagoya meteorological observatory is located near to Gifu, and has almost similar weather condition as compare to Tsu that is why the error between Gifu and Nagoya are too small. The comparison results of temperature and relative humidity of the three observation points for the entire month of January are shown in Figs. 3.21 and 3.22.

3.4.3 Evaluation of Dew Condensation at Ooeyousui Bridge

Herein, we describe an evaluation of dew condensation using IDW at Ooeyousui bridge from the Nagoya, Gifu, and Tsu meteorological observatories as shown in Fig. 3.23. The latitude and longitudes, distances

of each meteorological observatory, and weight factor (w_i) from Ooeyousui bridge are given in Table 3.6. The dew-point temperature were calculated from the atmospheric temperature and relative humidity at saturated vapor pressure as it was described in section 3.2. The difference between the girder temperature and dew point temperature became small and continuously increased the tendency of dew condensation from 9:00, 1/8 to 9:00, 1/9, as shown in Fig. 3.24. However, the girder temperature did not fall below the dew point temperature during this period of time, but because the temperature differences are too small at about 0.4 °C, which means both girder temperature and dew-point temperature is almost the same, that the dew condensation could occurred.

Moreover, the evaluation of dew condensation for the entire month of January 2018 for this bridge can be observed from Fig. 3.25. The tendency for the occurrence of dew condensation is high on particular days which is strongly indicative of dew condensation around the bridge. In addition, if we compare the results of evaluation of dew condensation using IDW with an evaluation of the dew condensation using the ACM sensor for this bridge as shown in Fig. 3.14. Both indicates the occurrence of dew condensation during the same period of time, which means similar results from a field observation and IDW method.

3.5 Concluding Remarks

The field measurement was carried out for the Ooeyousui and Sanbonmatsu bridge in the flat and mountainous areas in the Aichi prefecture. The atmospheric temperature and relative humidity of both bridge were obtained using sensors, then their results were compared with Nagoya meteorological observatory. Additionally, an evaluation of dew condensation was conducted for the both bridges using atmospheric temperature /relative humidity, and the ACM sensor. Moreover, the evaluation of dew condensation was performed using IDW to describe specifically the use and employment of the IDW technique, and also the results were compared with field observation. From the above field observation the following summary can be made:

1) The changes in temperature and relative humidity at Ooeyousui and Sanbonmatsu bridge are extremely linked with the changing rate at the Nagoya meteorological observatory, but the value of temperature and relative humidity of these three points (Ooeyousui, Sanbonmatsu, and Nagoya meteorological observatory) are not quite the same. Therefore, an evaluation of dew condensation due to atmospheric temperature and relative humidity of the entire prefecture only from Nagoya meteorological observatory is not suitable. It is necessary to evaluate for each single points using IDW technique.
2) The investigation revealed the lower atmospheric temperature and higher relative humidity at Sanbonmatsu compare to Ooeyousui bridge, this might be due to location of Sanbonmatsu at mountainous area. Therefore, the dew condensation more likely occurred in Sanbonmatsu as compared to Ooeyousui bridge.

3) The evaluation outcome of the dew condensation due to atmospheric temperature and relative humidity when using IDW technique and field measurement were quite similar, and both confirmed the dew condensation at Ooeyousui bridge. Thus, it is concluded that the IDW can be effective.
4) In this study, the evaluation of dew condensation was carried out only at Ooeyousui bridge as a case study using IDW technique to show its employment and confirmed validity. However, the IDW can be applied for the evaluation dew condensation for any arbitrary point as well.

References

Daiichi – kagaku.co.jp,"Humidity calculation 1", https://www.daiichi-kagaku.co.jp/situdo/note/arekore08/.

https://www.nims.go.jp/stx-21/jp/publications/stpanf/pdf/corrosion6.pdf.

Imai, R., Miyasou, T. and Aso, T., (2020)," An evaluation of dew condensation on steel plate girder bridges", Journal of Structural Engineering, Vol.66A, pp.443-451.

JMA, (2018), "Japan Meteorological Agency", https://www.data.jma.go.jp/gmd/risk/obsdl/index.php.

Motoda, S., Suzuki, Y., Shinohara, T., Kojima, Y., Tsujikawa, S., Oshikawa, W., Itomura, S., Fukushima, T. and Izumo, S., (1994), "ACM (Atmospheric Corrosion Monitoring) type corrosion sensor to evaluate corrosively of marine atmosphere", Zairyo-to-Kankyo 43, pp.550-556.

Nagata, K., Naito, R., Yagi, C. and Kitahara., (2016), " Evaluation method of dew condensation of steel girders using weather data", "Journal of Structural Engineering, Vol.62A, pp.796-803.

National institute for materials science. (2004): Weathering steel/ Corrosion analysis.

Shrinks Co., Ltd, "Principle and outline of ACM sensor measurements", https://www.syrinx.co.jp/acm-spec/about-acm.htm.

(a) ACM sensor

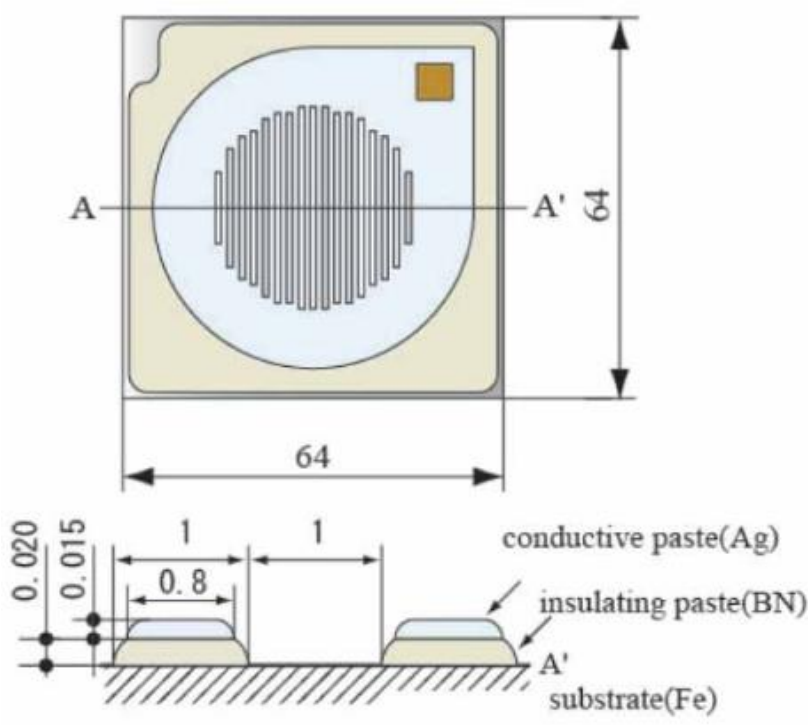

(b) Cross section of the ACM sensor at A-A`

Fig. 3.1 shows the ACM sensor, and its cross section

(a) EL-USB-TC temperature data logger

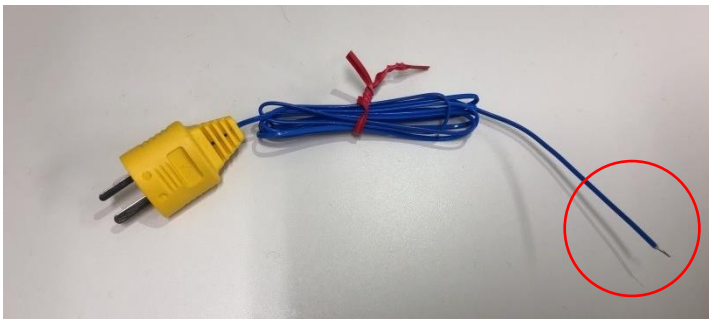

(b) T-type thermocouple

Fig. 3.2 shows the thermocouple used in the field measurements

Table 3.1 Specification of thermocouples

	K type thermocouple
Measurement range	-200 ~ +1350ºC
Accuracy	±1ºC

Fig. 3. 3 Atmospheric temperature and relative humidity sensor

Table 3.2 Specification of atmospheric and relative humidity sensor

	Atmospheric temperature	Relative humidity
Measurement range	-35 ~ +80ºC	0% ~ 100%
Accuracy	±0.5	±3%(20~80%); ±5% max

Fig. 3.4 Location of monitoring bridge

Photo 3.1 Ooeyousui bridge

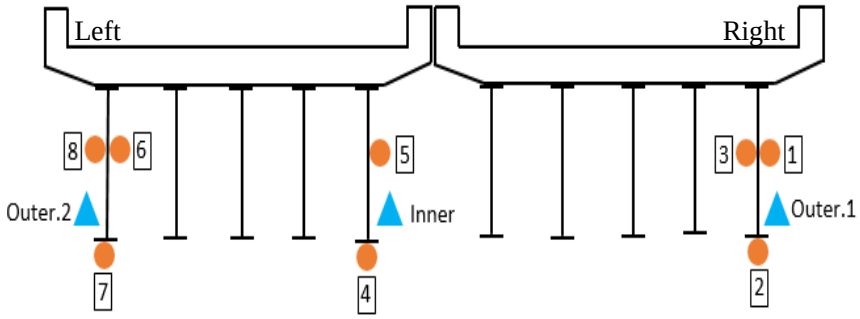

Fig. 3.5 Set position of measuring instrument and cross section of Ooeyousui bridge

Photo 3.2 ACM sensor on the web of girder

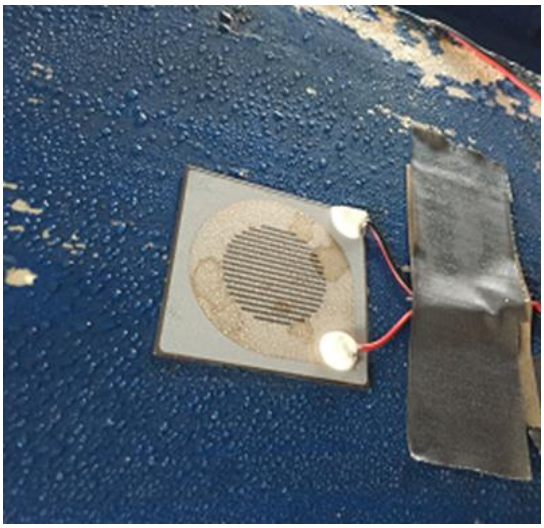

Photo 3.4 ACM sensor on the flange of girder

Photo 3.5 Exterior atmospheric and relative humidity sensor

Photo 3.6 Interior atmospheric temperature and relative humidity sensor

Fig. 3.6 Location of monitoring bridge

Photo 3.7 Sanbonmatsu bridge

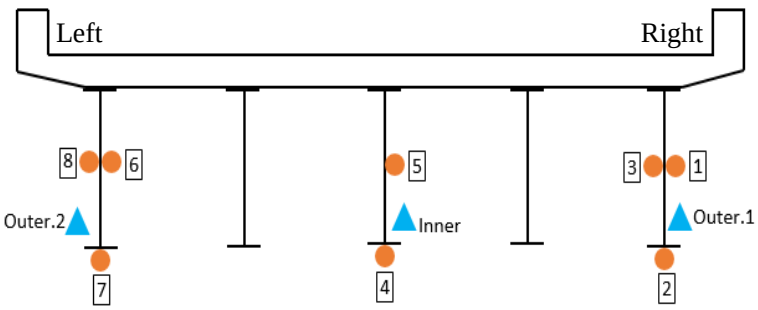

Fig. 3.7 Set position of measuring instrument and cross section of Sanbonmatsu bridge

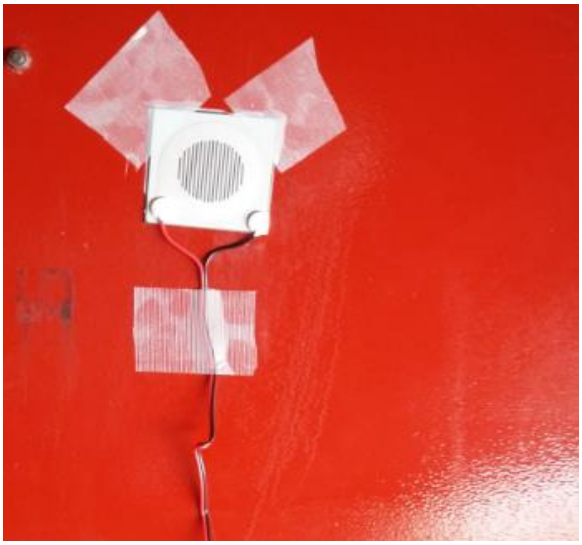

Photo 3.8 ACM sensor

Photo 3.9 Atmospheric temperature and relative humidity

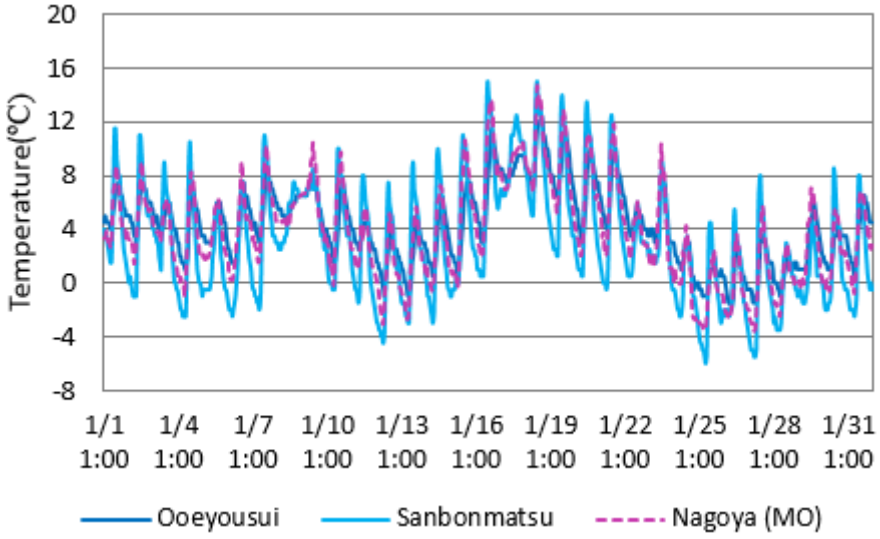

Fig. 3.8 Comparison of temperature of both Ooeyousui and Sanbonmatsu using NMO in January 2018

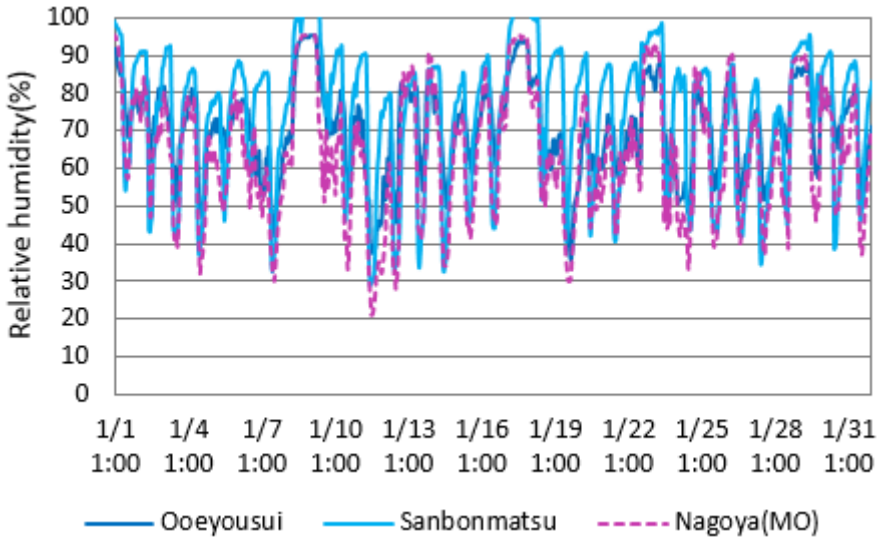

Fig. 3.9 Comparison of relative humidity of both Ooeyousui and Sanbonmatsu using NMO in January 2018

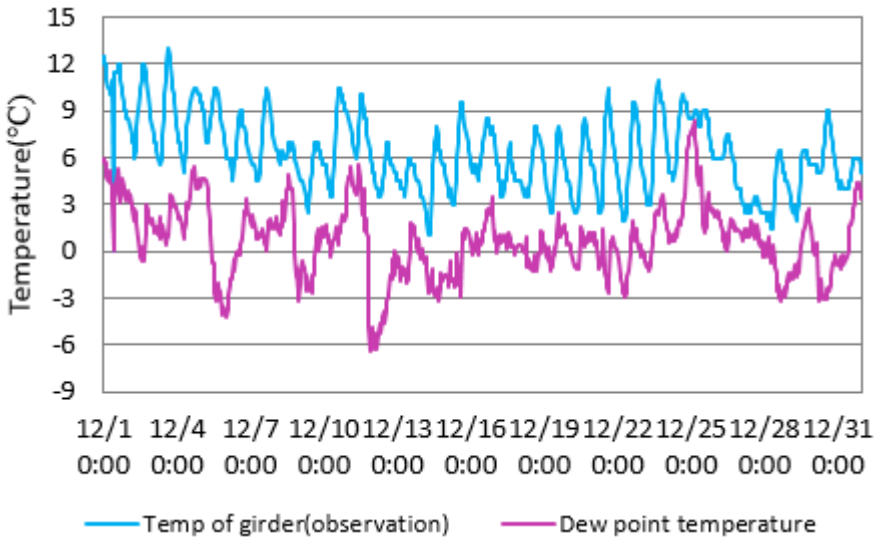

Fig. 3. 10 Evaluation results of dew condensation at Ooeyousui bridge by field measurement for December 2017

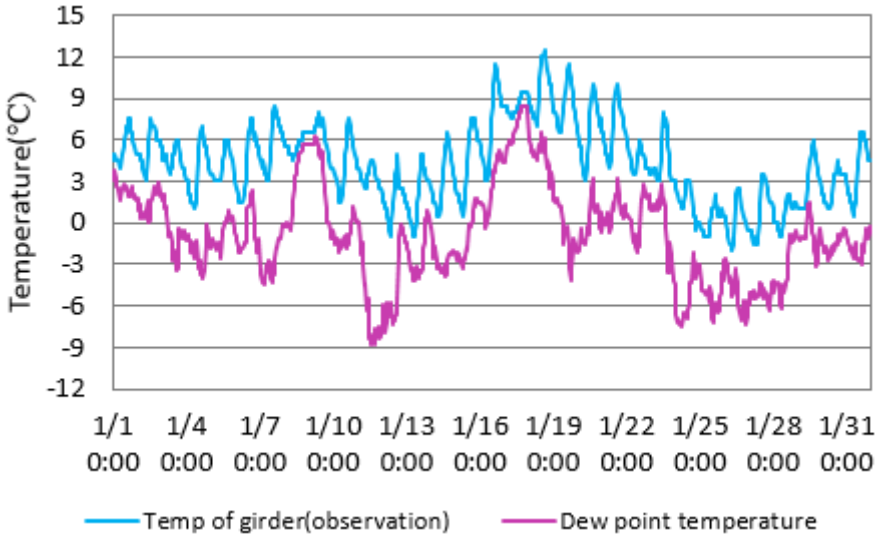

Fig. 3. 11 Evaluation results of dew condensation at Ooeyousui bridge by field measurement for January 2018

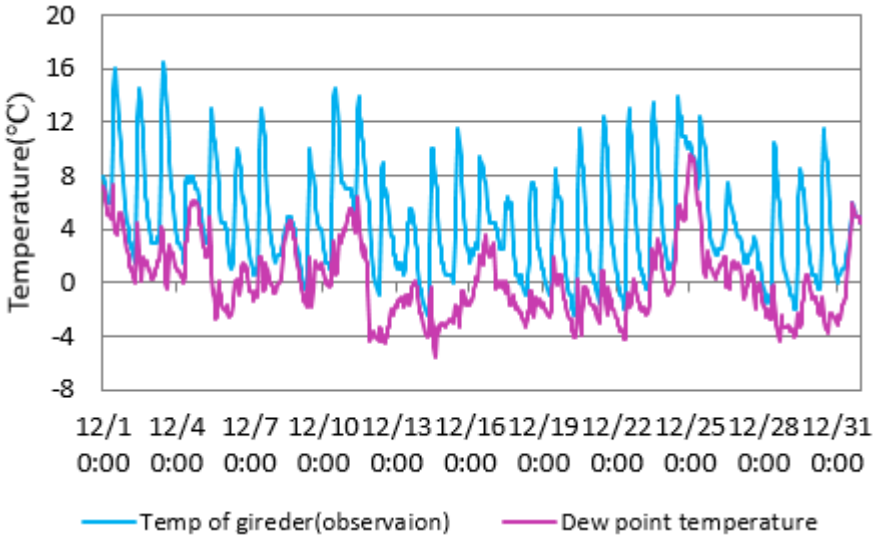

Fig. 3. 12 Evaluation results of dew condensation at Sanbonmatsu bridge by field measurement for December 2017

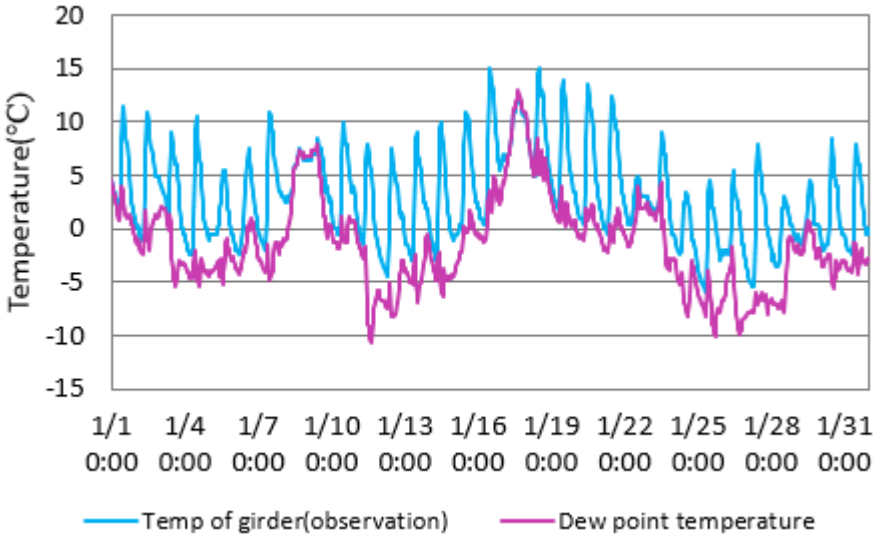

Fig. 3. 13 Evaluation results of dew condensation at Sanbonmatsu bridge by field measurement for January 2018

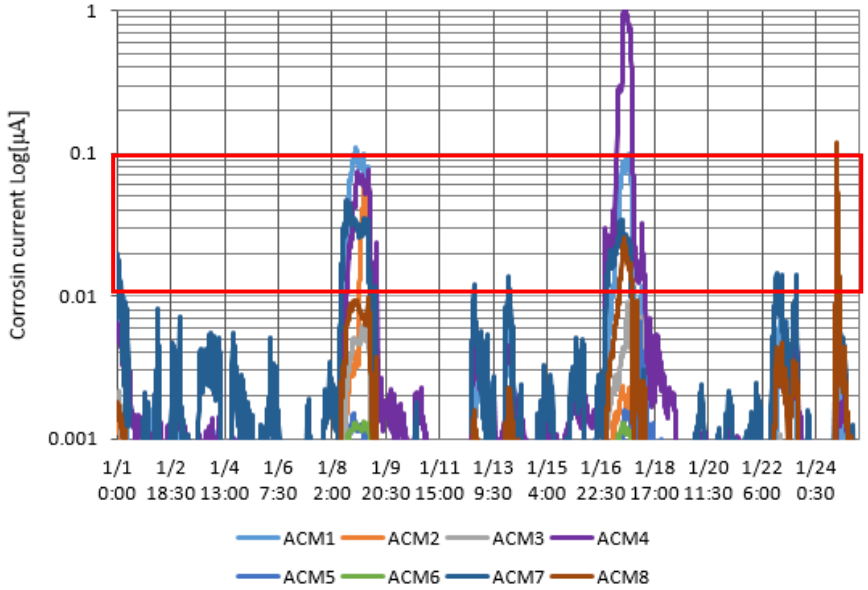

Fig. 3.14 Evaluation of dew condensation at Ooeyousui bridge using ACM sensor

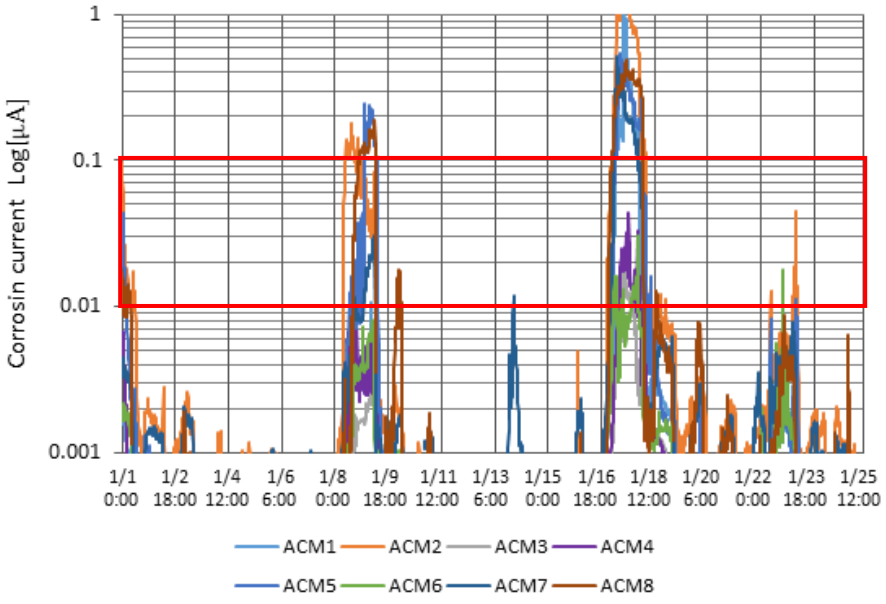

Fig. 3.15 Evaluation of dew condensation at Sanbonmatsu bridge using ACM sensor

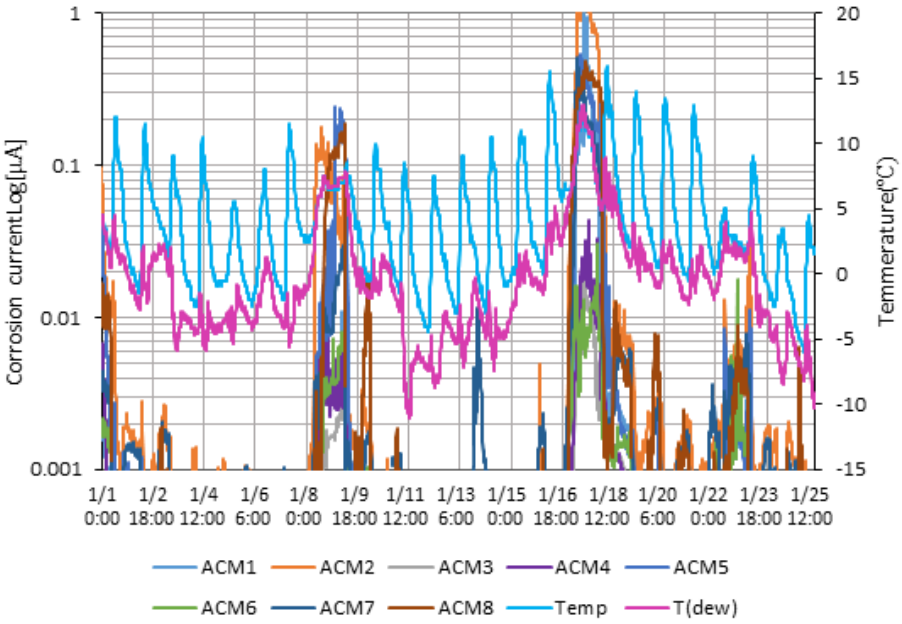

Fig. 3.16 Evaluation result of dew condensation using ACM and temperature/ humidity sensor

Fig. 3.17 Nagoya and its surrounding meteorological observatory with their elevation

Table 3.3 Latitude, longitude, distance and weight factor of each meteorological from Nagoya

Meteorological observatory	Latitude (°)	Longitude (°)	Altitude (m)	Distance (km)	Weight factor (w_i)
Gifu	35.401	136.762	12.7	31.70	0.71
Tsu	34.734	136.520	2.7	63.10	0.81
Hamamatsu	34.754	137.712	45.9	82.30	0.11

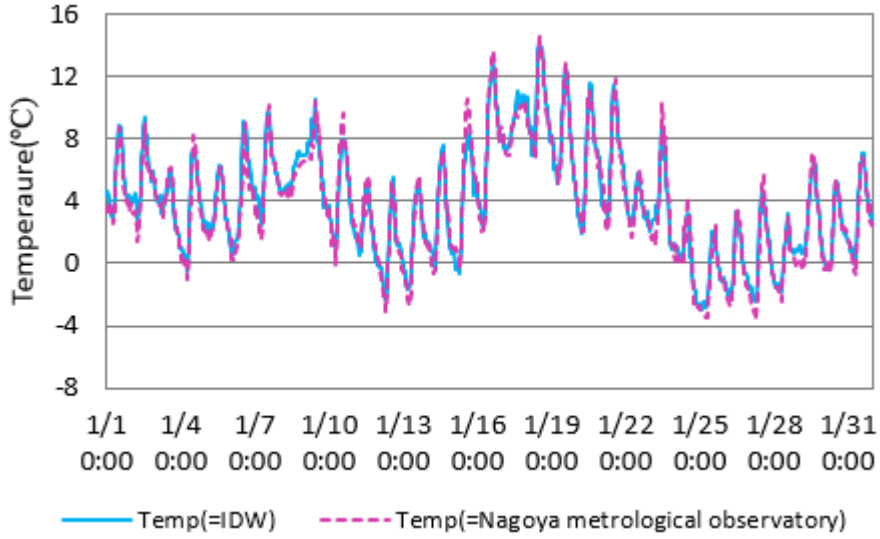

Fig. 3.18 Comparison results of temperature of IDW using Nagoya meteorological observatory

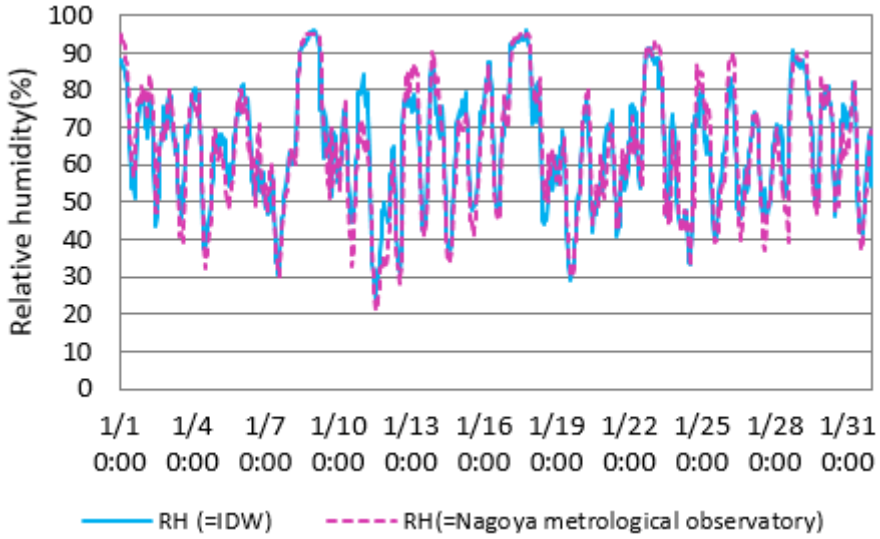

Fig. 3.19 Comparison results of relative humidity of IDW using Nagoya meteorological observatory

Table 3.4 ME and RMSE of temperature and relative humidity

	Temperature(°C)		Humidity (%)	
Meteorological observatory	ME	RMSE	ME	RMSE
Gifu, Tsu and Hamamatsu	0.19	0.72	0.76	6.20

Table 3.5 Geographical information of three meteorological observatories

Station name (weather data)	Latitude (°)	Longitude (°)	Altitude (m)
Gifu	35.401	136.762	12.7
Tsu	34.734	136.520	2.7
Nagoya	35.168	136.965	51.1

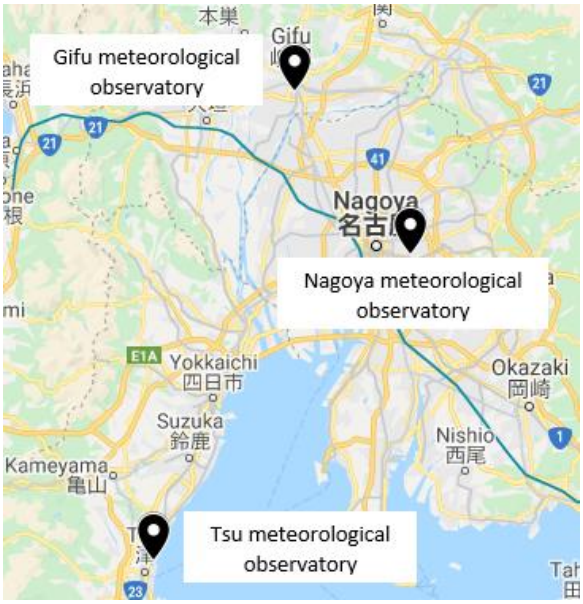

Fig. 3.20 Three interpolation points of Gifu, Nagoya, and Tsu meteorological observatories

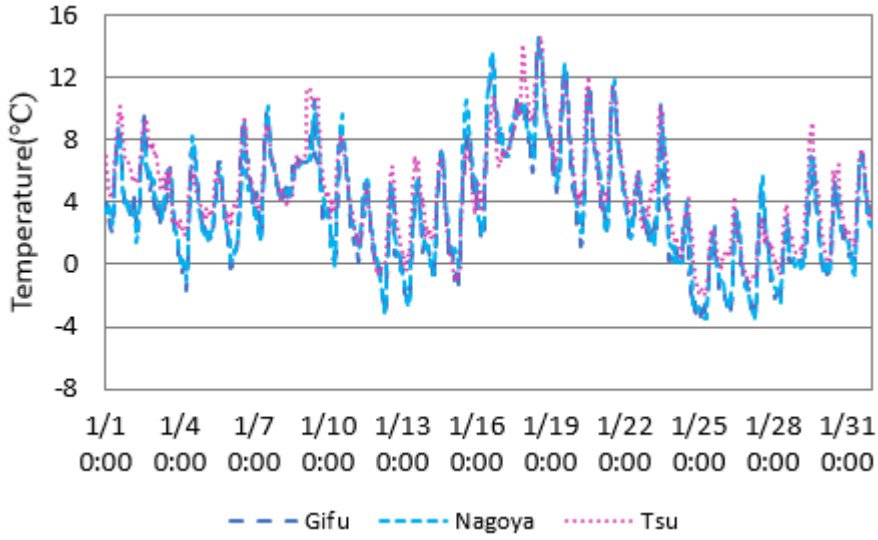

Fig. 3.21 Comparison results of atmospheric temperature of three interpolation points of Gifu, Nagoya, and Tsu

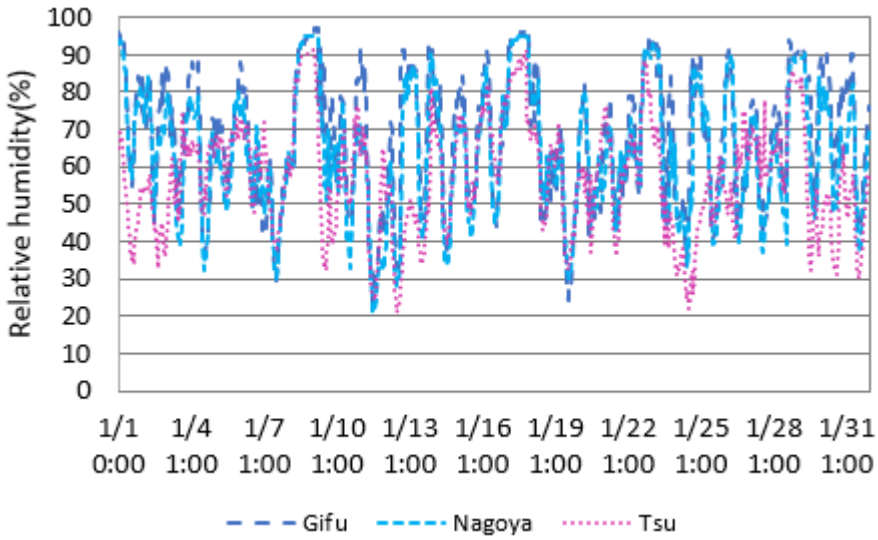

Fig. 3.22 Comparison results of relative humidity of three interpolation points of Gifu, Nagoya, and Tsu

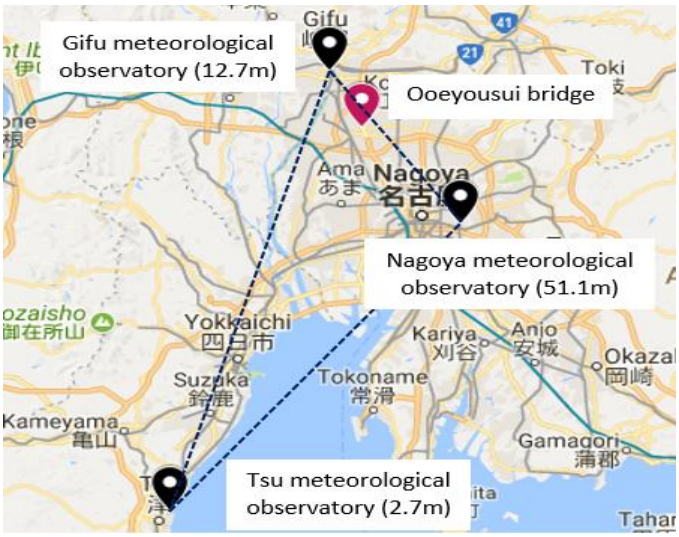

Fig. 3.23 Three interpolation points from the targeted bridge (image generated using Google Maps)

Table 3.6 Latitude and longitude, altitude, distance and weight factor of each meteorological from Ooeyousui bridge

Meteorological observatory	Latitude (°)	Longitude (°)	Altitude (m)	Distance (km)	Weight factor (w_i)
Gifu	35.401	136.762	12.7	10.50	0.79
Tsu	34.734	136.520	2.7	70.20	0.02
Nagoya	35.168	136.965	51.1	21.50	0.19

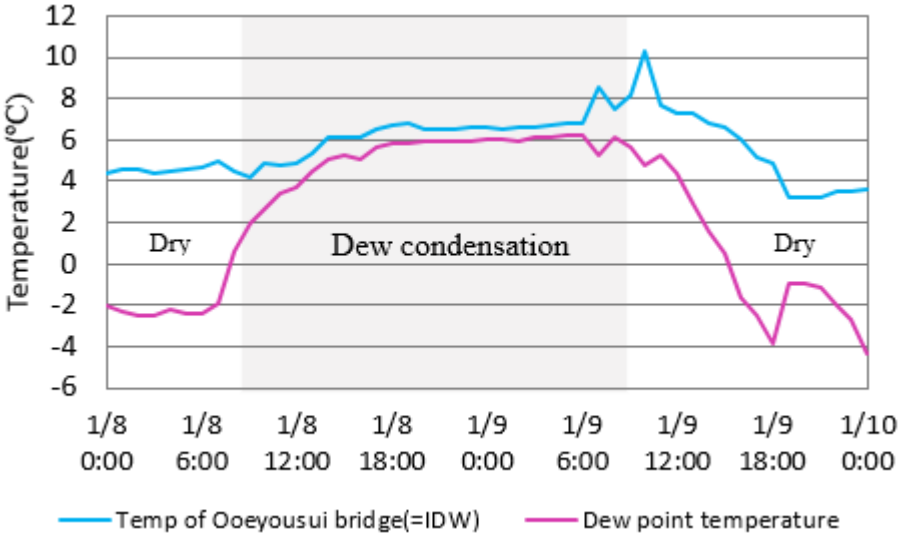

Fig. 3.24 Evaluation results of dew condensation from 00:00, 1/8 to 00:00, 1/10 in January 2018 at Ooeyousui bridge using IDW

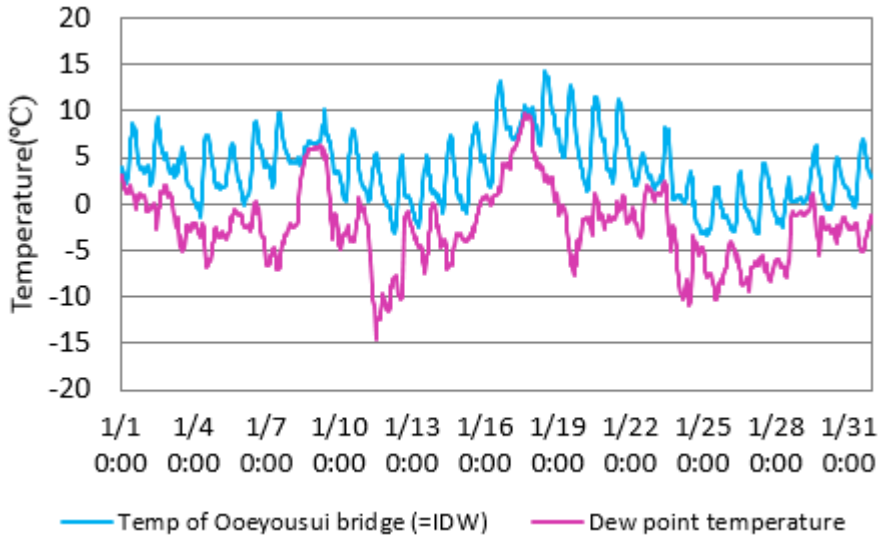

Fig. 3.25 Evaluation results of dew condensation in January 2018 at Ooeyousui bridge using IDW

Chapter 4

Improvement of Accuracy for the Evaluation of Dew Condensation using WRF technique

4.1 Introduction

It is important to accurately evaluate the corrosion environment of steel bridges for its prevention and maintenance (Obata et al., 2011). There are many factors that cause corrosion of steel infrastructures (Noguchi et al., 2017), one of them is being dew condensation due to temperature and relative humidity (Imai et al., 2020). Previously, a simple method was developed for corrosion environment evaluation due to dew condensation using a weather research and forecasting (WRF) numerical weather prediction, and inverse distance weighting (IDW) techniques (Nagata et al., 2016; Rasoli et al., 2019). Then, the dew condensation was investigated quantitatively across Aichi prefecture (Rasoli et al., 2018). The investigation revealed that the WRF has a significant potential to evaluate dew condensation for any arbitrary point without limitation. However, there are no sufficient studies on the improvement of WRF accuracy for the evaluation of corrosion environment.

Principally, the land use is a parameter that describes the land surface properties and it regulates the exchange of heat band momentum between soil and air. Urbanization increases temperature due to land surface change characteristics and deforestation affect the evapotranspiration. As the evaluation of dew condensation is carried out owing to temperature and relative humidity. Therefore, it is necessary to examine the effect of land surface in the model. By default, the WRF model uses land-use data based on the United State Geological Survey (USGS) (Anderson et al., 1976), which may not represent the real land situation in Japan, and might yields inaccurate results to a certain extent. Currently, the more reliable land use data is provided by the Geospatial Information Authority of Japan (GSI), and the digital map can be freely obtained by downloading the national land numerical information from the GIS home page (Geographical information System, 2019), which can be integrated into the WRF simulation model to improve the calculation accuracy.

In this study, initially the default land used data and GSI were integrated into the WRF model separately, subsequently the investigation was conducted, and their results were compared. The investigation outcome of the model, more accurately represented the real situation of Japan based on GSI land use data as compare to USGS, and take into account the land surface change. Also, it was found that the WRF-GSI can improve the accuracy of calculation particularly in the flat area where the land use is being change due to urbanization as compare that of with mountainous areas where the land surface change

is rarely can be occurred. Secondly, a quantitative investigation of dew condensation was carried out across the Aichi and Gifu prefecture based on both WRF-USGS and WRF-GSI land use data, respectively, and also their results were compared. Here, the investigation was conducted for the both Aichi and Gifu prefecture, however the results obtained from the study, are applicable for the entire the country. Finally, this chapter focused on the improvement of accuracy for the evaluation of corrosion environment of steel bridge using WRF technique, with pay attention to the land used data.

4.2 Numerical Modeling

In this study, the weather research and forecasting model is used to calculate the atmospheric temperature and relative humidity for the evaluation of corrosion environment of bridges. Therefore, it is essential to have sufficient knowledge about the WRF model and its employment. This section describes, the modeling approach, model execution process, investigated area with simulation domains, and land-use data.

4.2.1 Model Approach

The WRF model is a mesoscale numerical weather prediction system designed to serve both operational forecasting and atmospheric research needs (Khandaka and Moritmi, 2013). The WRF model development was a collaborative partnership, mainly among the National Center for Environmental Prediction (NCEP), National Center for Atmospheric Research (NCAR), National Oceanic and Atmospheric Administration (NOAA), Forecast System Laboratory (FSL), Air Force Weather Agency (AFWA), Naval Research Laboratory (NRL), Oklahoma University, and Federal Aviation Administration (FAA) (Janjic et al., 2010; Skamarock et al., 2008). This model is capable of creating forecasts using real time data, or idealized atmospheric simulations, and also it serves a wide range of meteorological application across scales from tens thousands of kilometers.

The WRF model is fully compressible and Euler non-hydrostatic model with a terrain-following hydrostatic pressure coordinates. It calculate winds (winds components u, v, and w), the perturbation temperature, perturbation geopotential, and the perturbation surface pressure of dry air. The model also optionally provides other variables such as turbulent kinetic energy, the water vapor mixing ratio, rain/snow mixing ratio, and cloud water/ ice mixing ratio. The different WRF options can be combined in several ways. The model has different parameterization for microphysics, long wave-radiation, short wave-radiation, cumulus, surface layer, planetary boundary layer (PBL), and land surface parameter, as physical options. Moreover, the model can also be set as either a one-way, two-way nesting or a moving nest model, these option allow the model to be versatile for both research and operational application.

4.2.2 Governing Equation

The WRF model takes the terrain-following hydrostatic pressure vertical coordinate system devised by Laprise (1992). This vertical coordinate system also can be referred to as the traditional sigma or vertical

coordinate system as shown in Fig. 4.1. The terrain-following hydrostatic pressure vertical coordinate is denoted by η and is defined by the following Eq. (4.1) and Eq. (4.2).

$$\eta = \frac{(p_h - p_{ht})}{\mu_d} \tag{4.1}$$

$$\mu_d = p_{hs} - p_{ht} \tag{4.2}$$

where μ_d is the mass of the dry air in the column, p_h is the hydrostatic component of the pressure bounded by the top and bottom layers p_{ht} and p_{hs} respectively. The value of η varies within range of 0 at the top layer and 1 at the bottom layer. Then, the terrain-following coordinate system can be combined with vertical height (z), which given by Eq. 4.3. In the equation g is the acceleration of gravity and ρ_d is density.

$$\mu(x, y)\Delta\eta = \Delta p_h = -g\rho_d \Delta z \tag{4.3}$$

The Euler flux equation including the effect of moisture in the atmosphere can be obtained from the η coordinate system (Skamarock et al., 2008) as following:

$$\partial_t U + (\nabla \cdot V_u) + \mu_d \alpha \partial_x p + \left(\frac{\alpha}{\alpha_d}\right) \partial_\eta p \partial_x \varphi = F_U \tag{4.4}$$

$$\partial_t V + (\nabla \cdot V_V) + \mu_d \alpha \partial_y p + \left(\frac{\alpha}{\alpha_d}\right) \partial_\eta p \partial_y \varphi = F_V \tag{4.5}$$

$$\partial_t W + (\nabla \cdot V_w) - g\left[\left(\frac{\alpha}{\alpha_d}\right) \partial_d p - \mu_d\right] = F_W \tag{4.6}$$

$$\partial_t \mu_d + (\nabla \cdot V) = 0 \tag{4.7}$$

$$\partial_t \varphi - \mu_d^{-1}\left[(\mathrm{V} \cdot \nabla_\varphi - gW)\right] = 0 \tag{4.8}$$

$$\partial_t \Theta + (\nabla \cdot \mathrm{V}\theta) = F_\Theta \tag{4.9}$$

$$\partial_t Q_m + (\nabla \cdot V q_m) = F_{Qm} \tag{4.10}$$

$$\partial_\eta \varphi = -\omega \alpha_d \mu_d \tag{4.11}$$

$$\mathrm{p} = p_0 (R_d \theta_m / p_0 \alpha_d)^\gamma \tag{4.12}$$

where Eq.4.4 and 4.5 represent the horizontal momentum equation, Eq. 4.6 denotes the vertical momentum, Eq. 4.7 represent continuity equation, Eq. 4.8 is the geopotential height equation, Eq.4.9 and Eq.4.10 is the thermodynamic equation, Eq.4.11 represent the hydrostatic equilibrium equation, and Eq.4.12 is the equation of state.

In the above equations u, v, and w are the wind components in the x, y, z directions,$\mathrm{U} = \mu_d u$ $\mathrm{V}=\mu_d v$, $\mathrm{W} = \mu_d v$ are the horizontal and vertical momentum, $\Theta = \mu_d \theta$ is flux temperature, θ is potential temperature, $Q_m = \mu_d q_m$ is water flux with q_m mixing ratios for water vapor, cloud, rain, ice and etc. F is represent forcing terms arising from model physics, turbulent mixing, spherical projection and the earth's

rotation,α_d represent the inverse density of the dry air ($1/\rho_d$) and α is the inverse density of full parcel density $\alpha = \alpha_d(1 + q_v + q_c + q_r + q_i + \cdots)^{-1}$. Also in these equations q are the mixing ratios (mass per mass of dry air) for water vapor, cloud, rain, ice, etc., γ is the ration of the heat capacity for dry air, R_d is the gas constant for dry air P_0 is a reference pressure (=1000hPascal), and $\theta_m = \theta\left[1 + \left(\frac{R_v}{R_d}\right) q_m\right] \approx \theta(1 + 1.61q_m)$.

4.2.3 WRF Execution Process

As shown in Fig. 4.2, the WRF preprocessing system (WPS) is used to prepare a domain (land area) for WRF, and also the model data have to be initialized by the WPS before it can be fed into the WRF system. The WPS consists of three independent programs: geogrid, ungrib, and metgrid. The purpose of geogrid is to define the simulation domains (analysis region, analysis period, and analysis center point) and interpolate the various terrestrial data sets to the model grids. The geographical data comes in file formats that are not readable by the WRF, thus, the WPS is capable of convert these types of data into a readable format by running preprogram (Wang et al., 2011). The ungrib program reads the GRIdded Binary (GRIB) files, degribs the data (extracted weather data from GRIB files for the defined model), and write the data into a simple format, called the intermediate file format. The metgrid program horizontally interpolates the intermediate format of the meteorological data extracted by the ungrib program into the simulation domains defined by the geogrid program. The meteorological data is prepared now for the REAL program (Wang et al., 2011). This program is responsible for initializing the data that is going to be used as the initial and lateral boundary condition. That is to say, once the REAL program has prepared the data, it can be fed into the WRF model. After editing the parameters, the initial value and boundary data are generated by running real.exe. The results file are obtained by executing the wrf.exe. Finally, the atmospheric temperature and relative humidity are obtained from the results files using the Griads Analysis and Display System (GrADS) as the numerical data.

4.2.4 Tow-Way Nesting

As shown in Fig. 4.3, a two-way nesting technique is employed normally when multiple model domain with different resolution are expected to run at the same time and exchange data between each other. In a two-way nested model, the parent domain provided boundary values for the nested domain, on the other hand, the nested domain provides down-scaled data back to its parent (wang et al., 2011). The downscaled data provided to the parent is often beneficial as it provides the coarse domain with information about small-scale process that it wouldn't be able to capture. To make sure that the coarse and fine grids are consistent at coincident points, the WRF check the reference state of each prognostic variable within the model. If there are some discontinuities present at the lateral boundaries, the model makes the necessary adjustment to ensure that stability within the model maintained (Shamrock et al., 2008). In this study, the nesting technics has been used to make the fine resolution for the targeted area. Also it is preferred that the nesting ratio should be odd number.

4.2.5 Weather Data Used in the Model

In this study, the initial and lateral boundary conditions for the meteorological components were taken from (NCEP), and FNL (Final) Operational global analysis data has been prepared at every six hours interval with a special resolution of $1.0^0 \times 1.0^0$ (NCAR, NCEP FNL Operational model global tropospheric analysis, continuing from 1999). This data is provided by the Global Data Assimilation System which is obtained from the collection of observational data of Global telecommunication system, and many other sources. Moreover, the FNL parameters include surface pressure, sea level pressure, geopotential height, temperature, sea surface temperature, soil value, ice cover, relative humidity, U- and V- winds, Vertical motion, skin temperature, vorticity and ozone. In this study, the WRF model used to reanalyze the past weathers data.

4.2.6 Investigated Area and Simulation Domains

The adapted WRF model had three nested domains in Aichi Prefecture, with size of 1,000 km x 1,000 km, 300 km x 300 km, and 100 km x 100 km, from the coarser to the inner most nested domain, respectively. The nested domain were defined using a Mercator projection as shown in Fig. 3.4. The domain setting and configuration options are listed in Table 3.1. The initial and lateral boundary conditions were taken from the (NCEP), and the FNL (final) Global Analysis data were available at 1° resolution and six hour interval. In this study, the WRF model was adopted for Gifu Prefecture as well, the domain setting and configuration options considered similar to Aichi prefecture. Here, the investigation was conducted for both Aichi and Gifu prefecture, however the results obtained from this work is applicable across the country.

4.2.7 Land Use Data

Land use is a very important parameter that describes the land surface properties including modification due to human activities. It regulates the exchange of heat and momentum between soil and air, which in numerical models determine the meteorological magnitudes near the surface (Clarke et al., 20120; Cheng and Byun, 2008; Pineda et al., 2004). Some studies show that the twine process of urbanization and deforestation can change land surfaces properties. Urbanization increases the temperature due to change in land surface characteristics, such as increasing paving, rooftop, building, and other urban infrastructures. Meanwhile, deforestation affect evapotranspiration process (Yi Change et al., 2013; Samanta et al., 2011). As the evaluation of corrosion environment steel bridges owing to atmospheric temperature and relative humidity is discussed in this chapter, it is necessary to examine the effect of land use in our simulation.

Numerous studies have been conducted to enhance the performance of air quality and meteorological models, and it has been confirmed that the surface heterogeneity plays a key role in atmospheric modeling. Thus, regularly updating, and accurately representation of the land use change can be considered an important subject to maintain the quality issue in the modeling (Cheng et al., 2013; Civerolo et al., 2007; Lam et al., 2006). Also, it is considered to increase the model grid resolution for the complex terrain with abrupt slopes (Arnold et al., 2012). This provide the advantage of better prediction of

magnitude such as atmospheric temperature, relative humidity, and wind speed. However, most of default land use datasets don't have the finer resolution below 1 km, and it is required for adapting new land use datasets in the model.

4.2.8 Land Use Classification

This section briefly describes the differences between the land use and land cover based on their definition. Land cover refers to the state or physical appearance of the land surface such as forest, grassland, wetlands, croplands, bare soil, exposed rock…etc. while, land use refers to the specified purpose of land from human perspective like; extensively or intensively, residential, commercial services, for development or conservation (Burian et al., 2002). The present study doesn't focus on differentiation between those two definitions, it is considered the whole data as land- use, although it is significantly related to the land cover, because the variables are called land-use in the WRF numerical prediction model, and there no distinction is mad. In this study, two sets of land-use data are employed in our WRF simulation, which consist of USGS and GSI, and their details are discussed as flowing.

As shown in Table 4.2 and 4.3, the currently available USGS land use data contain 25 categories and have resolution of roughly 1 km, used by default. This is the oldest and most widely used global land cover datasets based on the global land cover characterization (GLCC) that was created by the US Geological Survey, the University of Nebraska-Lincoln, and the European Commission`s Joint Research Center. The 1-km advanced very high-resolution radiometer 10-days normalized difference vegetation index composites spanning the period from April 1992 through March 1993 (Irvem and El-Sadek., 2014). These data are not updated regularly, although the national land cover datasets of USGS are updated, it covers the United States only (MRLC, 2020). The land-use categories are characterized by the physical parameters such as; the roughness length, thermal inertia, soil moisture availability, albedo, surface heat capacity, and surface emissivity. In addition, in this study, the GSI land use data were used in simulation model. However, it contains 12 land use classifications that need to be remapped (Obata and Murakami. 2014) to corresponding USGS type as shown in Table 4.3. The GSI land use data from the year of 2009 was employed to the model, these data are updated regularly.

4.3 Evaluation of Dew Condensation

Firstly, the comparative investigation of land use data based on USGS and GSI was carried out for Aichi and Gifu prefecture. Subsequently, an evaluation of dew condensation as a results of atmospheric temperature and relative humidity were conducted for the both prefectures respectively. The evaluation method, and its mathematical procedure were demonstrated in chapter 3.

4.3.1 Comparison of USGS and GSI Land Use Data in Aichi Prefecture

The comparison of USGS and GSI land use data was carried out using WRF model to examine the land use distribution situation. Fig. 4.5 shows the land use type based on USGS classification after running WRF

model in Aichi prefecture, the domain size, investigation area, domain setting and its configuration options are described in section 4.2.6. Based on the USGS land use data, almost the entire analysis domain, except the east part of the target domain, is classified as Cropland/Grassland Mosaic, and Mixed Shrubland/Grassland, which is outdated, and does not take into account urbanization over the recent decades, as the analysis domain covers the Nagoya city and Nagoya port which are urban areas.

Fig. 4.6 demonstrates the land use type according to GSI land use data, when the new data are integrated into the WRF model instead of default land use (USGS). The wider urban area has been accurately identified along with, industrial area including well distribution of irrigated cropland and forest. Further, if the USGS and GSI land use distribution are compared with the actual map, as shown in Fig. 4.7, it can be seen clearly, that WRF-GSI results are more similar to the actual map and confirms the accuracy of GSI land use when compared to WRF-USGS, thus accurately representing the current land situation in Japan. Additionally, this comparison also shows that mapping of GSI land use to USGS has successfully been done and completely confirmed by the actual map.

The comparison result between USGS and GSI land use data as shown in Fig.4.5 and 4.6 explicitly demonstrates that the land use change due to urbanization, and industrialization. However, the right- hand side of both Fig. 4.5 and 4.6, which are mountainous and covered with forest, are quite similar, and remain unchanged. This is because of the mountainous areas are rarely exposed to the land surface changes due to urbanization or other human activities as compared to other land types. Therefore, consideration of accurate land use data for WRF simulation domain as a statics geographical input while running WRF model is required.

Finally, this comparison was performed for a quite small WRF domain around Nagoya Port to determine the land use situation based on the USGS and GSI classification. In the next section the, the evaluation of dew condensation will be conducted directly and the results will be described quantitatively.

4.3.2 Evaluation of Dew Condensation in Aichi Prefecture

The evaluation of dew condensation due to the atmospheric temperature and relative humidity in Aichi Prefecture is discussed. The dew-point temperatures were obtained by the third region analysis domain of WRF at center point with 0.05° intervals, from the innermost domain, which covered the entire prefecture within the range of 34.6° to 35.35° latitudes and 136.75° to 137.75° longitudes. Additionally, in this analysis, the steel girder temperature was assumed to be equal the atmospheric temperature and was obtained by the WRF technique. The mathematical calculation of the dew-point temperature and dew condensation is described in chapter 3. In the given figures of the prefecture, the vertical axis indicates the latitude and the horizontal axis indicates the longitude. Each point within this area is identified based on the latitude and longitude. Each coordinate pair of atmospheric temperature and relative humidity was obtained by the WRF technique. Further, the dew-point temperature was calculated from the saturated vapor pressure within the analysis domain. The dew condensation results were obtained by subtracting the

atmospheric temperature from the dew - point temperature, it is considered dew if the difference is greater than zero.

Finally, the frequency of dew condensation, which occurred during January 2017, was quantified as shown in Fig. 4.8 and Fig. 4.9 based on USGS and GSI land use data, respectively. The numbers denote the dew frequency that occurred over the period of one month. Additionally, the evaluation results of dew condensation for February 2017 can be observed in Fig. 4.10 and 4.11 based on USGS and GSI land use data, respectively. The evaluation was conducted during winter as; the possibility of dew is higher during this seasons.

4.3.3 Comparison of Dew Condensation in Aichi Prefecture

A comparison of dew condensation over the period of one month based on WRF-USGS and WRF-GSI is presented in this section. The dew condensation occurred normally across the Aichi Prefecture as shown in Fig. 4.8 and 4.9. Additionally, from the evaluation results, it is clear that although the occurrence tendency of dew condensation in Fig. 4.8 and 4.9 is quite similar, it is still not exactly the same. The frequency of dew condensation decreases when using WRF-GSI land use, as seen in Fig. 4.9, compared to WRF-USGS, as seen in Fig. 4.8. The counted reduced number reached almost 137 times in the entire prefecture. Particularly, the dew condensation frequency reduces significantly where the urban area has increased due to expenses compared to other type of lands, as indicated by the blue colored in the corresponding figures.

Furthermore, Fig. 4.10 and 4.11 demonstrate the comparison of dew condensation based on WRF-USGS and WRF-GSI during February, respectively. As seen in the figures, the dew condensation frequency reduces when using GSI land use as compares to USGS, especially in the western region of the prefecture. The behavioral change of dew condensation is quite similar to the comparison results of Fig. 4.8 and 4.9, respectively. This might be due to urbanization that increases the atmospheric temperature; and decreases the relative humidity. Thus, increasing the temperature when relative humidity decreases, also leads to a decrease in the dew condensation.

Finally, the comparison results of Fig. 4.8 and 4.9 during January 2017, and Fig 4.10 and 4.11 during February 2017 show that the dew condensation frequency can be changed when integrating WRF-GSI instead of using the default land use data into the WRF model.

4.3.4 Comparison of USGS and GSI Land Use Data in Gifu Prefecture

The comparative investigation of USGS and GSI land use data were conducted for Gifu prefecture using WRF model. The main purpose of this investigation is to see the difference in land distribution before and after employment of GSI. According to Fig. 4.12, the entire analysis domain is classified as forest, Cropland/Grassland Mosaic, Savanna, and Mixed Shrubland/Grassland based on USGS land use. However, as major part of the prefecture is covered with forest. Fig. 4.13 shows the land distribution after employing the GSI land use data in the model. The wider urban area has been accurately identified in the south part of the prefecture, but still the major part is classified as forest area. If we compare both Fig. 4.12 and 4.13

with actual map, as shown in Fig. 4.14, it seen that the WRF-GSI results are more similar to actual map compare to WRF-USGS. Although, there exist slight differences between Fig. 4.12, Fig. 4.13 and 4.14, still the major areas are classified as forest and similar. Hence, it is concluded that Gifu prefecture is almost totally covered with forest.

4.3.5 Evaluation of Dew Condensation in Gifu Prefecture

In this section, the evaluation results of dew condensation are demonstrated for the Gifu Prefecture. The atmospheric temperature and relative humidity were obtained from the third region analysis domain (inner most domain) using the WRF technique for, the analysis domain located within the range of 35°. 25° – 36.45° latitude and 136.3° – 137.6° longitude. The dew- point temperature was calculated at the center point with 0.05° intervals, and the evaluation was conducted during January and February 2017. The main purpose of this evaluation was to examine the dew condensation, and sufficiently describe all the aspects of dew occurrence. Gifu Prefecture is mountainous and almost covered with forest. The land use type and surface characteristics of Gifu Prefecture are completely different from Aichi Prefecture.

The evaluation of dew condensation was carried out across Gifu Prefecture. The study revealed that, the dew condensation occurred the entire the prefecture as shown in Figs. 4.15 and 4.16 for the month of January 2017 and Fig. 4.17 and 4.18 during February based on USGS and GSI respectively. Secondly, dew occurrence tendency in this prefecture is high. Further, dew frequency can vary for each single point and might depend on temperature and relative humidity of the coordinate points. From Fig. 4.17, it is clear that the dew frequency is slightly higher in WRF-USGS as compared to the dew frequency when using WRF-GSI during January, as shown in Fig. 4.18. Similarly the frequency of dew condensation is higher based on the WRF-USGS during February as shown in Fig. 4.17 compare to the frequency number of dew based on WRF-GSI as shown in Fig. 4.18. Although, slight differences exists, but it is extremely minor which can be ignored. As Gifu is a mountainous prefecture and covered with forest, the evaluation results of the dew are quite identical when using WRF-USGS and WRF-GSI. Thus, it can be concluded that for mountainous areas, the WRF-USGS can be used for accurate and easy evaluation of dew condensation.

4.3.6 Comparison of Dew Condensation in Aichi and Gifu Prefecture

The comparison of dew condensation, conducted during January 2017, is presented from different points of view of the prefecture in this section. The main purpose of this comparison is to see the impact of land use on the quantitative evaluation of dew condensation in different prefectures. The evaluation results of dew for Aichi Prefecture are described in section 4.3.2 ~ 4.3.3. As indicated in Figs. 4.8 and 4.9 for the month of January, where dew was overestimated when using WRF-USGS in comparison to WRF-GSI land use. From this comparison we know that the behavioral changes (increasing or decreasing) of dew condensation are linked to the change of land use type to a certain extent.

With respect to dew condensation in Gifu Prefecture, as indicated in section 4.3.5, the evaluation outcome of dew based on WRF-USGS and WRF-GSI is almost the same as shown in Figs. 4.15 and 4.16

for the month of January 2017, respectively. Moreover, the tendency of dew condensation looks higher in Gifu than in Aichi Prefecture, because this prefecture mountains ranges that are mostly covered with forest.

Finally, it can be clearly stated that for mountainous areas like Gifu, the occurrence tendency of dew is higher. Further, although the default land use is quite suitable and simple, the GSI land use also can be utilized for the accurate evaluation of dew condensation.

4.4 Concluding Remarks

The improvement of accuracy for the evaluation of dew condensation was investigated using WRF technique. As the evaluation of dew condensation due to atmospheric temperature and relative humidity was discussed using WRF model in this chapter, thus, it is necessary to consider the effect of land use data into the simulation model, because the urbanization increases temperature due to land surface characteristics and deforestation affect the evapotranspiration. Land use has a crucial important role that demonstrates the land surface properties and its modification owing to human activities, the exchange of heat and moment between soil and air can be regulated through land use parameters as well. In this study, the GSI and USGS land use data were employed into the model and their results were compared.

The investigation revealed that the default USGS data currently utilized in WRF modeling system, classify most of the land use type as Mixed Shrubland/Grassland; and Cropland/Grassland Mosaic. It means, the USGS data partially misrepresents the land use in the analysis domain, whereas the GSI data accurately reflects the recent development of urban structures, industrial/ commercial, and forest as well as the distribution of cropland as it was described in section 4.3.1. Further, the evaluation of dew condensation based on WRF-USGS and GSI were conducted for both Aichi and Gifu prefecture, and their results were compared. From the above study the following summary can be made:

1) The default USGS data currently utilized in WFR partially misrepresent the real situation of land in Japan, whereas the GSI data is more accurate, and take into account the land use change due to urbanization and other related activities.
2) For evaluation of the corrosion environment of steel bridges with the use of the WRF technique, for mountainous areas, USGS land use data can be used without any changes. However, for urban areas the GSI land use data should be used.
3) The GSI land use data modified and integrated into the model. The modification process of GSI land use data to USGS was described in this chapter, and the validity of the GSI land use data was confirmed using real map.

References

Anderson, J.R., Hardy, E.E., Roach, J.T. and Witmer, R.E., (1976), “A land use and land cover classification system for use with remote sensor data”, Geological Survey Professional Paper 964, U.S. Government Printing Office.

Arnold, D., Morton, D., Schicker, I., Seibert, P., Rotach, M., Horvath, K., Dudhia, J., Satomura, T., Muller, M., Zangl, G. and others.,(2012), " High resolution modelling in complex terrain", Report on the HiRCoT Workshop, Vienna, 21-23 February.

Burian, S.J., Broun, M.J. and McPherson, T.N., (2002), "Evaluation of land use/land cover datasets for urban watershed modeling", Water Science and Technology, Vol.45, N0.9, pp. 269-276.

Cheng, F.Y. and Byun, D.W., (2008), "Application of high resolution land use and land cover data for atmospheric modeling in the Houston-Galveston metropolitan area", Part 1: Meteorological simulation results, Atmospheric Environment, Vol.42, No.33, pp.7795-7811.

Civerolo, K., Hogrefe, C., Lynn, B., Rosenthal, J., Ku, J. Y., Solecki, W., … and Kinnyey, P., (2007), " Estimating the effects of increased urbanization on surface meteorology and ozone concentrations in the New York City metropolitan region", Atmospheric environment, Vol. 41, No.9, pp.1803-1818.

Clarke, S.G., Zehnder, J.A., Loridan, T. and Grimmond, C.S.B., (2010), "Contribution of land use change to near-surface air temperatures during recent summer extreme heat events in the Phoenix Metropolitan area", American Meteorological Society, pp.1649-1664.

GIS home page, (2019), "National land numerical information download services", http://nlftp.mlit.go.jp/ksj.

GSI, (2019), "Geospatial Information Authority of Japan", http://www.gsi.go.org.

Imai, R., Miyasou, T. and Aso, T., (2020), "An evaluation of dew condensation on steel plate girder bridges", Journal of Structural Engineering, Vol. 66A, pp. 443-451 (in Japanese).

Janjic, Z., Gall, R. and Pyle, M.E., (2010), "Scientific documentation for the NMM solve", National Center for Environmental Prediction Office, NCEP. NCAR Tech. Note NCAR/TN-475+SR, 54pp.

Khandar, M.H.A. and Moritomi, H.,(2013), "Numerical simulation for regional ozone concentration: A case study by weather research and forecasting/ chemistry (WRF/Chem) model", International Journal of energy and environment, Vol.4, No.6, pp.933-954.

Lam, J.S.L., Lau, A.K.H., and Fung, J.C.H., (2006), "Application of refined land-use catagories for high resolution mesoscale atmospheric modelling", Boundary-layer meteorological, Vol.119, No.2, pp. 263-288.

Laprise, A., (1992), "The Euler equations of motion with hydrostatic pressure as a independent variable", Mon.Wea.Rev, pp. 197-207.

MRLC, "Multi-Resolution Land Characteristics (MRLC) Consortium", https://www.mrlc.gov/.

Nagata, K., Naito, R., Yagi, C. and Kitahara, T., (2016), "Evaluation method of dew condensation of steel girders using weather data", Journal of Structural Engineering, Vol.62A, pp.796-803 (in Japanese).

NCAR, "NCEP FNL Operational model global tropospheric analysis, continuing from 1999", https://rda.ucar.edu/datasets/ds083.2.

Noguchi, K., Shirato, H. and Yagi, T., (2017), “Numerical evaluation of sea salt amount deposit on bridge girder”, Journal of Bridge Engineering, Vol.22, No.7.

Obata, M. and Murakami. (2014), “Observation of sea salt particles and its numerical simulation as estimation of corrosive environment”, Journal of Structural Engineering, Vol.60A, pp.596-604 (in Japanese).

Obata, M., Watanabe, Y., Goto, G.T.LI., and Goto, Y., (2011), “Prediction of adhered behavior of sea-salt particles on bridge girder”, Procedia Engineering, Vol.14, pp.1043-1050.

Pineda, N., Jorba, O., Jorge, J. and Baldasano, J.M., (2004), “Using NOAA AVHRR and SPOT VGT data to estimate surface parameters: application to a mesoscale meteorological model”, International Journal of Remote Sensing, Vol. 25.No.1, pp. 129-143.

Raoli, Z., Nagata, K., Miyawaki, Y. and Kitahara, T., (2019), “Study on evaluation of corrosion environment on steel bridges using inverse distance weighting method”, Journal of Structural Engineering, Vol. 65A, pp. 479-491.

Rasoli, Z., Nagata, K. and Kitahara, T., (2018), “Monitoring of corrosive environment focusing on dew condensation in steel bridges”, Proceeding of the Sixth International Symposium on Life-Cycle Civil Engineering (IALCCE2018), pp.1175-1182.

Sadek, A. and El-Sadek, A., (2014), “ Evaluating the impact of land use uncertainty on the simulated streamflow and sediment yield of the Seyhan river basin using the SWAT model”, Turkish Journal of Agriculture and Forestry, Vol.38, pp. 515-530.

Samanta, S., Pal, D.K., Lohar, D. and Pal, B.,(2011), “Preparation of digital data sets on land use/ land cover, soil and digital elevation model for temperature modelling using remote sensing and GIS techniques”, Indian Journal of Science and Technology, Vol. 4, No.6, pp.636-642.

Skamarock, C.W., Klemp, J.B., Dudhia, J., Gill, D.O., Barker, D.M., Duda, M.G., Huang, X.Y. Wang, W. and Powers, J.G., (2008), “A description of the advance research WRF version 3”, NCAR Tech. Note NCAR/TN-475+STR, 13pp.

Wang, W., Bruyere, C., Duda, M., Dudhia, J., Gill, D., Lin, H., Michalakes, J., Rizvi, S., Zang, X., Beezley, J., Coen, J. and Mandel, J., (2011), “ARW version modeling systems usuer guide”, NCAR, pp.202.

Yi Cheng, F., Ching Hus, Y. and Liam Lin, P., (2013), “Investigation of the effects of the effects of different land use and land cover patterns on mesoscale meteorological simulation in the Taiwan area”, Journal of applied meteorological and climatology, Vol.52, pp.570-587.

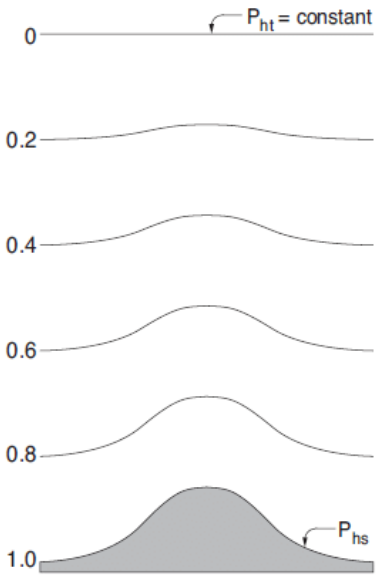

Fig. 4.1 the WRF eta vertical coordinate system as shown in Skamarock et al. (2008)

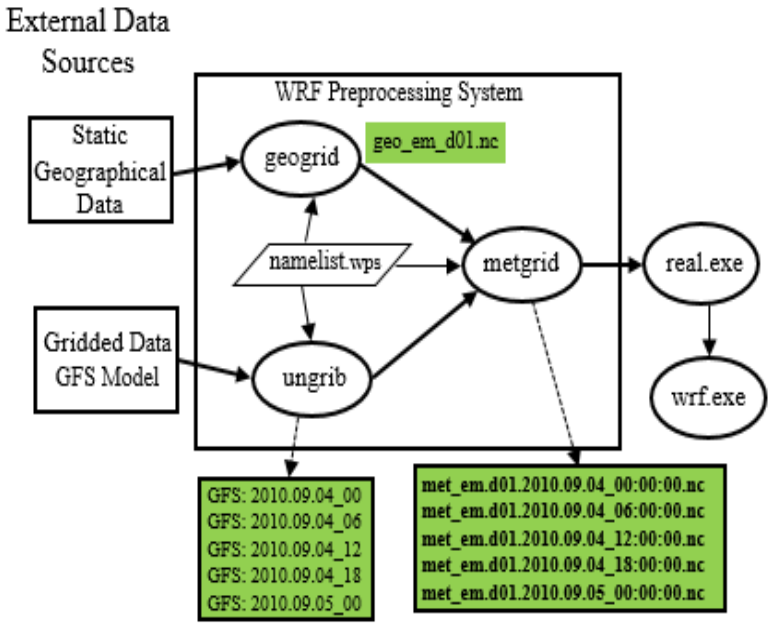

Fig. 4.2 WRF execution process

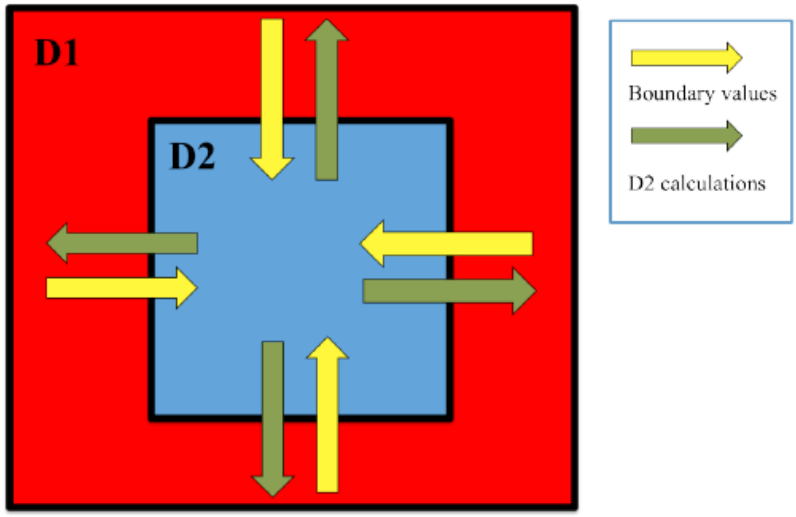

Fig. 4.3 Parent and nested domain labeled with D1 and D2 respectively. The yellow arrow represents lateral boundary providing for nested domain, while the green arrows shows the calculation provided to the parent by nest domain

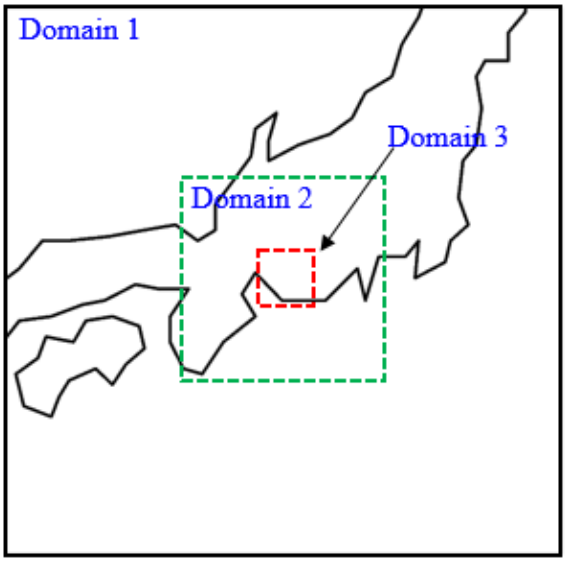

Fig. 4.4 Modeled simulation domains

Table 4.1 WRF model domain setting and configurations

Vertical resolution	40 levels		
Domains	Domain 1	Domain 2	Domain 3
Horizontal resolution	1000 km	300 km	100 km
Domains of integration	34.98 N - 137.28 E	35.14N - 137.17E	35.07N -137.30E
Interval of grids	25 km	5 km	1 km
Microphysics	WSW6-class group scheme	//	//
Longwave radiation	RRTM	//	//
Shortwave radiation	Dudhia	//	//
Surface layer	Monin-Oebukhov (Janjic Eta)	//	//
Land surface model	Noah	//	//
Boundary Layer	Mellor-Yamada-Janjic Tke	//	//
Cumulus parameterization	Kian-Fritsch(new Eta)scheme	//	//
Soil layer	Noah	//	//

Table 4.2 Description of 25-land use category of USGS, vegetation categories and their physical parameter for summer seasons

Land use index	Albedo	Moisture Avail.	Emissivity	Roughness Length	Thermal inertial	Definition
1	15	10	88	80	0.03	urban
2	17	30	98.5	15	0.04	Dryln Crop. Past.
3	18	50	98.5	15	0.04	Irrg. Crop. Past.
4	18	25	98.5	15	0.04	Mix. Dry/Irrg. C.P.
5	18	25	99	14	0.04	Crop./ Grs. Mosaic
6	16	35	98.5	20	0.04	Crop. /Wood Mosc
7	19	15	98.5	12	0.03	Grassland
8	22	10	88	10	0.03	Shrubland
9	20	15	90	11	0.03	Mix Shrb. /Grs
10	20	15	92	15	0.03	Savanna
11	16	30	93	50	0.04	Decids. Broadlf
12	14	30	94	50	0.04	Decids. Needlf
13	12	50	95	50	0.05	Evergrn. Braoddlf
14	12	30	95	50	0.04	Evergrn. Needlf.
15	13	30	94	50	0.04	Mixed Forest
16	8	100	98	0.01	0.06	Water Bodes
17	14	60	95	20	0.06	Herb. Wetland
18	14	35	95	40	0.05	Wooded wetland
19	25	2	85	10	0.02	Bar. Sparse Veg.
20	15	50	92	10	0.05	Herb. Tundra
21	15	50	93	30	0.05	Wooden Tender
22	15	50	92	15	0.05	Mixed Tundera
23	25	2	85	10	0.02	Bare Grn. Tundra
24	55	95	95	5	0.05	Snow or ICE
25	-	-	-	-	-	No data

Table 4.3 Description of 25-land use category of USGS, vegetation categories and their physical parameter for winter seasons

Land use index	Albedo	Moisture Avail.	Emissivity	Roughness Length	Thermal inertial	Definition
1	15	10	88	80	0.03	urban
2	20	60	92	5	0.04	Dryln Crop. Past.
3	20	50	93	2	0.04	Irrg. Crop. Past.
4	20	50	92	5	0.04	Mix. Dry/Irrg. C.P.
5	20	40	92	5	0.04	Crop./ Grs. Mosaic
6	20	60	93	20	0.04	Crop. /Wood Mosc
7	23	30	92	10	0.04	Grassland
8	22	20	93	1	0.04	Shrubland
9	22	25	93	1	0.04	Mix Shrb. /Grs
10	20	15	92	15	0.03	Savanna
11	17	60	93	50	0.05	Decids. Broadlf
12	15	60	93	50	0.05	Decids. Needlf
13	12	50	95	50	0.05	Evergrn. Braoddlf
14	12	60	95	50	0.05	Evergrn. Needlf.
15	14	60	93	20	0.06	Mixed Forest
16	8	1	98	0.01	0.06	Water Bodes
17	14	75	95	20	0.06	Herb. Wetland
18	14	70	95	40	0.06	Wooded wetland
19	23	0.05	90	1	0.02	Bar. Sparse Veg.
20	15	60	92	10	0.05	Herb. Tundra
21	15	60	93	30	0.05	Wooden Tender
22	15	60	92	15	0.05	Mixed Tundera
23	25	0.05	90	5	0.05	Bare Grn. Tundra
24	70	95	95	0.1	0.05	Snow or ICE
25	-	-	-	-	-	No data

Table 4.4 Land use mapping from GSI to USGS classifications

GSI	USGS
Paddy field	Irrigated Cropland and Pasture
Other agricultural land	Mixed Dry land/Irrigated Cropland and pasture
Forest	Mixed Forest
Wasteland	Barren or Sparsely Vegetated
Building site	Urban and Build-Up Land
Other sites	Industrial or Commercial
River and lakes	Lakes
Beach	Barren or Sparsely Vegetated
Sea water	Water Bodies
Golf course	Mixed Shrubland / Grassland
Road	Urban and Build-Up land
Railway	Urban and Build-Up land

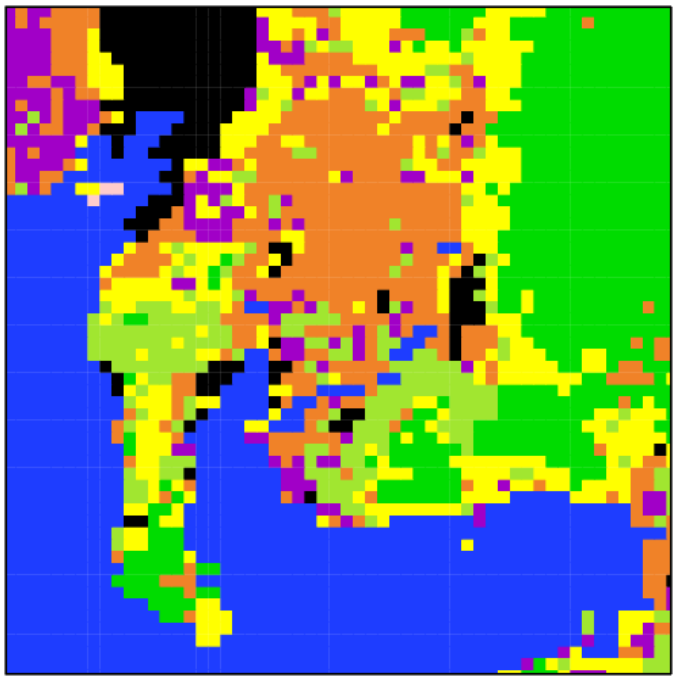

Fig. 4.5 Distribution of land from WRF domain around Nagoya port using USGS land use data

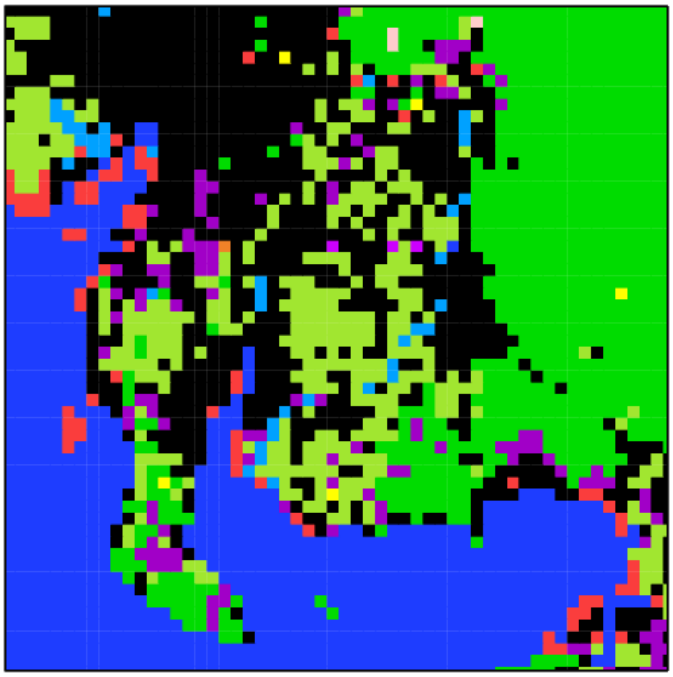

Fig. 4.6 Distribution of land from WRF domain around Nagoya port using GSI land use data

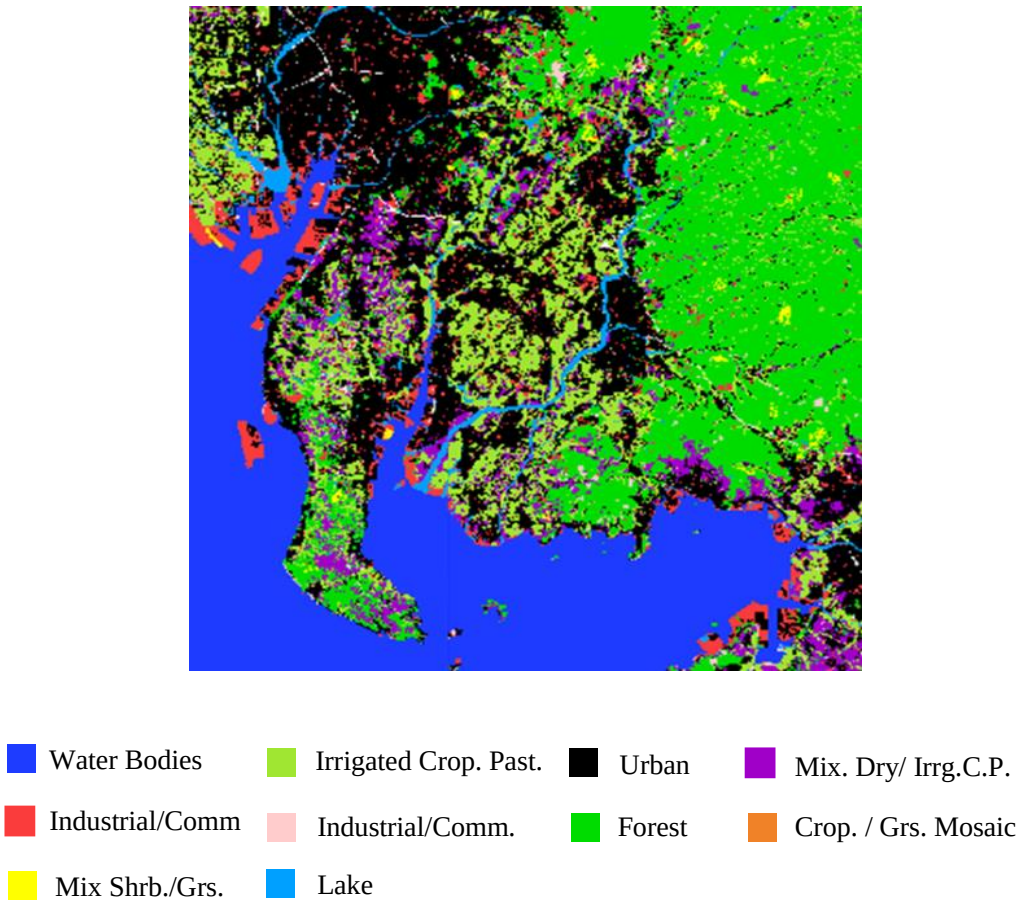

Fig. 4.7 Real map land use distribution data (map generated using national land numerical information)

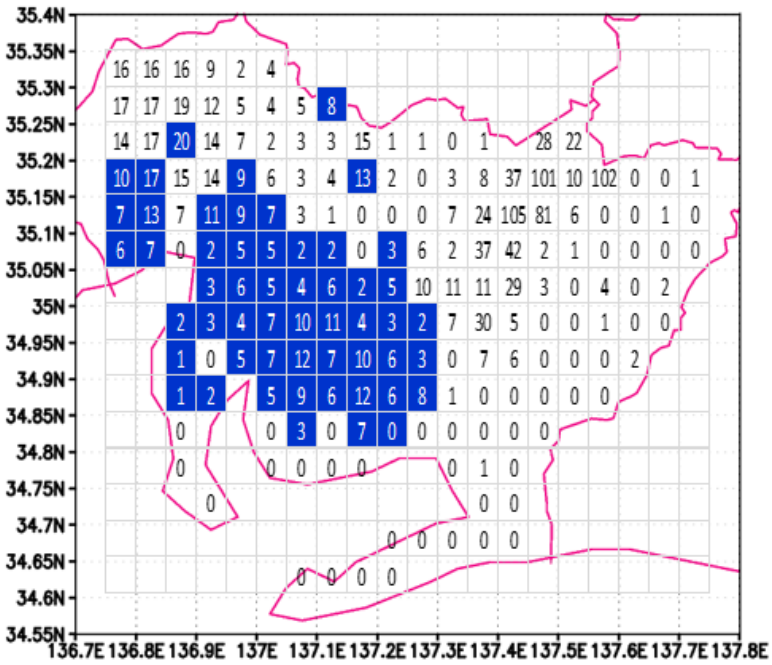

Fig. 4.8 Evaluation results of dew condensation using WRF- USGS in Aichi Prefecture during January 2017

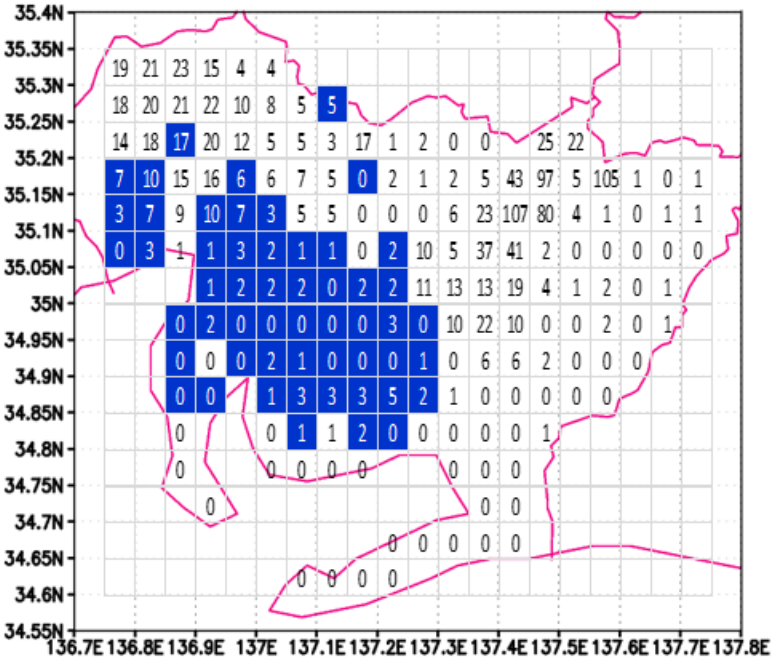

Fig. 4.9 Evaluation results of dew condensation using WRF- GSI in Aichi Prefecture during January 2017

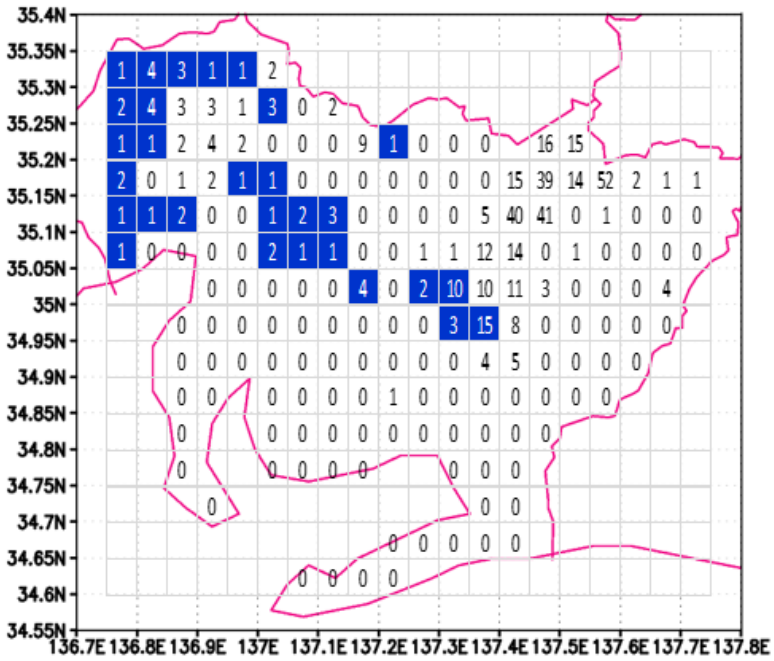

Fig. 4.10 Evaluation results of dew condensation using WRF- USGS in Aichi Prefecture during February 2017

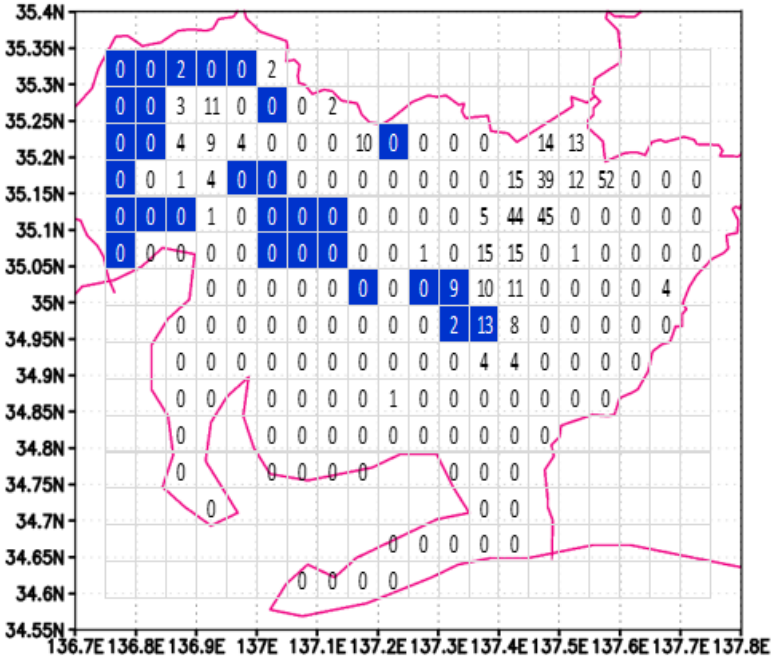

Fig. 4. 11 Evaluation results of dew condensation using WRF- GSI in Aichi Prefecture during February 2017

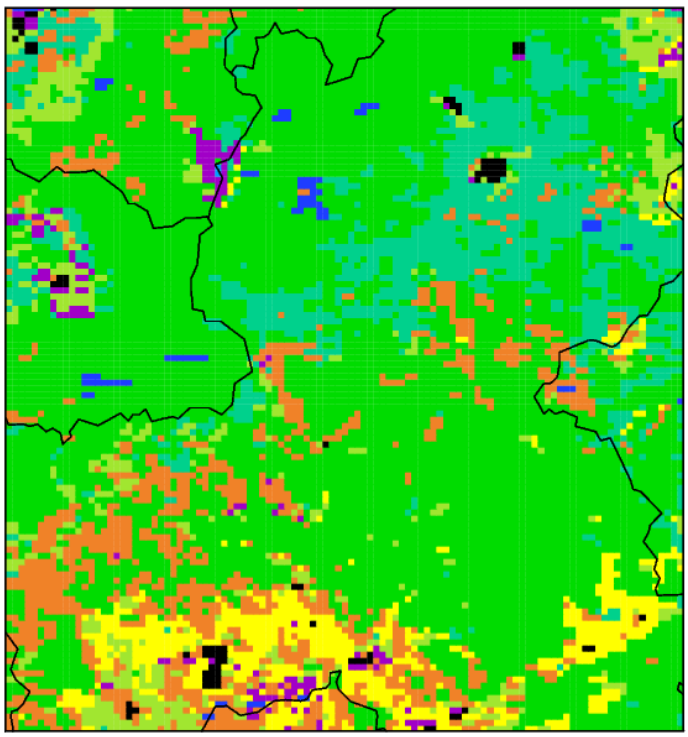

Fig. 4.12 Distribution of land from WRF domain for Gifu using USGS land use data

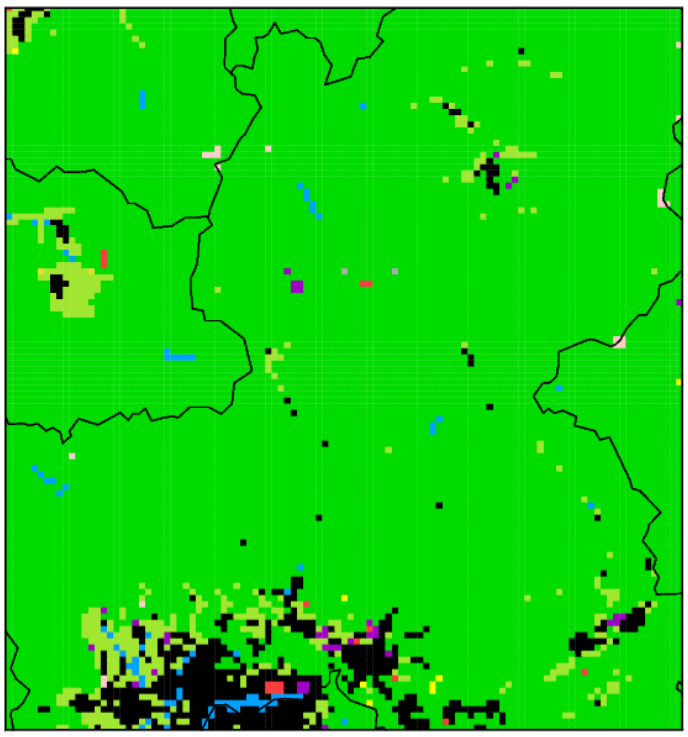

Fig. 4.13 Distribution of land from WRF domain for Gifu using GSI land use data

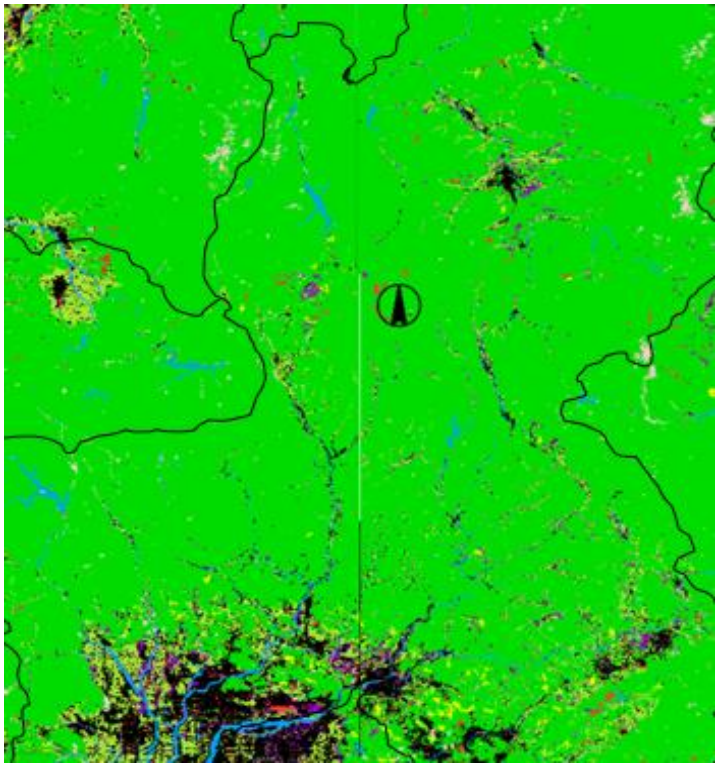

Fig. 4.14 Real map land use distribution data (map generated using national land numerical information)

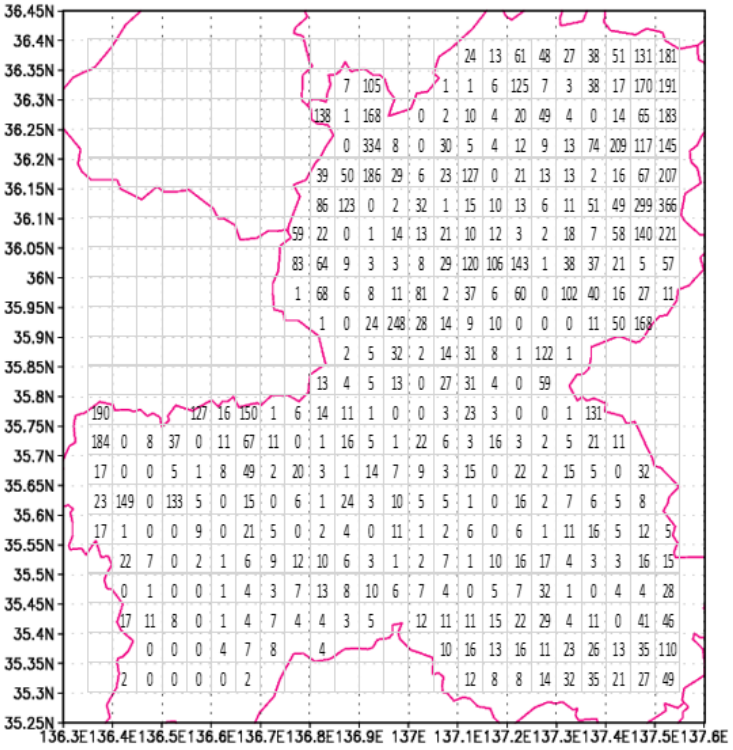

Fig. 4.15 Evaluation results of dew condensation using WRF- USGS in Gifu Prefecture during January 2017

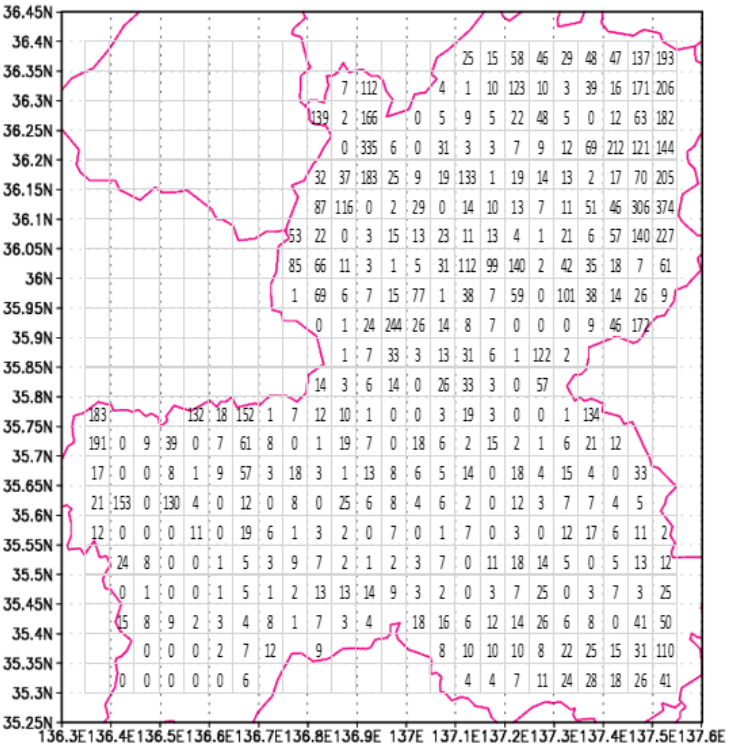

Fig. 4.16 Evaluation results of dew condensation using WRF- GSI in Gifu Prefecture during January 2017

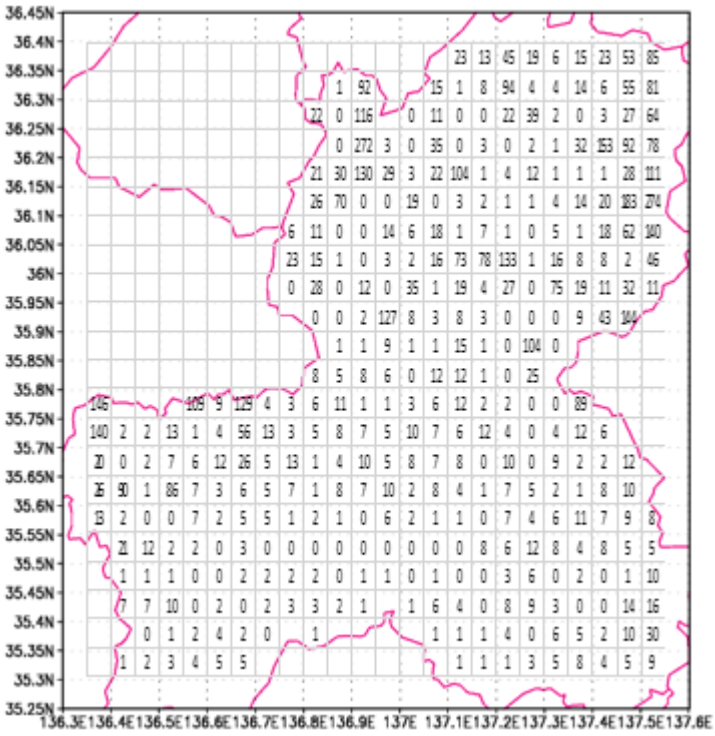

Fig. 4.17 Evaluation results of dew condensation using WRF- USGS in Gifu Prefecture during February 2017

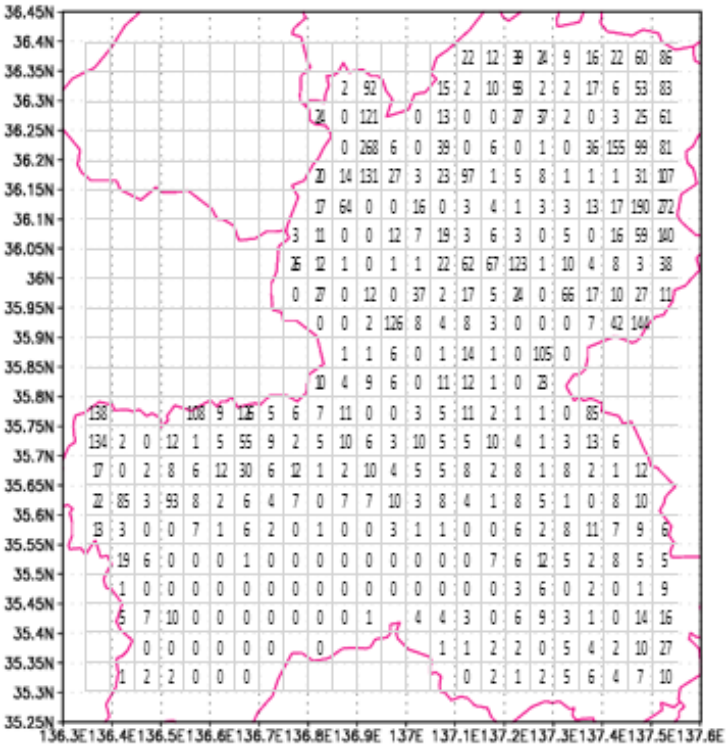

Fig. 4.18 Evaluation results of dew condensation using WRF- GSI in Gifu Prefecture during February 2017

Chapter 5

Investigation of Relationship between Girder Temperature and Atmospheric Temperature

5.1 Introduction

In this study, the girder temperature assumed to be equal to the atmospheric temperature. Based on this, the evaluation of dew condensation was carried out (Nagata et al., 2016). However, in reality, there is a minor difference between the atmospheric temperature and actual girder temperature. Therefore, to equalize them a modification factor is proposed. First, the atmospheric temperature and girder temperature were obtained from the field measurement at Sanbonmatsu bridge using atmospheric temperature/relative humidity sensor, and a thermocouple. Subsequently, their relationship were investigated by calculation of the mean error (ME) and root mean square error (RMSE) (Chiai and Draxler, 2014). The investigation revealed that the monthly temperature RMSE is almost 0.8 ℃ at flange of girder and 1.3 ℃ at web of girder. It means, the girder temperature is higher compare to atmospheric temperature.

Secondly, the evaluation of dew condensation was performed in Aichi prefecture based on the temperature modification factor. The temperature and humidity were obtained using WRF model, then the temperature modification factor applied to obtain the girder temperature. Based on the girder temperature and relative humidity the frequency of dew condensation were calculated. The results before and after applying temperature modification were compared, and it is found that the frequency of dew reduced after applying modification factor.

Thirdly, the field observation were conducted for the Toyokuni bridge as well as Sanbonmatsu bridge, these two bridges are located in the northeast of Aichi prefecture which is in mountainous areas. The dew condensation evaluation was conducted for the bridges using atmospheric temperature/ relative humidity sensor, and atmospheric corrosion monitoring (ACM) sensor. The investigation revealed that even the girder temperature is higher than dew point temperature, and the difference between girder and dew-point temperature reach almost 2℃ from the results of atmospheric sensor, but the dew condensation can occur because the ACM corrosion current shows dew in the same period of field measurement. In this situation, the dew condensation is thought to be due to fog, because the fog normally forms when the difference between air temperature and dew-point is less than 2.5 ℃ (Fog-AMA Glossary) also the foggy weather condition was observed most of time around these bridges. Finally, an evaluation of dew condensation was proposed using WRF technique.

5.2 Observation Site Overview

This section describes the bridge location, type of sensor used in the present study, and the set position of sensors in the bridges as following.

5.2.1 Bridges to Be Studied

One-site, observation has been conducted at Toyokuni bridge in the northeast (35.084° N, 137.448° E) of Aichi prefecture. Fig. 5.1 shows the monitoring location of the bridge (image generated using Google Map), and photo 5.1 shows an overview of the bridge, which was built in 1997. This is a steel girder bridge with length of 180m. Further, the sensors were set for the Sanbonmatsu bridge as well as Toyokuni bridge, the location of Sanbonmatsu and its overview were already described in chapter 3.

5.2.2 Set Position of Measurement Instruments

Fig. 5.2 shows the cross section and set position measuring instruments in the bridge. In this study, two ACM sensors were set on the bottom flange and web of exterior girder on the right-hand side of bridge, to evaluate the dew condensation for both web and flange of girder. Photo 5.2 and 5.3 shows the actual ACM on the web and flange of girder respectively. Additionally, atmospheric temperature/relative humidity sensor, and thermocouple were set for the girder to evaluate the atmospheric temperature and relative humidity around the girder, and girder temperature. Photo 5.4 and 5.5 show the actual sensor after installation in the bridge. The measurement was conducted during December 2017, and June 2019 for Sanbonmatsu and Toyokuni bridges, respectively. Moreover, the atmospheric temperature obtained by field measurement is assumed to be equal to the temperature estimated by WRF.

5.3 Relationship between Girder Temperature and Atmospheric Temperature

It is important to evaluate the dew condensation on steel girder bridge rather than the bridge construction point. Previously, the evaluation of dew condensation as a results of atmospheric temperature and relative humidity was carried out using WRF technique. The results obtained by WRF represents dew on the bridge construction points (around the bridge) not exactly on the bridge members. Therefore, it is essential to obtain the girder temperature form atmospheric temperature directly for accurate evaluation of corrosion environment of bridges. In the following section, a temperature modification factor is proposed, and the relation of girder temperature and atmospheric temperature were expressed mathematically.

5.3.1 Temperature Modification Factor

In this study, the girder temperature is assumed to be equal to the atmospheric temperature. Based on this, the evaluation of dew condensation was performed. However, in reality, there is a minor difference between the atmospheric temperature and actual girder temperature. To equalize them, a modification factor is proposed. In this study, both the girder temperature and atmospheric temperature were investigated at the

Sanbonmatsu bridge. The investigation was conducted during December 2017. The girder temperature was obtained through field measurement using a thermocouple, and a temperature/relative humidity sensor was used to obtain the atmospheric temperature for the exterior girder on the right side of the bridge. The location of the sensors and cross section of the bridge shown in Fig. 5.2. For our study, we obtained the modification factor based on the temperatures during winter. The difference in temperature was evaluated by the calculation of the mean error (ME) and root mean square error (RMSE).The ME was obtained by subtracting the atmospheric temperature from girder temperature. Because, the results of ME are positive for both web (point A) and flange of girder (point B), this meant that the girder temperature is higher in comparison to atmospheric temperature. The monthly temperature RMSE is about 1.3 °C at web and almost 0.8 °C at flange of girder for December 2017, as shown in the Table 5.1.

Figs 5.3 and 5.4 show the simultaneously comparison of girder temperature, atmospheric temperature, and modified temperature (after applying temperature modification factor) at web and flange of girder respectively, for the period of 10 days from 00:00, 1/12 to 00:00, 11/12 in December 2017. The main purpose of this comparison is to clearly describe the temperature differences before and after applying the modification factor with respect to girder temperature. According to the graphs the lowest value of atmospheric temperature is lower compare to girder temperature, the difference in the lower point of girder and atmospheric temperature became minimized by applying the modification factor. However, the highest value of girder temperature is higher compare to modified temperature, and further higher compare to atmospheric for Fig. 5.3. Similarly, the simultaneously comparison results of girder temperature, atmospheric temperature and modified temperature at web and flange of girder from 00:00, 11/12 to 00:00, 21/12 in December are demonstrated in Fig. 5.5 and 5.6. According to the figures the difference in temperature between girder and atmospheric temperature became minimized after applying the modification factor. Although, the maximum value of girder temperature (blue color) is higher compare to modified temperature (red color) and more higher compare to atmospheric temperature (black color) for the web, but still the modified temperature represents similar results to girder temperature. The present investigation revealed that the temperature difference is varied from 0.8 °C to 1.3 °C with respect to flange and web of girder. Hence, for simplicity we take the temperature difference at flange (which is 0.8℃) as 1 °C, this value is almost equal to the average difference of temperature at flange and web.

In short, for dew condensation to occur, low atmospheric temperature and high relative humidity is required. Hence, the temperature modification factor was considered based on the lowest temperature difference. The approximate mathematical relationship between girder and atmospheric temperature can be expressed using Eq. (5.1).

$$T_{girder} = T_{atm} + 1\ ^{\circ}C \tag{5.1}$$

where T_{girder} is the temperature of the steel girder, and T_{atm} is the atmospheric temperature.

5.3.2 Evaluation of Dew Condensation Based on Modification Factor

This section presents, the evaluation of dew condensation based on the temperature modification factor. The actual girder temperature can be easily obtained from the atmospheric temperature by applying Eq. (5.1). Firstly, the evaluation of dew condensation as a results of atmospheric temperature and relative humidity was carried out using WRF model for the month of January 2017, as shown in Fig. 5.7. Subsequently, the evaluation of dew condensation was conducted after applying the temperature modification factor during January, and the results can be observed form Fig. 5.8. The frequency number of dew reduced after applying the medication factor, the total reduced dew frequency for the entire month is 265, in comparison to the evaluation results of dew condensation before applying the modification factor across the Aichi.

Moreover, the evaluation results of dew condensation without using temperature modification during February 2017 is shown in Fig. 5.9. Then, the dew condensation evaluation was performed based on the actual girder temperature for the same month of February, and their results were compared. According Fig. 5.10 after applying the temperature modification factor, the dew condensation frequency decreased to 130, in comparison to the evaluation results without using the temperature modification factor as shown in Fig. 5.9. This was due to a temperature increase while calculating the dew-point temperature. As the temperature increase and relative humidity decreases accordingly. Finally, Fig. 5.8 and 5.10 show the possible accurate results of dew condensation after applying the temperature modification factor in the Aichi Prefecture. The dew condensation frequency is extremely high in the northeast and northwest regions of the prefecture as compare that of the rest part of the prefecture.

5.4 Evaluation of Dew Condensation by Field Measurement

This section, focused on the evaluation of corrosion environment of bridges using field observation. The main factor considered the atmospheric temperature and relative humidity, then dew condensation was investigated from the real data using sensor. Firstly, the weather environment around the Toyokuni bridge was described, then the evaluation of dew due foggy weather condition is demonstrated using ACM sensor. The details about the Toyokuni bridge is explained in the following:

5.4.1 Atmospheric Temperature and Relative Humidity

The atmospheric temperature and relative humidity were obtained by using atmospheric temperature and relative humidity sensor at Toyokuni bridge, then their results were compared with Nagoya and Shinshiro meteorological observatories. The main purpose this comparison is to see the weather situation around this bridge and confirms the measurement results. Fig. 5.11 shows, the simultaneously comparison results of temperature from the field measurement along with Nagoya and Shinshiro meteorological observatories (JMA,2018). According to the figures, the temperature of Toyokuni is lower compare to Nagoya and Shinshiro in the entire month of December 2018. Second, the change in behavior of Toyokuni bridge is

extremely linked with rate of change in meteorological observatories, but still the temperatures are not quite the same.

Fig. 5.12 demonstrates the comparison results of relative humidity at Toyokuni bridge and Nagoya meteorological observatory. This comparison was conducted only with Nagoya because the Shinshiro observatory doesn't recode the humidity. According to the figure, the humidity is higher at Toyokuni compare to Nagoya meteorological observatory in the entire month, particularly the maximum value of humidity is higher as compare to Nagoya meteorological observatory. From this comparison, it is clearly concluded that the lower temperature and high relative humidity was observed around the bridge. This situation lead to dew condensation which easily can occur, and the environment could be corrosive. Therefore, it is important to examine the corrosion environment of Toyokuni bridge owing to weather condition.

5.4.2 Evaluation Results of Dew Condensation

The evaluation of dew condensation was conducted at Toyokuni bridge. First the atmospheric temperature and relative humidity was obtained using field measurement, then the dew condensation calculated at saturated vapor pressure using Sonntag's equation (Imai et al., 2020; Diaiichi-kagaku.co.jp: Humidity calculation 1). The dew can occur whenever the girder temperature is either equal or fall below the dew-point temperature. According to Fig. 5.13, the difference in temperature between girder and dew-point became small and continuously increased the tendency of dew condensation, as it is clearly seen from the figure in some instances the girder and dew-point temperature are same which shows the occurrence of dew.

Fig. 5.14 shows, the evaluation results of dew based on atmospheric corrosion monitoring (ACM) sensor. According to ACM sensors the dew condensation occur when the corrosion current falls within the range of 0.01-0.1 mA, the greater value from the 0.1 mA states the rain condition and the smaller value of 0.01 mA demonstrate the dry condition (National Institute for Material Science, 2004). As indicated by the graph dew occurred in ACM 1 and ACM 2, because the corrosion current value being within range the range of 0.01 to 0.1. This range is a remarkably accurate statement of dew condition.

The investigation results of dew based on the atmospheric temperature and relative humidity sensor and ACM sensor show the dew condition in this bridge, and both sensor confirms the investigation outcome of each other's. Finally, the outcome of present investigation is a significant evidence of corrosion environment in Toyokuni bridge, and confirmed dew.

5.4.3 Evaluation of Dew Condensation Owing to Fog

Most of time, the dew condensation tends to occur during winter seasons due to low temperature and high humidity (Nagata et al., 2016). However, in mountainous areas, the occurrence of dew condensation is not limited to the winter seasons (December, January, and February), and it can occur event in the others month of the years.

Fig. 5.15 shows the simultaneously comparison of girder temperature and the dew point – temperature at Toyokuni bridge, where the measurement period was during June 2019. The girder and dew point temperatures were obtained through field measurements using sensors. In the present investigation, the flange temperature of the girder at point B was considered for comparison with the dew point-temperature. As seen from the figure, the girder temperature is higher than the dew point temperature. The difference in temperature reach almost 2℃ during the measurement period. Additionally, Fig. 5.16 shows, the evaluation results of dew condensation in the bridge using atmospheric corrosion monitoring (ACM) sensor. As indicated by the graph, dew occurs in both ACM 1 and ACM 2, because the corrosion current value is within range of 0.01 to 0.1 mA, as shown by blue-colored rectangle. This range is a remarkably accurate statement of dew condensation. Moreover, the occurrence tendency of dew is higher in ACM 2 than ACM 1.

Similarly, the simultaneously comparison of girder temperature and dew point temperature was carried out at Sanbonmatsu bridge, the measurement period is from 00:00, 27/6 to 00:00 30/6 in June 2019. In this study, the girder temperature and dew point temperature were obtained by field measurement using sensors as well. The girder temperature was measured at point B at lower flange of girder. According to Fig. 5.17, the girder temperature is higher than dew point temperature, and the difference in temperature is about 2℃, almost similar to Toyokuni bridge. Moreover, the evaluation of dew condensation was carried for Sanbonmatsu using ACM sensor. According to Fig. 5.18, dew condensation occurs in the bridge as well, because the current corrosion value is within the range of 0.01 to 0.1 mA that clearly indicates the dew condition.

In short, the dew condensation normally occurs when the girder temperature is either equal or lower than the dew point temperature. In the present investigation, although, the girder temperature is higher than the dew-point temperature, dew condensation still occurs in the bridges. Thus, in such a situations the dew condensation is considered to occur as a results of fog, as fog normally forms when the difference between air-temperature and dew point is less than 2.5℃, and also most of time foggy, weather condition was observed around the bridges.

5.5 Evaluation of Dew Condensation Using WRF Technique

Fig. 5.19 shows the investigation results of dew condensation from 00:00, 28/5 to 00:00, 29/5 in May 2019 at Toyokuni bridge. According to the graph, the tendency of occurrence of dew condensation is high during this period of time, as the difference between girder temperature and dew point is too small. Additionally, Fig. 5.20 demonstrates the investigation results of dew condensation by using WRF technique during the month of May 2019. As, indicated by the graph, the girder temperature is higher in comparison to the dew point –temperature over the calculation period as well as field measurement during June 2019, as shown in Fig. 5.15. However, the difference in temperature between girder temperature and dew point temperature is reduced and the tendency occurrence of dew condensation at certain times continuously increases, the

difference in temperature reach below 2°C. This can, therefore, considered as a more accurate statement of fog condition by WRF technique.

That is to say, the investigation of dew condensation can be conducted due to fog using WRF technique, and it is important to consider the corrosion environment of bridge due to fog for more accurate evaluation of environment characteristics.

5.6 Concluding Remarks

As, it is very important to know the girder temperature for evaluating dew condensation on the bridge based on the actual girder temperature. Therefore, in this chapter, the relation between girder temperature and atmospheric temperature was investigated and a temperature modification factor was proposed to easily obtain the girder temperature from the atmospheric temperature. The WRF is capable of calculating the temperature and relative humidity for any arbitrary point, then, the girder temperature can be obtained simply by applying the proposed modification factor.

Further, a comparative investigation of temperature and relative humidity was carried out for Toyokuni bridge along with Nagoya and Shinshiro meteorological observatories to examine the weather condition around the bridge, and as a result the low temperature and high humidity were observed which indicates the possibility of occurrence dew. Moreover, the present investigation revealed that dew can occur even when the girder temperature is higher than the dew point temperature, this can be due to fog, because the fog forms when the difference between temperature and dew point reach 2.5 °C. This was the new phenomena that was observed at both Toyokuni and Sanbonmatsu bridges, and confirmed by field measurements. Finally, the evaluation of dew condensation was conducted by using WRF technique, and it was confirmed that dew condensation owing to fog can be evaluate by using WRF technique. From this study the following summary can be made:

1) The actual girder temperature could be easily obtained from the atmospheric temperature by applying the proposed modification factor. This is useful for the evaluation of dew condensation on steel bridges rather than at bridge construction point.
2) The comparison of dew condensation was carried out at Aichi prefecture before and after applying temperature modification factor. The outcome of present investigation revealed that the frequency of dew condensation significantly reduced after applying temperature modification factor as compare that of before applying the modification factor. The frequency of dew based on temperature modification factor represents the dew on steel bridge, and provide more accurate results.
3) The investigation revealed that dew condensation occur due to fog, even when the girder temperature is higher than the dew point temperature. Therefore, a calculation method was proposed by using WRF technique, and the validity of the proposed method was confirmed by field measurements.
4) Finally, for accurate evaluation of corrosion environment of bridge, it is significantly important to consider the occurrence of dew condensation as a results of fog, particularity, where the possibility of formation of fog is expected.

References

Chai, T. and Draxler, R.R., (2014), " Root mean square error (RMSE) or mean absolute error (MAE)-Arguments against avoiding RMSE in the literature", Geoscientific Model Development, pp. 1247-1250.

Daiichi – kagaku.co.jp,"Humidity calculation 1", https://www.daiichi-kagaku.co.jp/situdo/note/arekore08/.

Fog-AMS Glossary, https://glossary.ametsoc.org/wiki/Fog.

Imai, R., Miyasou, T. and Aso, T., (2020)," An evaluation of dew condensation on steel plate girder bridges", Journal of Structural Engineering, Vol.66A, pp.443-451.

JMA, (2018), "Japan Meteorological Agency", https://www.data.jma.go.jp/gmd/risk/obsdl/index.php.

Nagata, K., Naito, R., Yagi, C. and Kitahara.,(2016), " Evaluation method of dew condensation of steel girders using weather data", "Journal of Structural Engineering, Vol.62A, pp.796-803.

National institute for materials science. (2004): Weathering steel/ Corrosion analysis. https://www.nims.go.jp/stx-21/jp/publications/stpanf/pdf/corrosion6.pdf.

Fig. 5.1 Location of monitoring bridge

Photo 5.1 Toyokuni bridge

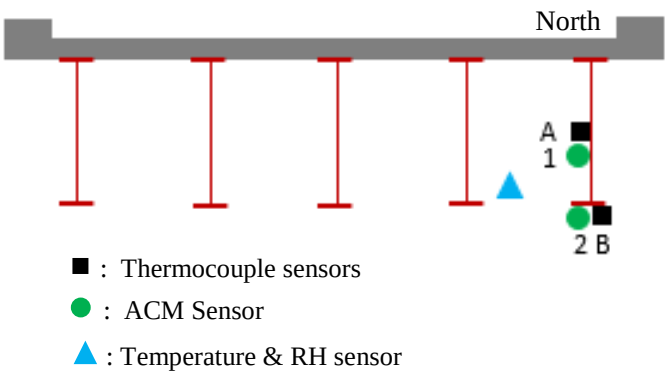

Fig. 5.2 Set position of measuring instrument and cross section of Toyokuni bridge

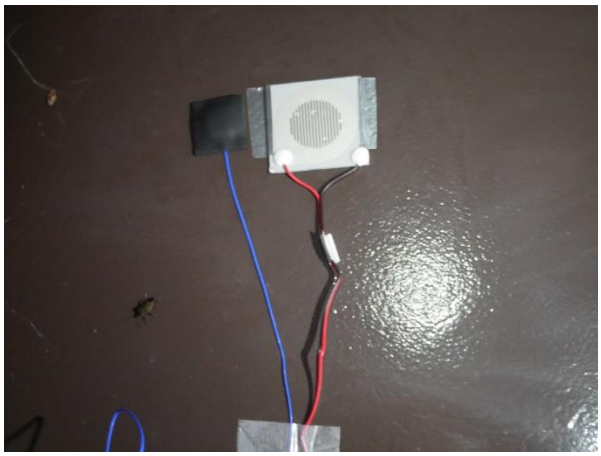

Photo 5.2 ACM sensor on the web of girder at point A.

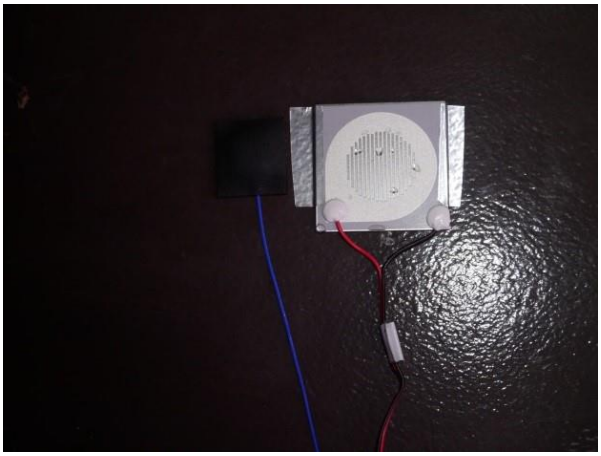

Photo 5.3 ACM sensor on the flange of girder at point B.

Photo 5.4 Atmospheric temperature and relative humidity sensor

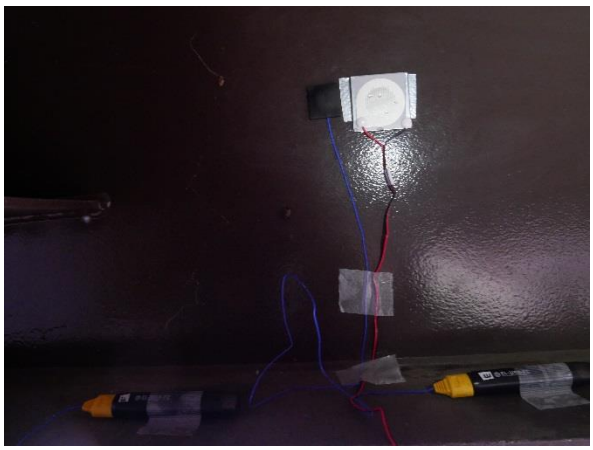

Photo 5.5 Thermocouple

Table 5.1 ME and RMSE of temperature in December 2017

No		Temperature (°C)	
1	Set position of sensors	ME	RMSE
2	Web of girder at point (A)	0.991	1.281
3	Flange of girder at point (B)	0.677	0.792

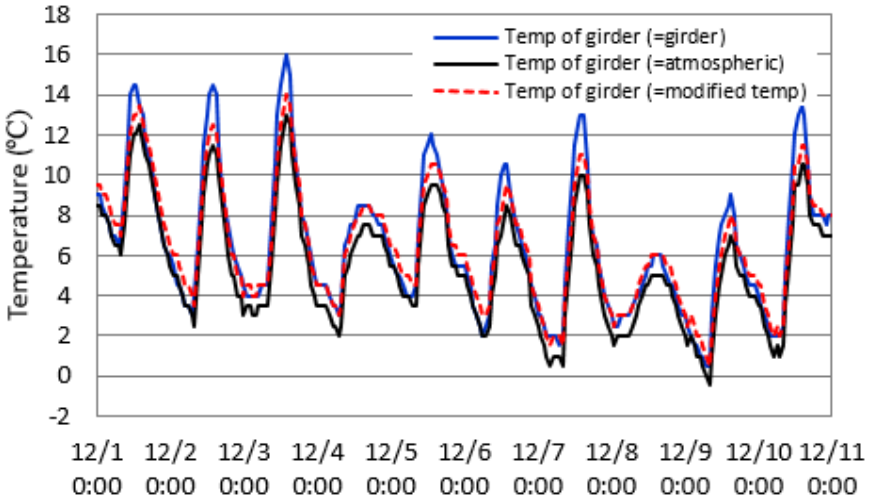

Fig. 5.3 Comparison of girder, atmospheric, and modified temperature of web at point A from 00:00, 1/12 to 00:00, 11/12 in December 2017

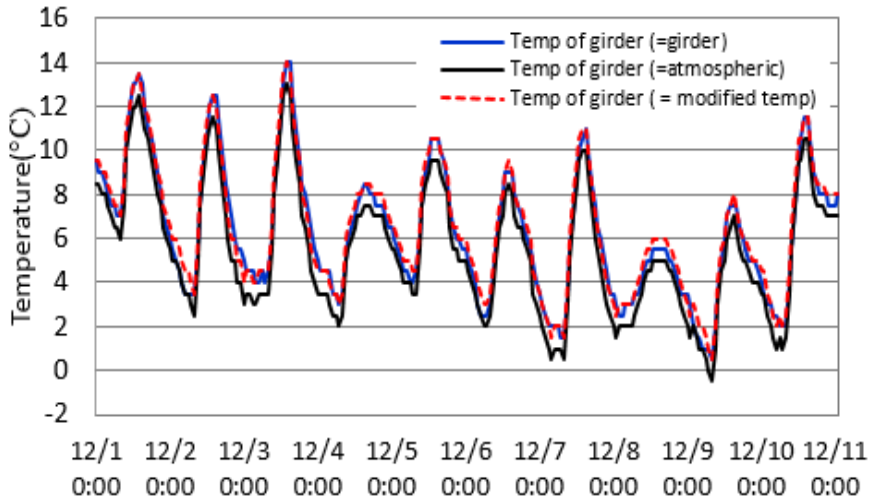

Fig. 5.4 Comparison of girder, atmospheric, and modified temperature of flange at point B from 00:00, 1/12 to 00:00, 11/12 in December 2017

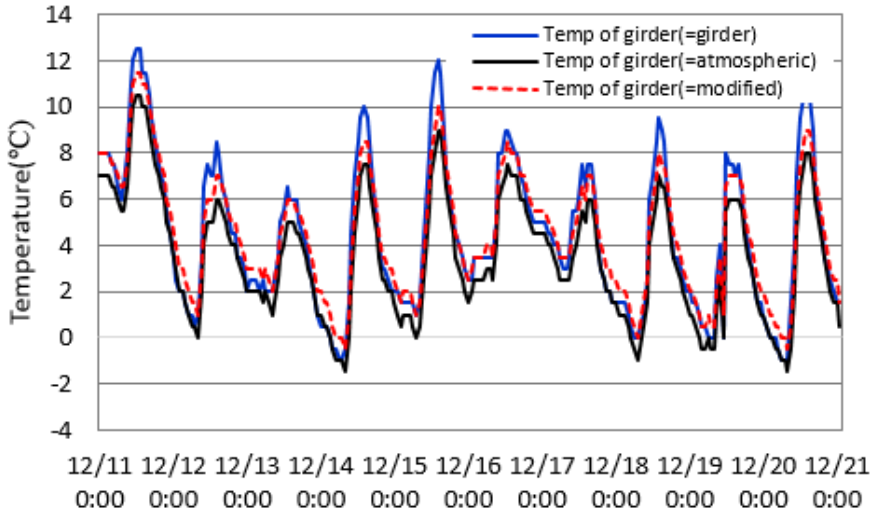

Fig. 5.5 Comparison of girder, atmospheric, and modified temperature of web at point A from 00:00, 11/12 to 00:00, 21/12 in December 2017

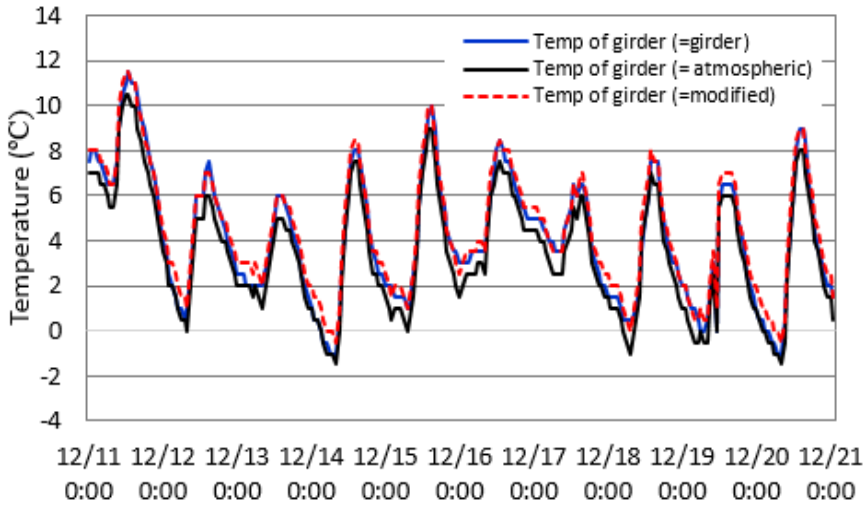

Fig. 5.6 Comparison of girder, atmospheric, and modified temperature of flange at point B from 00:00, 11/12 to 00:00, 21/12 in December 2017

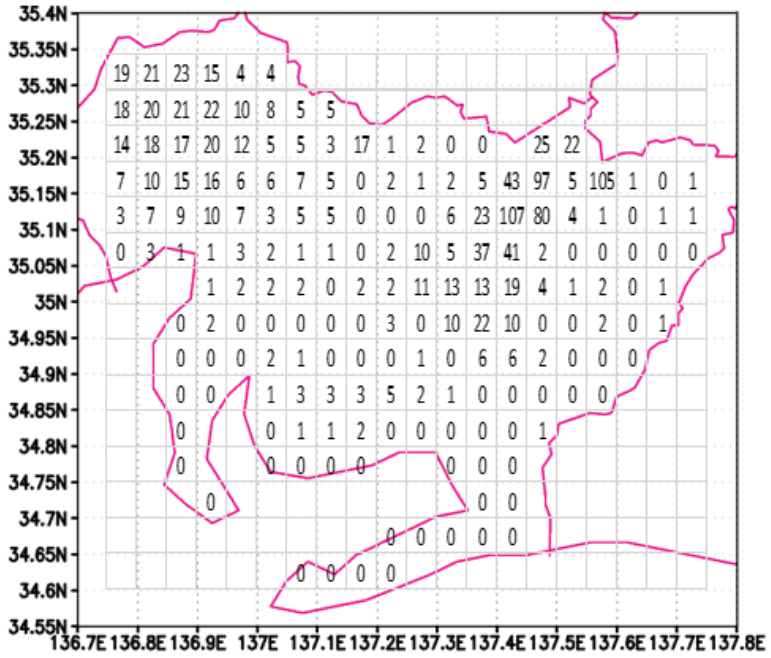

Fig. 5.7 Evaluation results of dew condensation in Aichi Prefecture during January 2017

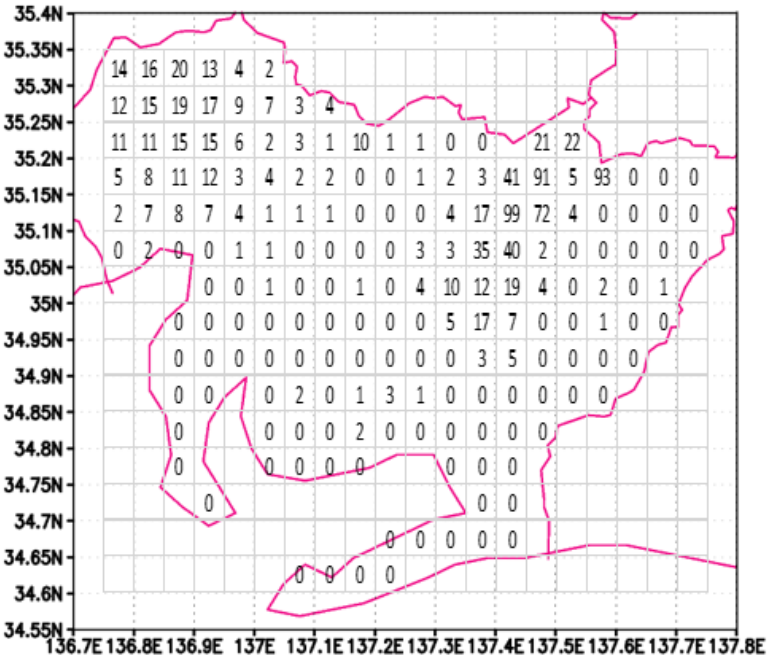

Fig. 5.8 Evaluation results of dew condensation after applying temperature modification in Aichi Prefecture during January 2017

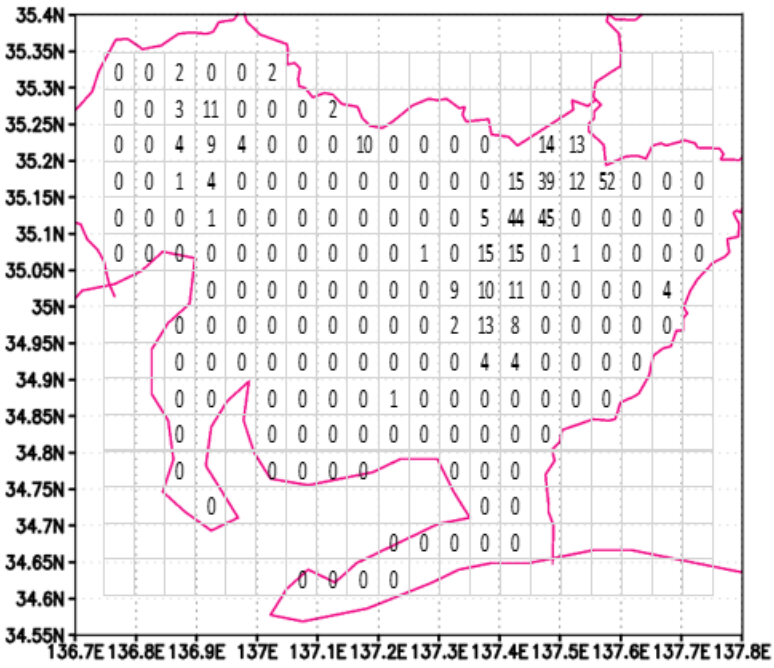

Fig. 5.9 Evaluation results of dew condensation in Aichi Prefecture during February 2017

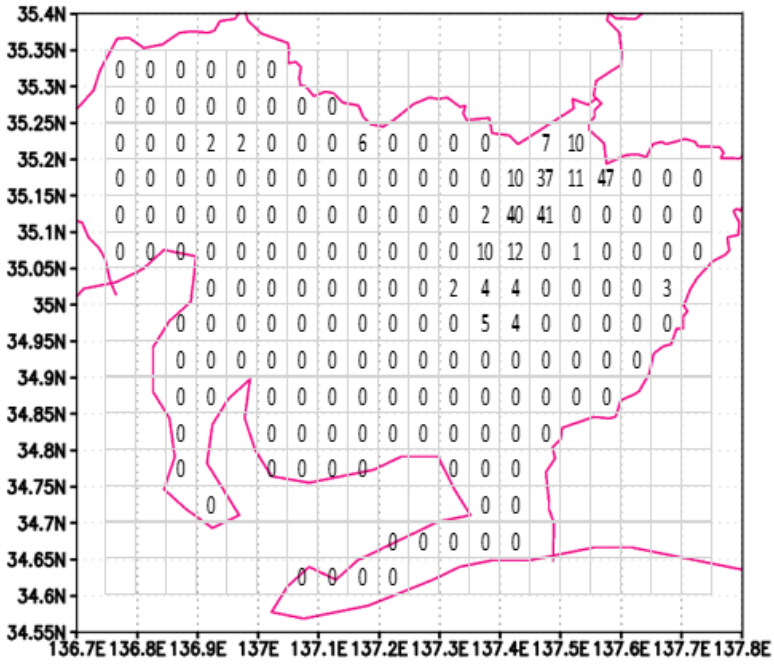

Fig. 5.10 Evaluation results of dew condensation after applying temperature modification in Aichi Prefecture during February 2017

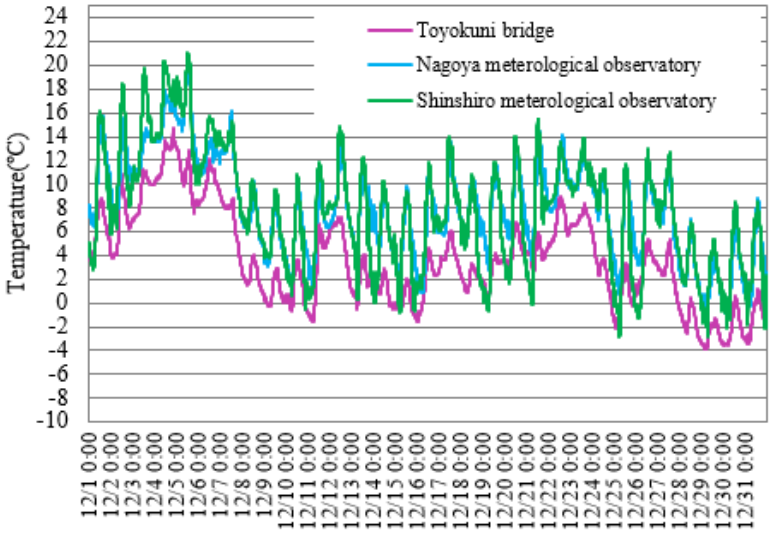

Fig. 5.11 Comparison results of temperature of Toyokni bridge with Nagoya and Shinshiro meteorological observatories

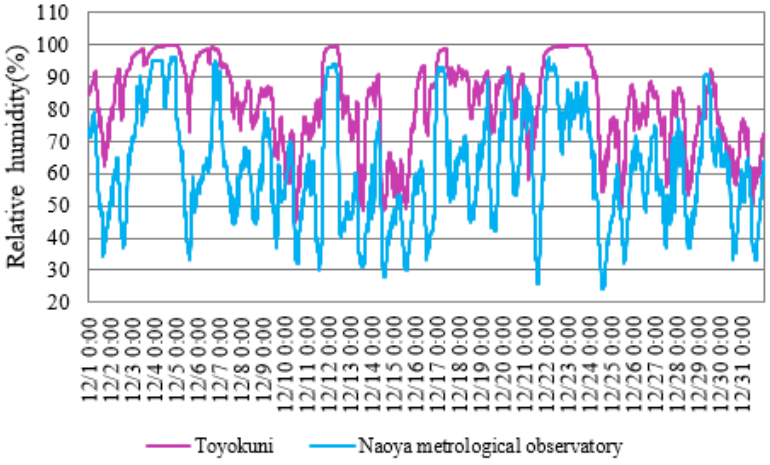

Fig. 5.12 Comparison results of relative humidity at Toyokni bridge with Nagoya and Shinshiro meteorological observatories

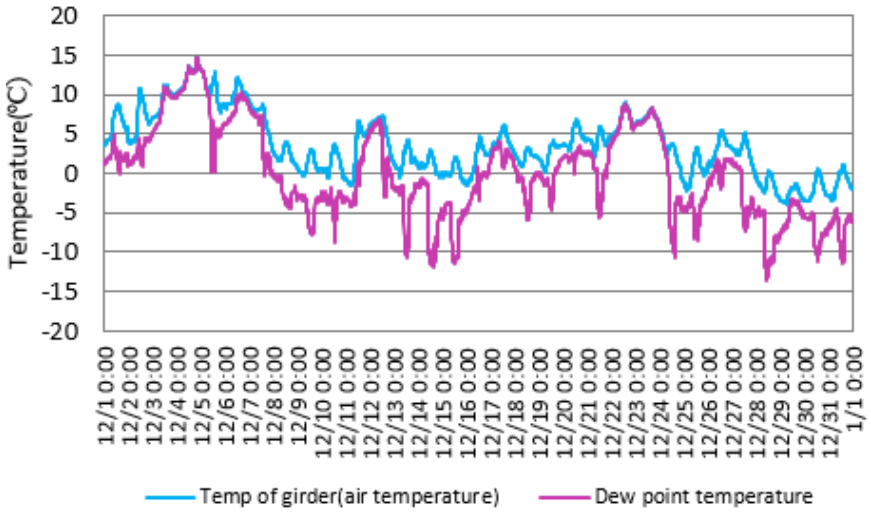

Fig. 5.13 Comparison of temperature with dew-point temperature at Toyokuni bridge

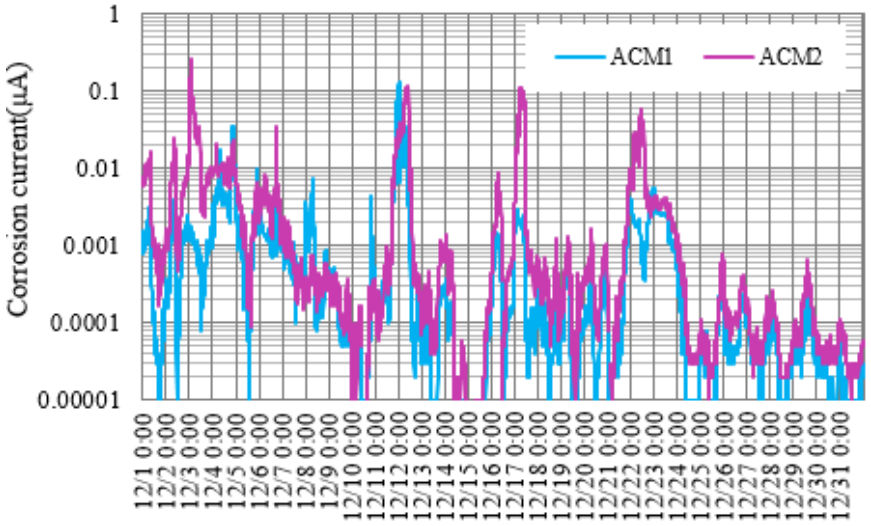

Fig. 5.14 Evaluation results of dew condensation using ACM sensor at Toyokuni bridge

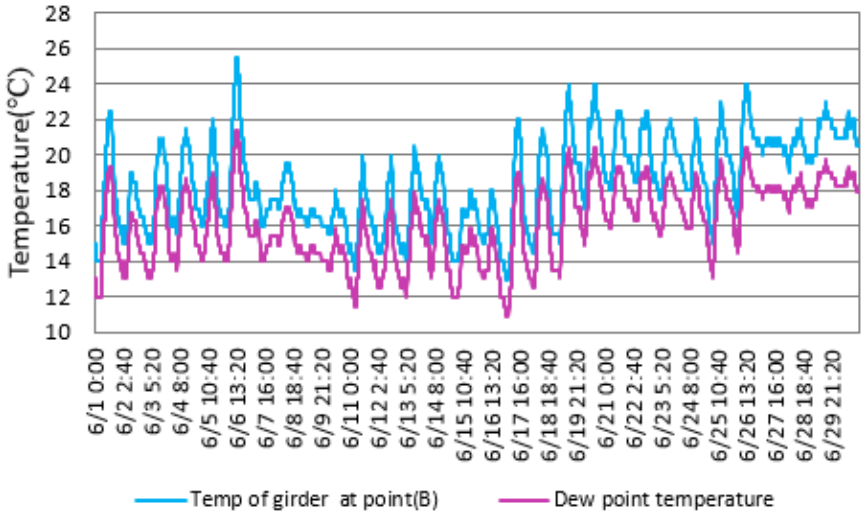

Fig. 5.15 Comparison of girder temperature with dew point-temperature at Toyokuni bridge during June 2019

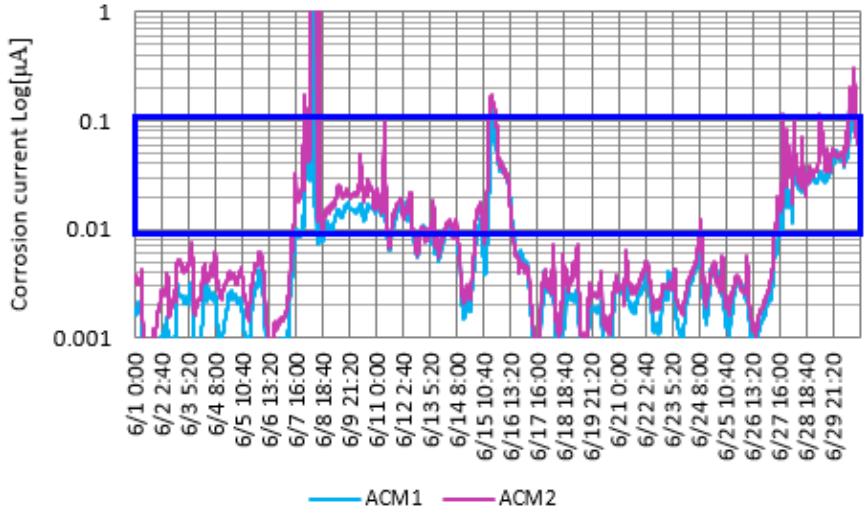

Fig. 5.16 Evaluation results of dew condensation using ACM sensor at Toyokuni bridge during June 2019

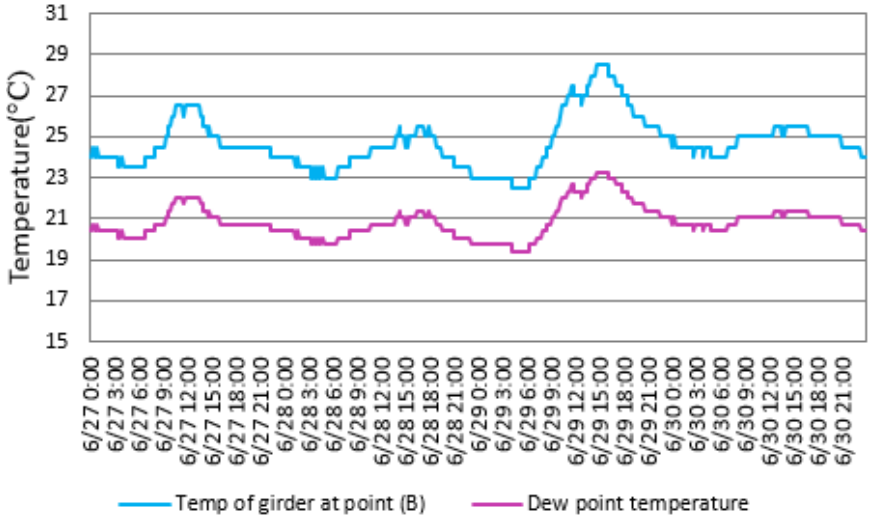

Fig. 5.17 Comparison of girder temperature with dew point-temperature at Sanbonmatsu bridge from 00:00, 27/6 to 00:00, 30/6 in June 2019

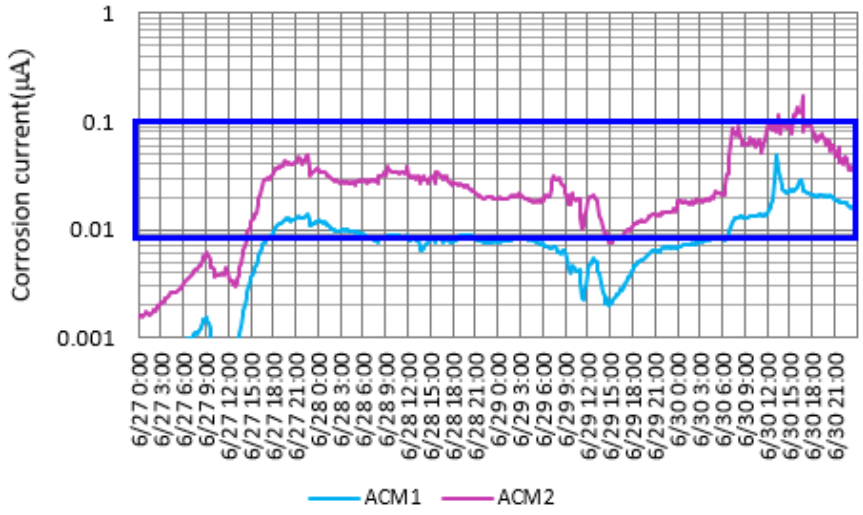

Fig. 5.18 Evaluation results of dew condensation using ACM sensor at Sanbonmatsu bridge from 00:00, 27/6 to 00:00, 30/6 in June 2019

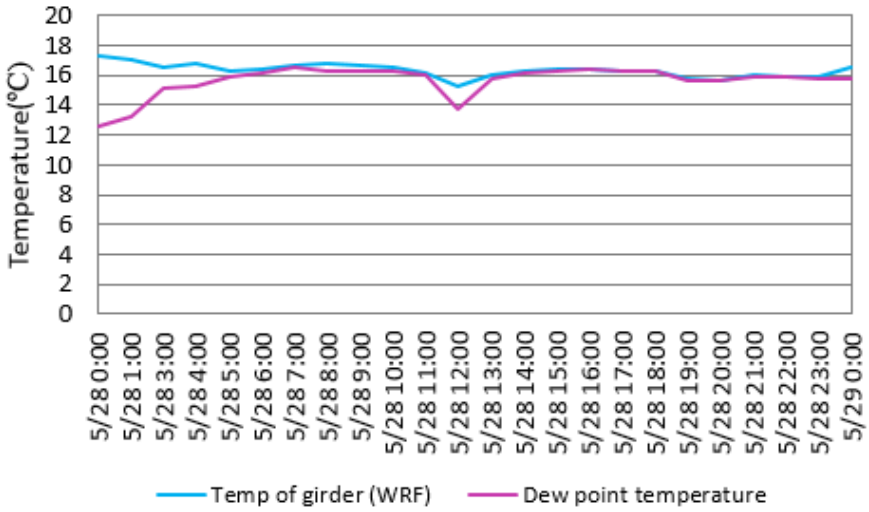

Fig. 5.19 Evaluation results of dew condensation using WRF technique at Toyokuni bridge from 00:00, 28/5 to 00:00, 29/5 in May 2019

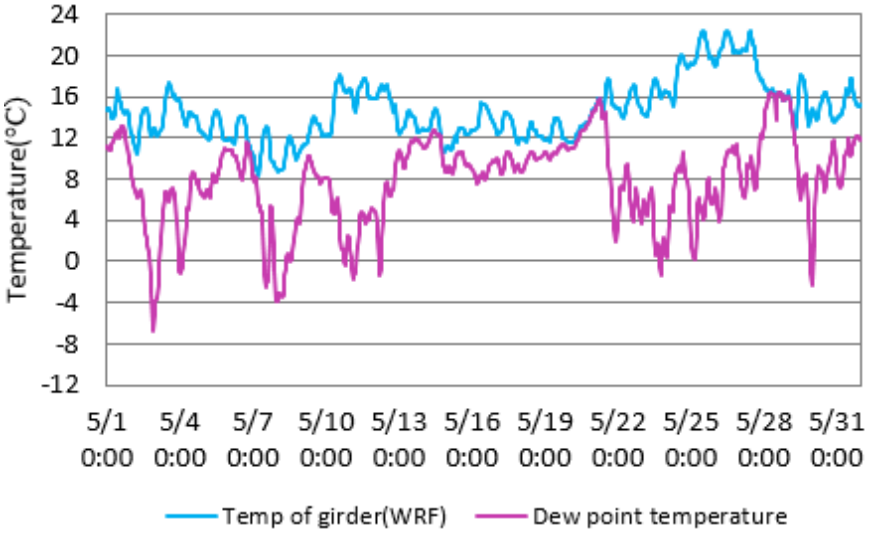

Fig. 5.20 Evaluation results of dew condensation using WRF technique at Toyokuni bridge during May 2019

Chapter 6

Development of a Total Evaluation Method for Dew Condensation on Steel Bridge

6.1 Introduction

Previously, a method for the evaluation of corrosion environment of bridges as a result of atmospheric temperature and relative humidity was proposed using a weather research and forecasting (WRF) numerical weather prediction technique and inverse distance weighting (IDW) technique (Nagata et al., 2016; Rasoli et al., 2018, 2019,2020). This method can easily evaluate the corrosion environment of bridges at global scale (around the bridge) rather than specifically on the bridge members as it was described in the previous chapters in details. This chapter aims, to develop a method for extensive evaluation of dew condensation on the structural members of the bridges at local scale (on the bridge girders), Also it is essential to know either the evaluation of dew condensation for steel bridges at global scale is sufficient or further evaluation at locale is needed. Therefore, a total evaluation method for corrosion environment caused by dew condensation was proposed which comprises of two major steps as they are described as following:

Step_ 1 is used for the evaluation of corrosion environment at a global scale, and the procedure in this step is as follows: select the targeted bridge and determine the coordination points (latitude and longitude), use the WRF or IDW technique to calculate the atmospheric temperature, relative humidity, and wind speed, subsequently conduct the evaluation of dew condensation at global scale.

Step_ 2 is employed when the corrosion environment of a bridge due to dew condensation is required for each structural members. In Step_ 2, the meteorological data such as; atmospheric temperature, relative humidity, and wind speed that are already obtained in Step_ 1 are used for the STAR_CCM+ software program, as input for proper boundary and initial conditions, and subsequently the evaluation is simply conducted. Fig. 6.1 shows the detailed description of the proposed evaluation method (Step_ 1 and Step_ 2) from beginning to end. Additionally, field measurements were carried out for the Ooeyousui bridge as a case study, to confirm the validity of the proposed method and will be described in the next section. In this study, initially evaluation of dew condensation was carried out using field measurements, then the evaluation of dew condensation was conducted using WRF technique for dry and dew cases, and lastly the dew condensation was conducted on bridge girder using STAR_CMM+.

Finally, this study aims to propose a total evaluation system of corrosion environment of bridges through WRF or IDW technique as large scale environmental information approach to proceed the

investigation of corrosion environment to a local scale on the bridge members using STAR_CCM+ program.

6.2 Evaluation of Dew Condensation by Field Measurements

In this study, the atmospheric corrosion monitoring (ACM) sensor was used to evaluate the dew condensation, and thermocouples were used to measure the girder temperature at Ooeyousui bridge by field measurement. The bridge overview, monitoring location, and its coordination points including the sensor specification were described in detailed in chapter 3. In the present investigation, totally eight ACM sensors were set for the web and flange of girder, three ACM sensors were for the exteriors girder and two ACM sensor for the middle girder. Additionally, three thermocouples were set for exteriors and middle girder on the web and flange of girders respectively. Fig. 6.2 shows the cross section of bridge, installation position of ACM, and thermocouples.

Fig. 6.3 (a) shows the evaluation results of dew condensation at the Ooeyousui bridge using ACM sensor from 00:9, 8/1 to 00:8, 9/1 in the month of January 2018. As indicated by the graph, dew was observed by ACM1, ACM2, ACM4, and ACM7. The corrosion current value within the range of 0.01 to 0.1 mA is highlighted by a red-colored rectangle in Fig. 6.3. This range is remarkably accurate indication of dew condensation (National institute for materials science, 2004). The ACM3, ACM5, ACM6 and ACM8 showed dry condition. Additionally, Fig. 6.3(b) shows the evaluation results of dew from 00:9, 2/1/2018 to 00:8, 3/1/2018, and the corrosion current value of ACM sensor is below 0.01 mA in this period. This is accurate indication of dry condition, and dew did not occur.

6.3 Model Description

In this study, the atmospheric temperature, relative humidity and wind speed are necessary to evaluate the dew condensation either in global or local scale. Therefore, this section briefly describes the modeling approach, simulation model, and the boundary conditions.

6.3.1 WRF and IDW Approach

The WRF model is a mesoscale numerical weather prediction system designed to serve both operational forecasting and atmospheric research needs (Khandaka and Moritmi, 2013; Janjic et al., 2010; Skamarock et al., 2008). The atmospheric temperature, relative humidity and wind speed can be predicted using WRF technique. Further, the IDW method is the simplest interpolation technique and can be applied to obtain the meteorological data using weights as a function of the distance between meteorological observatory and interpolation point (Chen and Liu, 2012; Setianto and Triandini., 2013; Wong., 2004; Moeletsi et al., 2016). The data of any arbitrary point (e.g., target Bridge) can be obtained using IDW method.

The details descriptions of IDW and WRF technique and their employments for the evaluation of corrosion environment for steel bridges are discussed in chapter 2 and chapter 4 of this thesis. Therefore,

the detailed explanation of these methods are avoided in this chapter. Here, a briefly information has been provided to connected the IDW and WRF as global approach with the new approach STAR_CCM+ which will be demonstrated in the next section.

6.3.2 STAR_CCM+ Approach

The numerical analysis was performed using general-purpose computational fluid dynamics (CFD) technique. The CFD is currently one of the most advanced and promising approaches used for analysis and solution of various problems involving flow domains in research and industrial applications (Bozzini et al., 2003).There are several commercial software packages such as; Numeca, Ansys and STAR_CCM+ used for CFD analysis. However, the present work was performed on STAR_CCM+ Software. STAR_CCM+ provides the most comprehensive engineering physics simulation inside a single integrated package. It is an entire engineering process for solving problems involving flow (of fluid or solids), heat transfer and stress. It provides a suite of integrated components that are combined to produce a powerful package that can address a wide variety of modeling needs. The components of this system include 3D-CAD modeler, surface preparation tools, automatic meshing technology, physics models and post-processing. Recently, the STAR-CCM+ became the first commercial CFD package that can mesh and solve a problem with over one billion cells. An object tree is provided for each live simulation; containing object representations of all the data associated with the simulation (Rajak et al., 2013; Zou et al., 2017; Yazgan-Birgi et al., 2019) .

In this study, STAR-CCM+ was used to simulate the dew condensation on structural members of a bridge. First, as an initial condition, a water droplet with a specific diameter was placed near the wall and directed toward the wall with a specific initial velocity and temperature. The water droplet stayed on the wall after colliding with wall it is considered dew if the water droplet gradually expands and its diameter is increased, whereas it is called evaporation if the water droplet diameter becomes smaller than initial value (Nagata et al., 2011; Nagata et al, 2016).

6.4 Simulation Domain and Boundary Conditions

In this study, the investigation of dew condensation was conducted for the only flange and the whole girder of bridge in local scale using STAR-CCM+ (Nagata et al, 2011; Nagata et al, 2016). This section demonstrates the simulation domain, boundary conditions, initial conditions, and analysis specification of the model.

6.4.1 Simulation Domain and Mesh Model

The model was prepared only for the a lower flange of exterior girder on the left-hand side of the bridge to show the validity of the proposed method rather than considering the entire cross section of the whole bridge. However, another model also was made for the entire cross section of a girder that will be described later. It should be reiterated, the main purpose of this study is to propose the evaluation system, and it doesn’t aims to evaluate the dew condensation in the real bridge model, thus, a simple model only for a

flange and a whole cross section of the girder was made which doesn't represent the real bridge model. That is to say, this model is an example to demonstrate the propose method and confirm its validity. The simulation domain size of flange was 2 m × 2 m in both horizontal and vertical direction. The flange of girder has width and thickness of 350 mm and 18 mm, respectively, as shown in Fig. 6.4(a). The model and mesh model for steel flange and airflow domain that created in STAR-CCM+ can be observed from Fig. 6.4(b) and Fig. 6.4(c), respectively. In this study, the 2D model (two dimension) was created for the analysis of dew condensation with finer mesh size for the flange of girder. The mesh size reaches to almost 2.5 mm as we approach to steel flange (in blue color) as shown in Fig. 6.4(d). The finer mesh size increases the accuracy of investigation compared with that of coarser mesh but requires longer time for simulation.

6.4.2 Boundary Conditions

In this study, to carry out simulation of dew condensation using STAR_CCM+, it is required to define the inlet, outlet, and the boundary condition of the model. Hence, an inlet was created on the left side of the model along AD from which air with a specific temperature, velocity, and water vapor entered. An outlet was provided on the right side along BC to allow the air to flow out. The upper and lower ends of the model were insulated walls, and the rate of heat exchange is zero. The AB and CD are frictionless boundary; the shear stress specification is slip, the wall species option is impermeable and the wall surface specification is smooth. The details of boundary conditions of the model can be seen in Fig. 6.5

6.4.3 Initial Conditions and Analysis Specifications

For this model, five water droplet were placed on the bottom face of the flange girder as shown in Fig. 6.6. As an initial condition, diameter of water droplet was set 1 mm, and it was considered as dew or evaporation when the diameter of water droplet increased or decreased from 1 mm respectively (Nagata et al, 2011; Nagata et al, 2016). Further, air flowed into the inlet with specified initial temperature and wind speed. The specification of air, water droplet, and steel girder used in the model are shown in Table 6.1 (a)-6.1(c).

6.5 Evaluation of Dew Condensation

In this section, the evaluation of dew condensation using numerical simulation model (WRF and IDW Technique) is described as following:

6.5.1 Evaluation of Dew Condensation Using WRF

This section demonstrate the evaluation of dew condensation using WRF technique. The main purpose of this section is to connect the previous study (Nagata et al., 2016; Rasoli et al., 2019, 2020) with the present one to develop a systematic relation. The evaluation of dew condensation due to atmospheric temperature and relative humidity was carried out at the Ooeyousui bridge considering the same period of field measurement as mentioned in section 6.2 of this chapter. The atmospheric temperature and relative humidity was obtained based on the bridge latitude and longitude using WRF technique. Subsequently, the

dew-point temperature was calculated at saturated vapor pressure. The dew can occur whenever the girder temperature is either equal or falls below the dew-point temperature. The mathematical procedure of dew condensation was described in Chapter 3.

As seen in Fig. 6.7(a), dew condensation occurred in the bridge from 00:9, 8/1/2018 to 00:8, 9/1/2018 because the difference between girder temperature and dew-point temperature is significantly small and even at some instances they are same which shows the high tendency of dew occurrence. During this period, dew condensation was also observed by field measurements using ACM sensors, as shown in Fig. 6.3(a). Additionally, Fig. 6.7(b) shows the evaluation results of dew from 00:9, 2/1 to 00:8, 3/1 in the month of January 2018. In this period, dew did not occur because the girder temperature was higher than the dew-point temperature, and the difference in temperatures were significantly large. Moreover, the field measurement results showed dry condition during the same period as shown in Fig. 6.3(b), and confirmed the WRF results. Based on this comparison, it is concluded that the evaluation results of dew condensation using WRF are similar to the field measurements, and it also provided the information of dew condensation at global scale (about overall the bridge) instead of the bridge girder only.

6.5.2 Evaluation of Condensation Using STAR-CCM+

The numerical simulation of dew condensation was conducted for the lower flange of exterior girder on left-hand side of the Ooeyousui bridge using STAR-CCM + program based on the model described in section 6.4.1 of this chapter. The main purpose of this investigation is to examine the difference in occurrence of dew condensation in each part of flange at local scale.

(a) Evaluation of Dew Condensation Considering Dry-Dew Case

During the field measurements, the girder temperature was observed as 6.5 °C at the center of lower flange. In this study, to accurately assess the local influence of flange for dew condensation, the girder temperature was set as 7.5 °C, 7 °C, 6.5 °C, 6 °C, and 5.5°C from left to the right side of flange in horizontal direction corresponding to the water droplet setting as shown in Fig. 6.6. The difference in temperature distribution was considered as 0.5 °C. Although, it is easy to set the constant temperature value for the whole flange of girder, it is preferable to know the influence of girder temperature distribution on the occurrence of dew in each part of the flange and examine the validity of the proposed method in all aspects. The weather data (atmospheric temperature, relative humidity, and wind speed) were obtained using WRF technique and inputted into STAR-CCM+ from 00:13, 8/1/2018.

Fig. 6.8 illustrates the simulation results of dew condensation. According to Fig. 6.8(a), the left side of the steel flange showed dry condition because the diameter of water droplet decreased from 1mm, and the rest part of flange show dew condition after the simulation time reached to 1 s. The tendency of dry condition increased on the left side whereas the tendency of dew increased from left to the right-hand side of the flange respectively until the simulation time reached to 196 s as shown in Fig. 6.8(b), this shows dry and dew conditions simultaneously, which can be called as the dry-dew case. Afterwards, the dry-dew

case totally changed to dew condition, and the dew condensation reproduced properly in the entire flange when the simulation time reached to 1255 s as shown in Fig. 6.8(c) because the diameter of water droplet exceeded from 1 mm, and subsequently, significant dew condensation was observed till the end of the simulation, as shown in Fig. 6.8(d).

It is assumed that the girder temperature has a close relation with dew condensation, therefore, it is important to assess the temperature distribution across the flange. The minimum and maximum temperatures were 5.5004 °C and 7.5000 °C, respectively, when the simulation time reached to 1 s as shown in Fig. 6.9(a). Afterwards, the temperature changed gradually, and tends to be further redistributed on the steel flange when the simulation time exceeded from 1 s as shown in Figs. 6.9(b), 6.9(c), and 6.9(d), respectively. The increase and decreases in the flange temperature can be influenced by the exchange of heat between air and flange. The decreasing temperature in each part of flange led to increasing occurrence tendency of dew on the corresponding part of flange. This can be clearly observed from comparison of flange temperature with dew condensation, as the flanges temperature decreased from the left to right side in Fig. 6.9 corresponding with the dew condensation increased from the left to right side as shown in Fig. 6.8.

Fig. 6.10(a) shows the variation in wind distribution. It is seen that the air flowed from inlet toward to the outlet in the simulation model, and the wind speed decreased when it reached near the surface of steel flange (blue color). Second, the airflow directly hit steel flange, which can cause the heat exchange between airflow and steel. Additionally, Fig. 6.10(b) is showing the overall condition of temperature in the model. The air temperature distribution appeared almost similar in the entire model (in red color) but it is different around steel flange (yellow), and for the steel flange itself (blue). The steel temperature is lower as compared with airflow temperature. Therefore, it is assumed the heat transfer occurred from air to the steel flange to some extent.

(b) Evaluation of Dew Condensation Considering the Dry Case

The numerical simulation of dew condensation was carried out for the flange of girder at local scale using STAR-CCM+. The girder temperature was observed 8.5 ℃ during field measurement using thermocouple at the center of lower flange. Therefore, the temperature was set as 9.5 ℃, 9 ℃, 8 .5 ℃, 8 ℃, and 7.5 ℃ from left to right side of the flange in horizontal direction as discussed in sub-section (a). The atmospheric temperature, relative humidity, and wind speed were obtained using WRF technique, and the simulation was conducted from 00:12, 2/1/2018.

According to simulation results presented in Fig. 6.11 (a), dew did not reproduce because the diameter of water droplet became smaller than 1 mm until the simulation time reached to 800 s. The simulation further continued to observe the behavior of water droplet. Consequently, the evaporation was observed instead of dew condensation, and two water droplets evaporated and three of them were remained when the simulation time reached to 1110 s as shown in Fig. 6.11(b). Finally, the tendency of evaporation

substantially increased as the simulation time reached to 1500 s as shown in Fig. 6.11(c). This is an accurate indication of dry condition, and this case can be termed as dry case.

As shown in Fig. 6.12(a), the minimum and maximum temperatures of flange reached to 7.4772 ℃ and 7.6486 ℃, respectively, when the simulation time reached to 800 s, and the temperature further distributed due to interaction of air flow with steel and caused exchange of heat. Further, the flange temperature decreased continuously as the numerical simulation run longer as shown in Figs. 6.12(b) and 6.12(c).This implies that the flange temperature is higher than air flow, and the flange tends to transfer heat into the air. This could be the reason due to which dew did not occur because the flange temperature is higher than that of air.

Fig. 6.13(a) shows the flow of air in the simulation model. It is seen that the air flow speed is lower around the flange surface, and the wind directly hit the steel, which caused the heat exchange between air and steel. Fig. 6.13(b) shows the temperature distribution in the entire model when the solution time reached to 1500 s. As seen in the figure, the air temperature is lower than that of the steel flange. Further, the difference in temperature between flange, around flange, and the whole simulation model as demonstrated in red, light blue, and blue color, respectively.

6.5.3 Evaluation of Dew Condensation Considering the Whole Girder

This section presents the details of the numerical simulation of dew condensation for the entire cross section of the girder. The main purpose of this section is to show the influence of structure on occurrence of dew condensation. The simulation model, meshing model, and boundary conditions are similar as described in section 6.4. For this particular case, 19 water droplets on the web and five were placed on the bottom flange of girders. The girder temperature was obtained as 6.5 °C at the center of lower flange during field measurement. To examine the structural influence on the occurrence of dew condensation and more accurately demonstrate the validity of local investigation of dew in each part of the girder, the temperature was distributed and set as 7.5 ℃, 7 ℃, 6.5 ℃, 6 ℃, and 5.5 ℃ from left to right side of the lower flange in horizontal direction similar to that as we discussed in section 6.5.2 for a single flange. As the difference in temperature between 7.5°C - 5.5 ℃ from extremely left to the right of flange reached to almost 2° C, therefore, a difference of 2°C was also considered for the web of girder from the bottom to upper part and distributed across the web in vertical direction. The meteorological data such as atmospheric temperature, relative humidity, and wind speed were obtained using WRF technique, and these data used as input for STAR-CCM+. The simulation was conducted from 00:13, 8/1/ 2018.

According to simulation results, the left side of the flange show dry condition, whereas on the right side of flange dew condensation reproduced properly because the diameter of water droplets increased from 1 mm. Additionally, the tendency of reproducing dew condensation is higher in the lower part of the web compared to that in upper part. Further, totally dry condition was observed from middle to the upper end of the web, and there is no dew as shown in Fig. 6.14 (a). Moreover, the dew condensation were totally reproduced on the flange of girder and lower part of the web when the simulation time reached to 1500 s,

as shown in Fig. 6.14(b). However, the higher tendency of dry condition was observed from middle to upper part of the web.

The dew and dry condition could be dependent on the girder temperature as well. Therefore, it is important to know the temperature distribution across the girder. The girder temperature is lower in the lower flange compared to that of the upper flange. Similarly, the girder temperature decreases from top to bottom across the web of girder as shown in Figs. 6.15(a) and 6.15(b), respectively. It is assumed that the tendency of dew occurrence increases as the girder temperature decreases, and that is why the tendency of dew occurrence was higher in lower part of the girder.

Fig. 6.16(a) shows the wind situation in the model. In this figure wind flows from the inlet, and it is increased when reached to near the flange. Therefore, each part of girder cannot receive the wind equally. Further, the model cannot receive the wind on the right side of the girder as easy as left side, and the wind speed becomes lower. This might be due to the influence of structure that each part cannot receive wind equally (whereas, the single flange could receive wind almost equally, as it was discussed in section 6.5.2 due to its horizontal location). Moreover, the air temperature is higher than that of lower part of the girder. However, the air temperature is lower compared to that in upper part of the girder and also the air temperature in right side of girder appeared lower (in light green color) than of the whole model temperature (in yellow color). Consequently, the variation of temperature in the girder and air model could be related to the structural influence in the mode. The detailed descriptions can be observed from Fig. 6.16(b).

6.6 Concluding Remarks

The evaluation results by WRF clearly revealed that the WRF and IDW techniques are very useful and effective to evaluate the corrosion environment of steel bridge at global scale (around the bridge), and there is no need for further investigation. However, this technique did not provide the sufficient information about the bridge members locally. Moreover, if further investigation is required for corrosion environment of dew condensation in each member of bridge, the second step needs to be performed using STAR-CCM+ software to determine the exact amount of dew at local scale.

The investigation revealed that the STAR-CCM+ can easily evaluate dew condensation locally in each part of the flange. It can show simultaneously the dry-dew case and dew case, and more specifically determine the critical parts of flange where the tendency of dew condensation is significantly high. The proposed method can provide comprehensive information regarding dew phenomena at local scale. Regarding the temperature distribution in the entire cross section of the flange and girder, it is continuously changed (increased and decreased) during the analysis period, and further redistributed as the simulation run from the beginning till end. The dew condensation is directly dependent on the girder temperature. The lower girder temperature increased the tendency of dew occurrence.

In short, the results of dew condensation obtained through field observation are in a good agreement with the numerical evaluation results using STAR-CCM+ software and confirmed the validity

of the proposed method. Furthermore, the numerical simulation can present further detailed description regarding dew condensation, evaporation, and the temperature distribution in the girder including the relationship between girder temperature and dew condensation in each part of the girder locally. Lastly, the presented investigation was conducted for a steel girder and a single flange to propose the total evaluation method, however, the results obtained in this investigation is applicable for the entire bridge. From the present study, the following summary can be made:

1) For the evaluation of corrosion environment at global scale (around the bridge), the IDW/WRF technique is sufficient. If more detailed information of dew condensation is needed in structural members of bridge, the local investigation should be conducted using STAR-CCM+ program.
2) The proposed evaluation system is useful to evaluate dew condensation for each member of bridge including structural influence for any arbitrary point without any field measurement.
3) The investigation revealed that the tendency of dew condensation is not similar for the each part of the girder. Therefore, it is important to evaluate the corrosion environment at local scale to determine the dew and dry part of the bridge members.
4) The numerical simulation results of dew condensation when using STAR-CCM+ software and field observation were similar. Hence, the validity of the proposed method was confirmed by field measurements.

References

Bozzini, B., Rcotti, E., Boniardi, M. and Mele, C., (2003), "Evaluation of erosion-corrosion in multiphase flow via CFD and experimental analysis", Science direct, wear, Vol.255, pp.237-245.

Chen, F. and Liu, C., (2012), "Estimation of the spatial rainfall distribution using inverse distance weighting (IDW) in the middle of Taiwan", Paddy Water Environ, Vol.10, pp. 209-222.

Janjic, Z., Gall, R. and Pyle, M.E., (2010), "Scientific documentation for the NMM solve", National Center for Environmental Prediction Office, NCEP. NCAR Tech. Note NCAR/TN-475+SR, 54pp.

Khandar, M.H.A. and Moritomi, H., (2013), "Numerical simulation for regional ozone concentration: A case study by weather research and forecasting/ chemistry (WRF/Chem) model", International Journal of energy and environment, Vol.4, No.6, pp.933-954.

Moeletsi, M.E., Shabalala, Z.P., Nysschen, G.D. and Walker, S., (2016)," Evaluation of an inverse distance weighting method for patching daily and dekadal rainfall over the Free State Province, South Africa", Water SA, Vol.42, No.3. Pp.466-474.

Nagata, K., Hotta, H., Hara, S., Yamaguchi, T. and Kitahara, T., (2016), "Study on prevention of dew condensation by using heat insulation coating", Journal of Structural Engineering, Vol.62A, pp.595-602(in Japanes).

Nagata, K., Ito, K., Yama, J., Obata, M. and Miyamoto, S., (2011), "Investigation of corrosion environment of a steel bridge for effective washing of girders", Journal of Structural Engineering, Vol.57A, pp.691-702(in Japanese).

Nagata, K., Naito, R., Yagi, C. and Kitahara, T., (2016), “Evaluation method of dew condensation of steel girders using weather data”, Journal of Structural Engineering, Vol.62A, pp.796-803 (in Japanese).

National institute for materials science. (2004): Weathering steel/ Corrosion analysis.

Rajak, U., Khare, R. and Prasad, V., (2013), “Flow simulation of elbow draft tube using STAR CCM+” Civil and Environmental Research, Vol.3, No.6, pp.105-110.

Raoli, Z., Nagata, K., Kitahara, T. and Sugiura, K., (2020), “Improvement of accuracy for the evaluation of corrosion environment on steel bridges using WRF technique”, Journal of Structural Engineering, Vol. 66A, pp. 452-465.

Raoli, Z., Nagata, K., Miyawaki, Y. and Kitahara, T., (2019), “Study on evaluation of corrosion environment on steel bridges using inverse distance weighting method”, Journal of Structural Engineering, Vol. 65A, pp. 479-491.

Rasoli, Z., Nagata, K. and Kitahara, T., (2018), “Monitoring of corrosive environment focusing on dew condensation in steel bridges”, Proceeding of the Sixth International Symposium on Life-Cycle Civil Engineering (IALCCE2018), pp.1175-1182.

Setianto, A. and Triandini. (2013), “Comparison of kriging and inverse distance weighting (IDW) interpolation method in Lineament extraction and analysis”, Journal of Southeast Asian Applied Geology, Vol.5, No.1, pp. 21-29.

Skamarock, C.W., Klemp, J.B., Dudhia, J., Gill, D.O., Barker, D.M., Duda, M.G., Huang, X.Y. Wang, W. and Powers, J.G., (2008), “A description of the advance research WRF version 3”, NCAR Tech. Note NCAR/TN-475+STR, 13pp.

Wong, D.W., Yuan, L. and Perlin, A.S.A., (2004), “Comparison of spatial interpolation methods for the estimation of air quality data”, Journal of Exposure Analysis and Environmental Epidemiology, Vol.14, pp. 404-415.

Yazgan-Birgi, P., Arafat, H.A. and Hassan Ali, M.I., (2019), “Implementation of two multiphase flow methods in modeling wetting of microporous hydrophobic membranes”, Science of the Total Environment, Vol.691, pp.1251-1261.

Zou, Y., Zhao, X. and Chen, Q., (2017), “Comparison of STAR-CCM+ and ANSYS Fluent for simulating indoor airflows”, Building Simulation, Vol.11, No.1, pp.165-174.

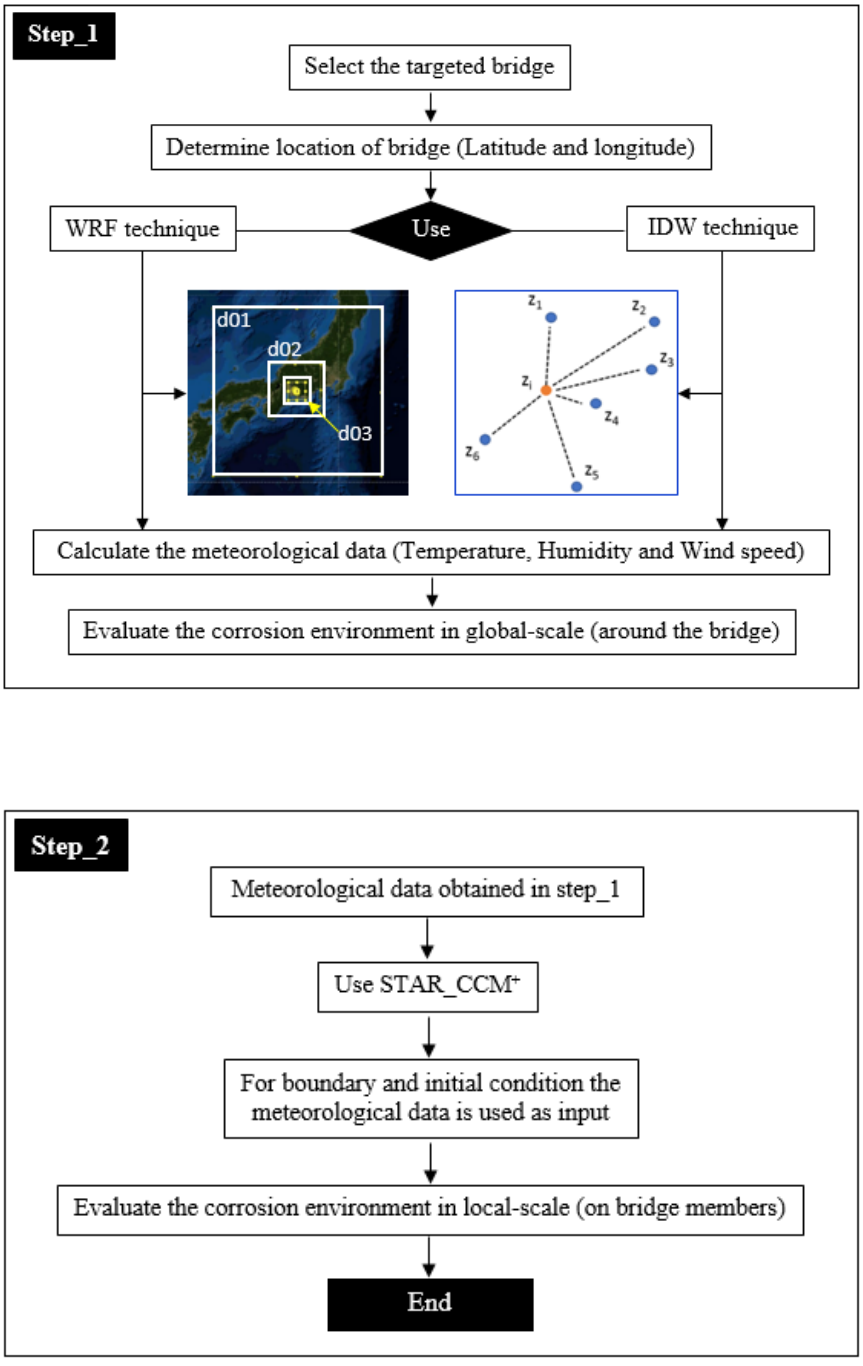

Fig. 6.1 Proposed total evaluation method of corrosion environment

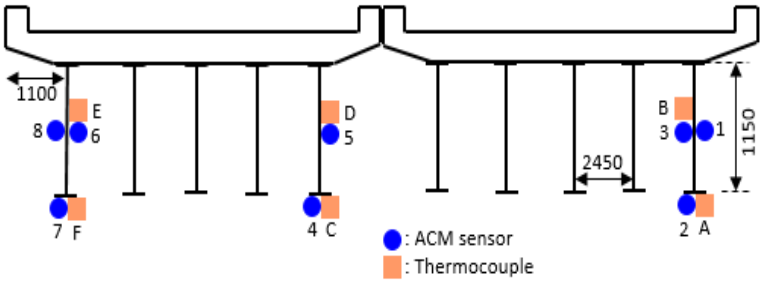

Fig. 6.2 shows the installation position of the ACM sensors and thermocouples

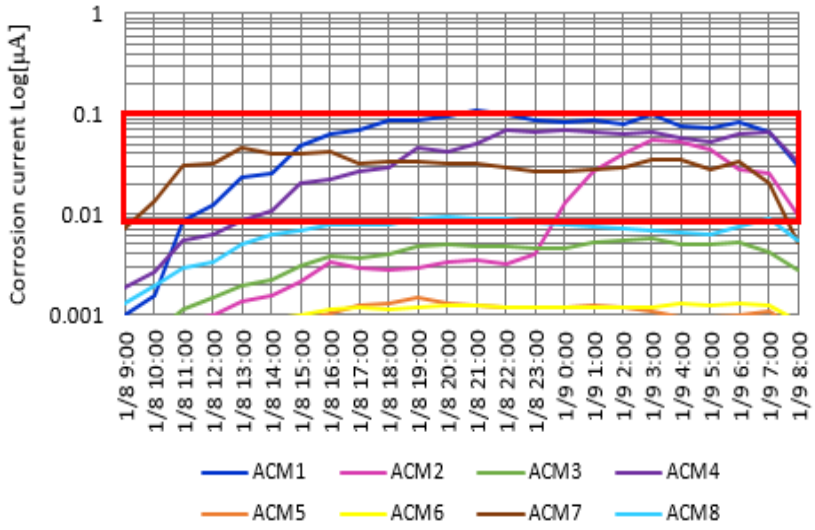

(a) Results of field observation from 00:9, 8/1 to 00:8, 9/1

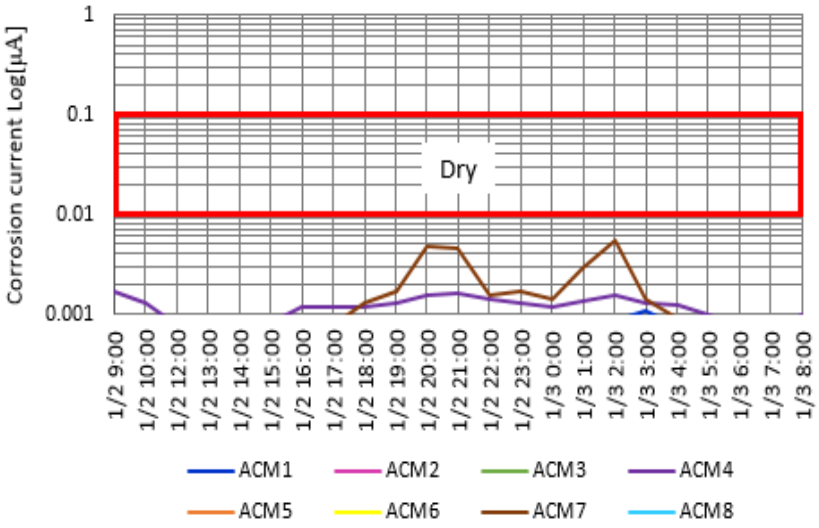

(b) Results of field observation from 00:9, 2/1 to 00: 8, 3/1

Fig. 6.3 shows the evaluation results of dew condensation at Ooeyousui bridge using ACM sensor during January 2018

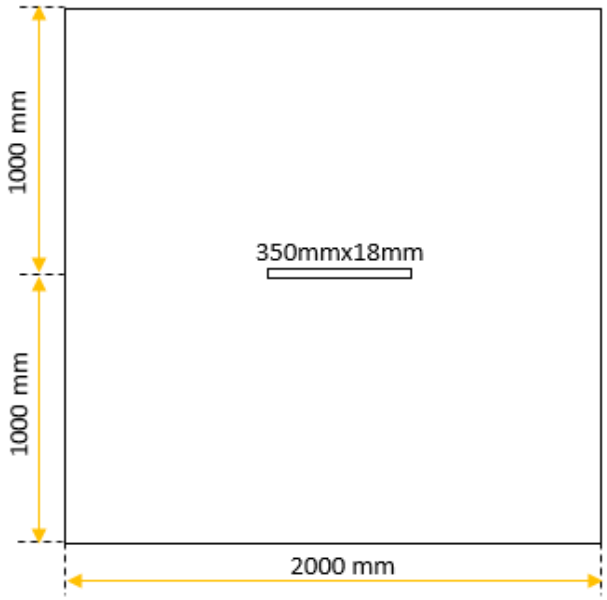

(a) Modeled domain

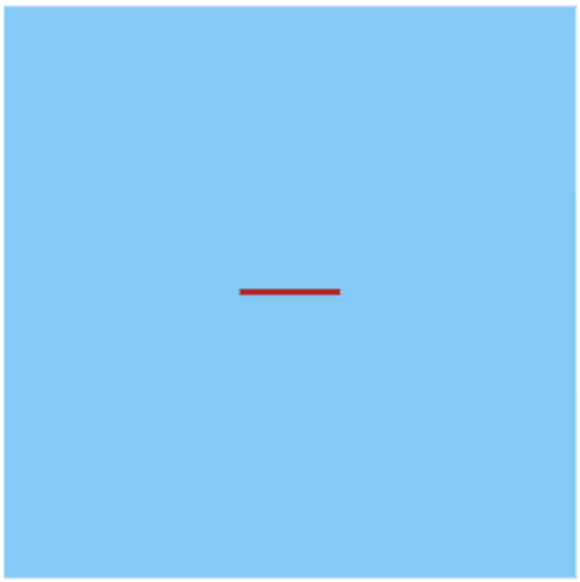

(b) Modeled domain (created by STAR-CCM+)

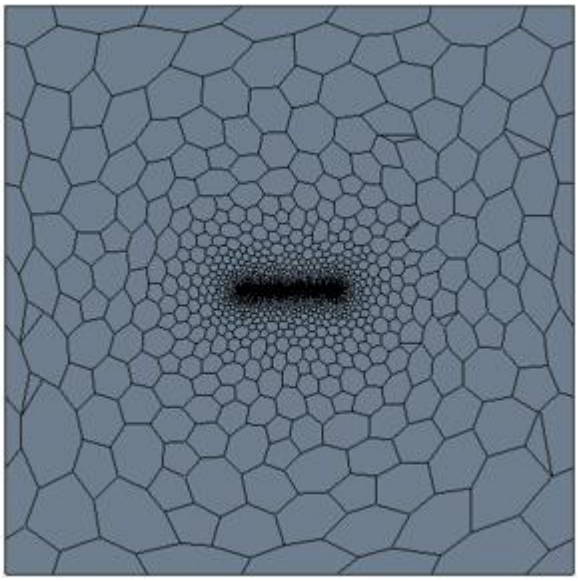

(c) Mesh modeled

(d) Mesh model around falnge

Fig. 6.4 Model size and mesh model created by STAR-CCM+

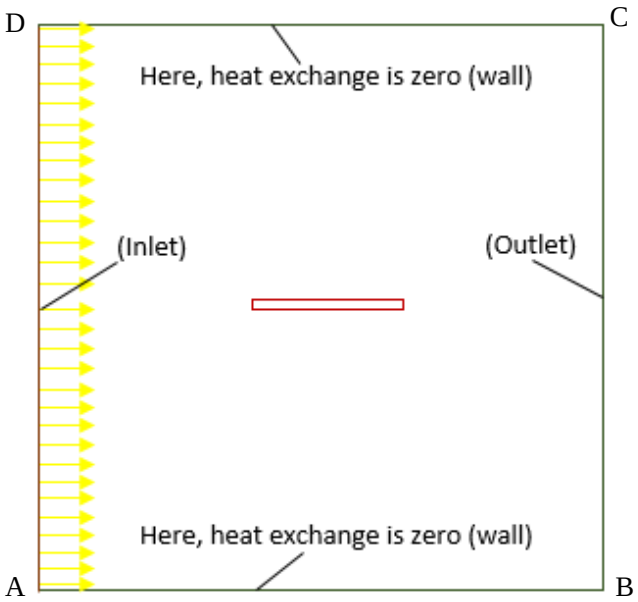

Fig. 6.5 Boundary conditions

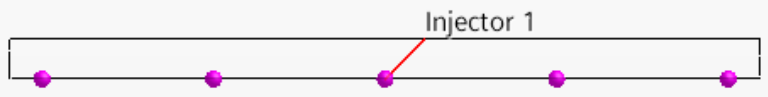

Fig. 6.6 Arrangement of water droplet on the flange

Table 6.1 (a) Specification of air

Molecular weight	28.96
Dynamic viscosity (pa-s)	1.85E-05
Specific heat (J/Kg-K)	1003.62
Thermal conductivity(W/m-k)	0.02603

Table 6.1 (b) Specification of water droplet

Molecular weight	18.015
Specific heat (J/Kg-K)	4181.7
Thermal conductivity(W/m-k)	0.62027
Heat of formation (J/Kg)	1.5866 E^{-7}
Density (Kg/m^3)	997.56
Surface tension (N/m)	0.072

Table 6.1 (c) Specification of steel

Density (Kg/m^3)	7800
Specific heat (J/kg-K)	448
Thermal conductivity(W/m-k)	80

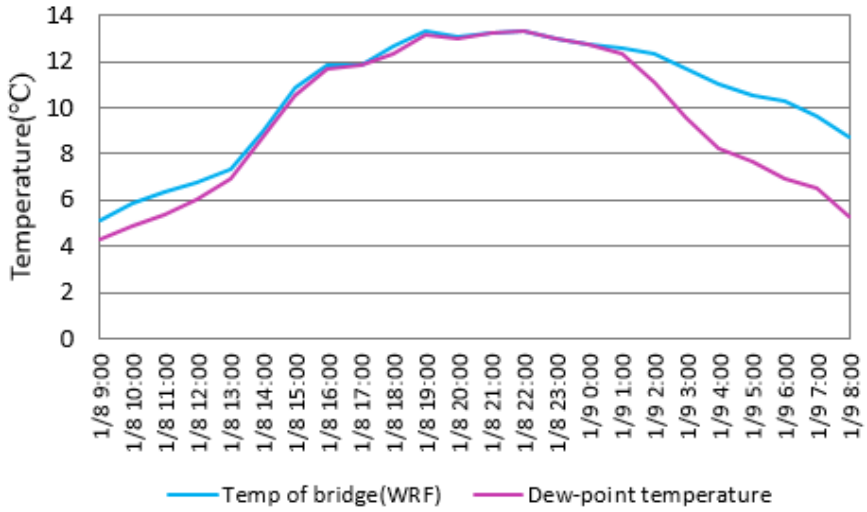

(a) Evaluation results of dew condensation from 00:9, 8/1 to 00:8, 9/1

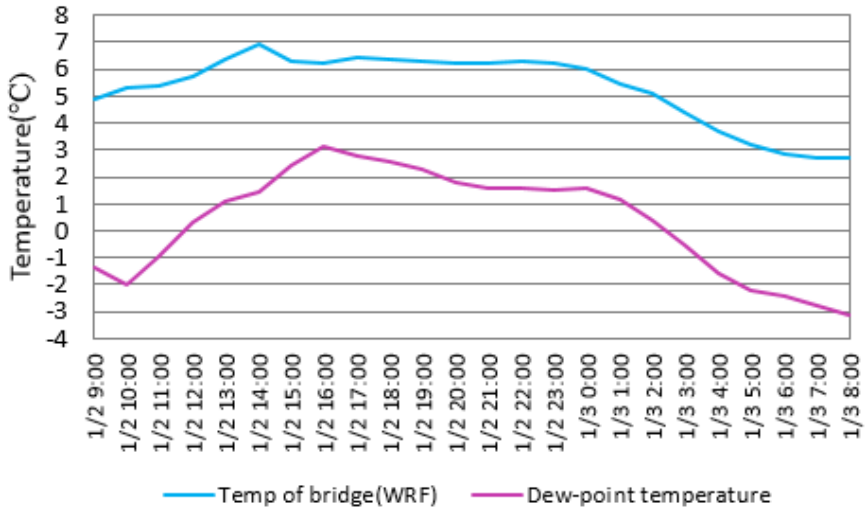

(b) Evaluation results of dew condensation from 00:9, 2/1 to 00:8, 3/1

Fig. 6.7 shows the evaluation results of dew condensation at Ooeyousui bridge using WRF during January 2018

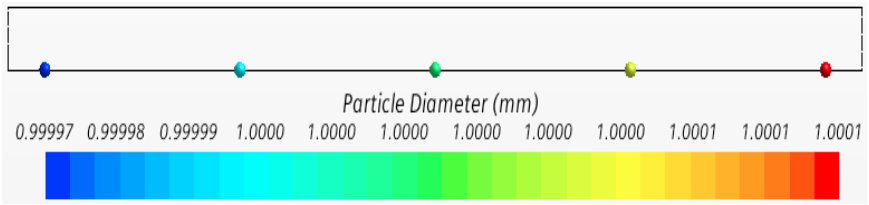

(a) Simulation Time = 1 s

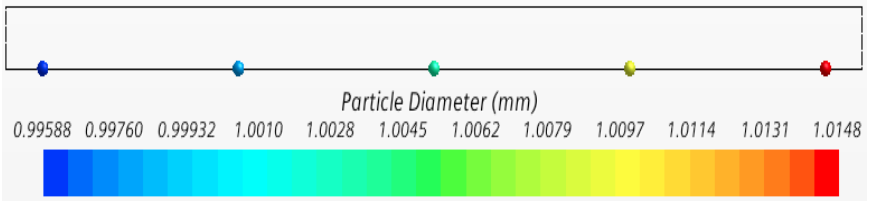

(b) Simulation Time = 196 s

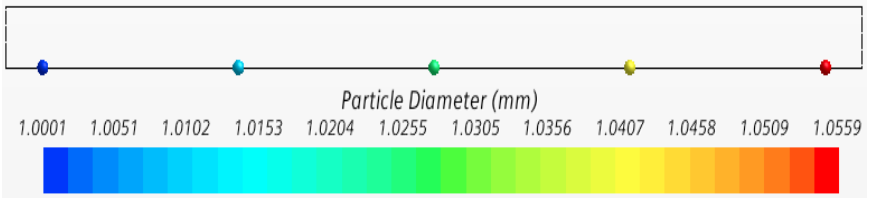

(c) Simulation Time = 1255 s

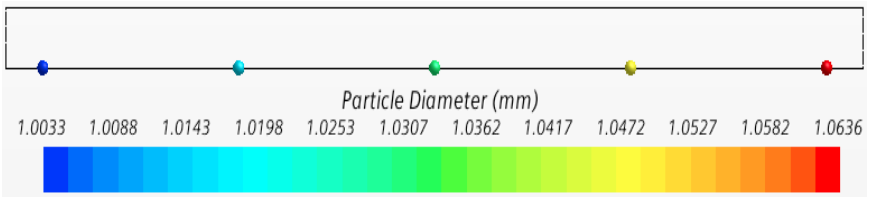

(d) Simulation Time = 1500 s

Fig. 6.8 Simulation results of dew condensation on steel flange using STAR-CCM+

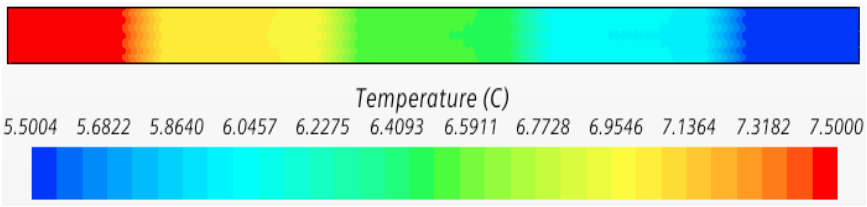

(a) Simulation Time = 1 s

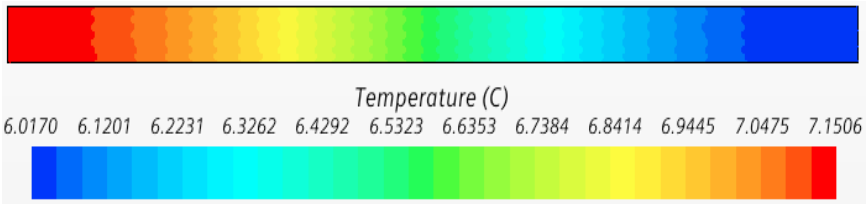

(b) Simulation Time = 196 s

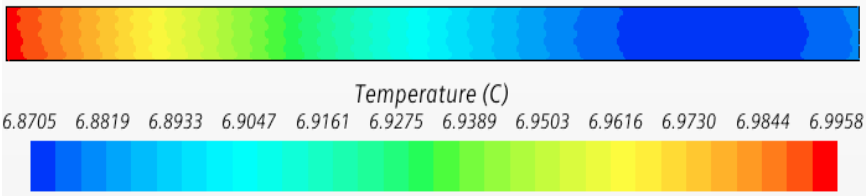

(c) Simulation Time = 1255 s

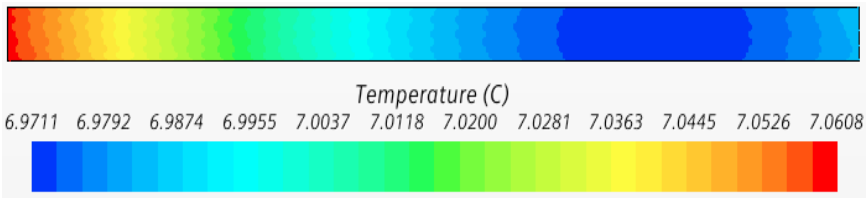

(d) Simulation Time = 1500 s

Fig. 6.9 Simulation results of temperature distribution on steel flange using STAR-CCM+

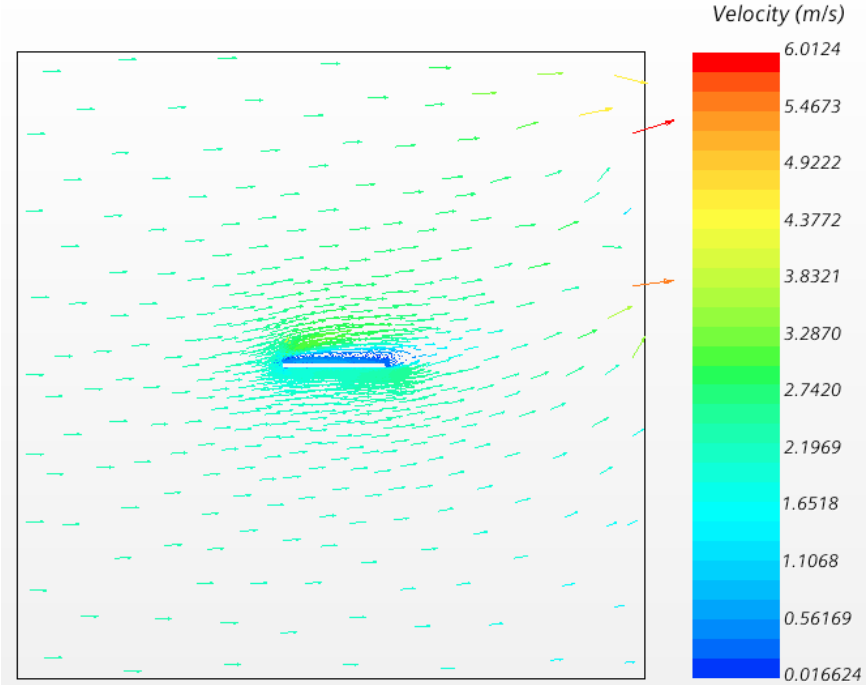

(a) Simulation Time = 1500 s

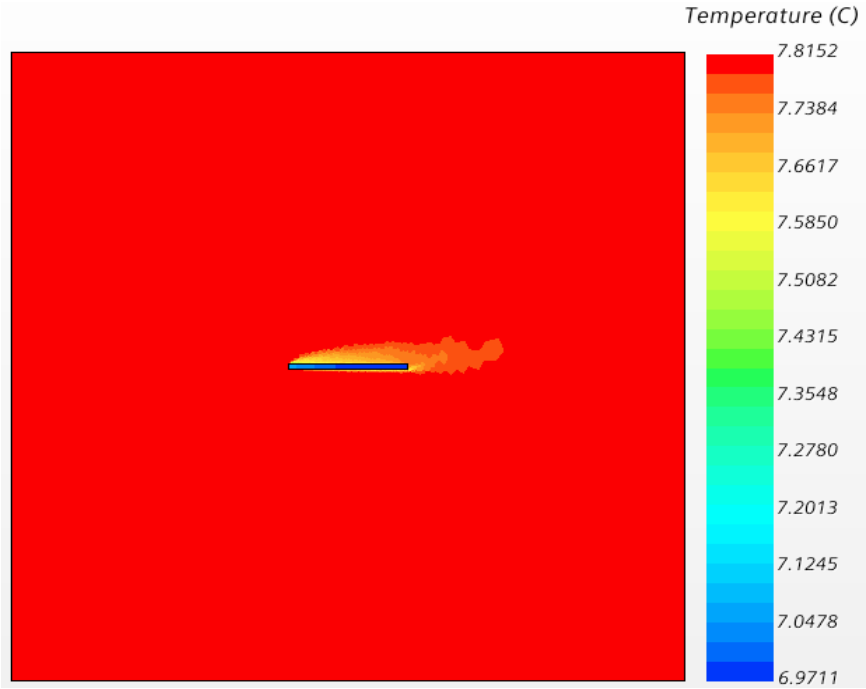

(b) Simulation Time = 1500 s

Fig. 6.10 shows the simulation results of (a) wind speed, and (b) temperature distribution in the model

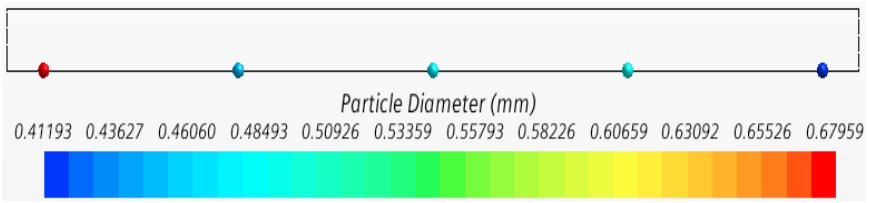

(a) Simulation Time = 800 s

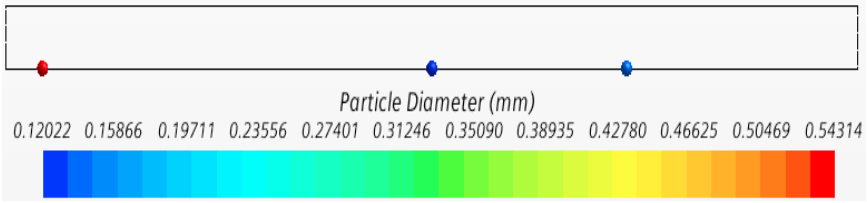

(b) Simulation Time = 1110 s

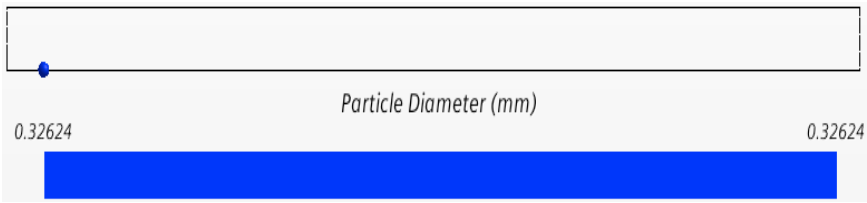

(c) Simulation Time = 1500 s

Fig. 6.11 Simulation results of dew condensation on steel flange using STAR-CCM+

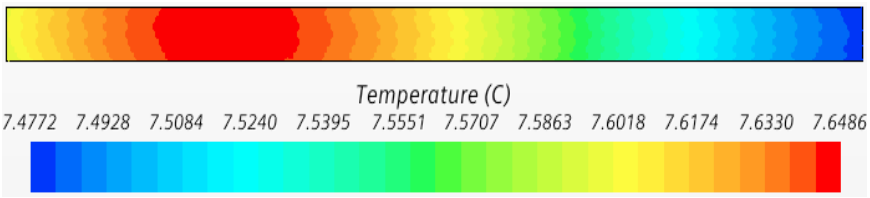

(a) Simulation Time = 800 s

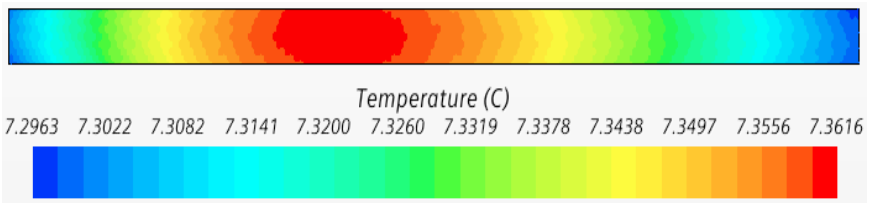

(b) Simulation Time = 1110 s

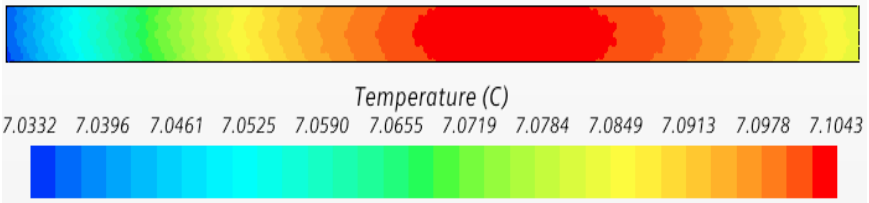

(c) Simulation Time = 800 s

Fig. 6.12 Simulation results of temperature distribution on steel flange using STAR-CCM+

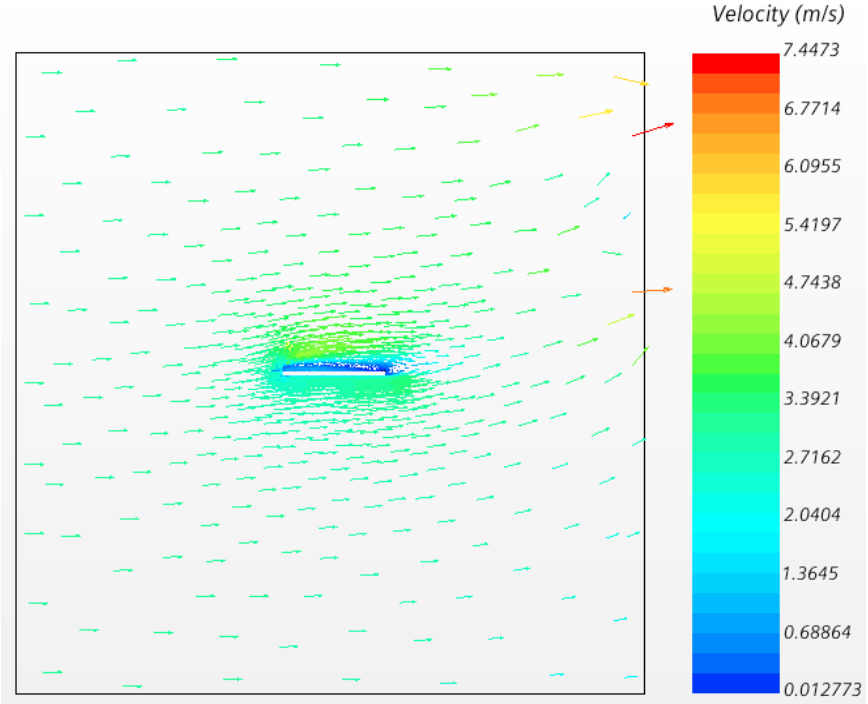

(a) Simulation Time = 1500 s

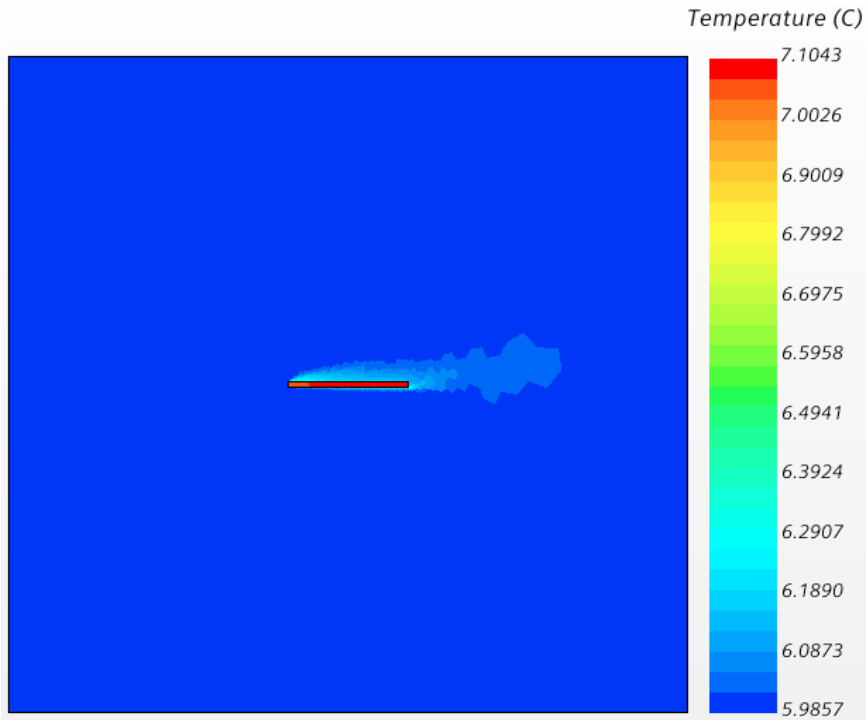

(b) Simulation Time = 1500 s

Fig. 6.13 shows the simulation results of (a) wind speed and (b) temperature distribution in the model

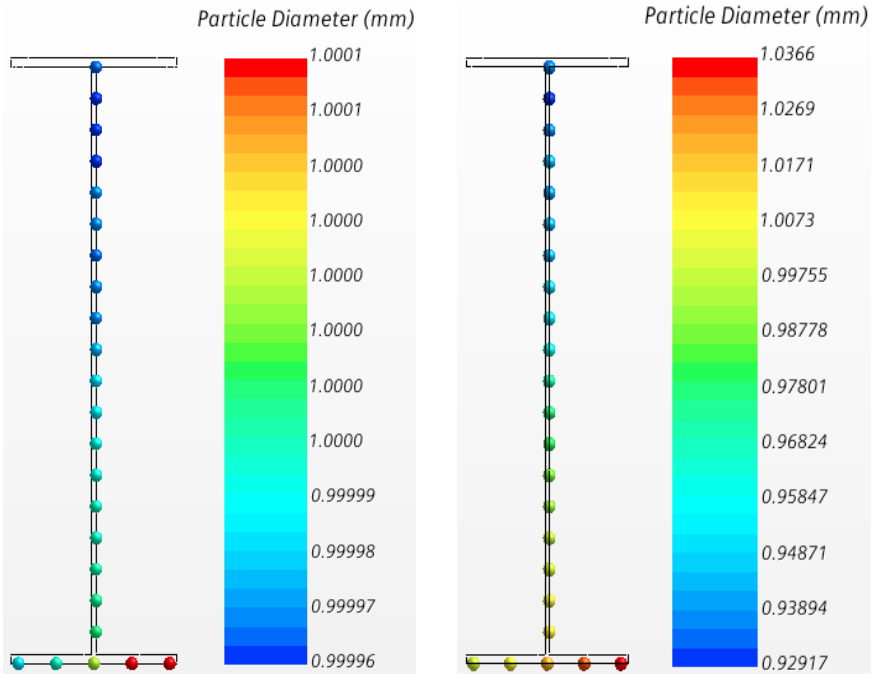

(a) Simulation Time = 1s (b) Simulation Time = 1s

Fig. 6.14 Simulation results of dew condensation on the entire cross section of girder using STAR-CCM+

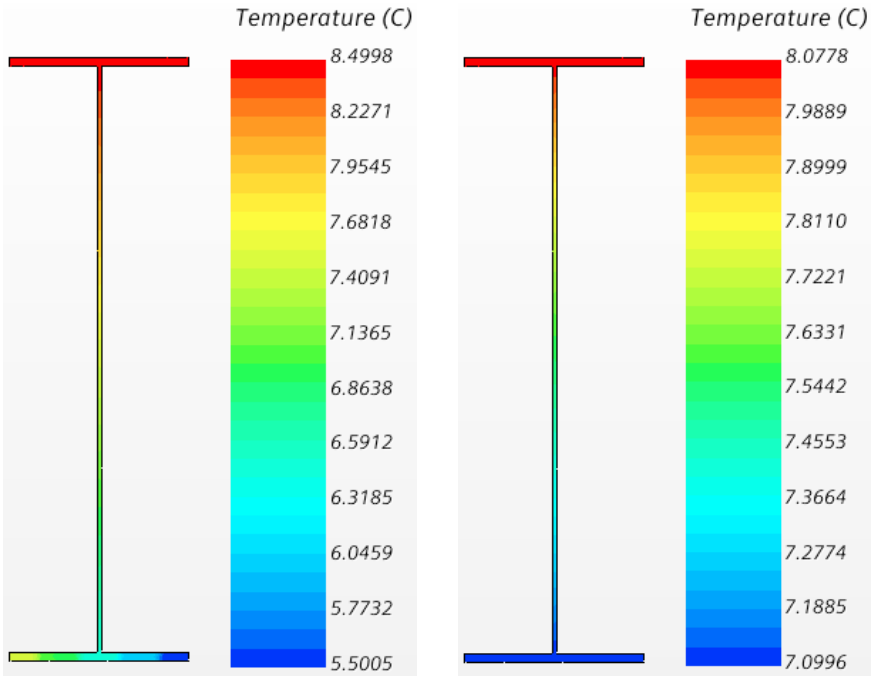

(a) Simulation Time = 1s (b) Simulation Time = 1s

Fig. 6.15 Simulation results of temperature distribution on the entire cross section of girder using STAR-CCM+

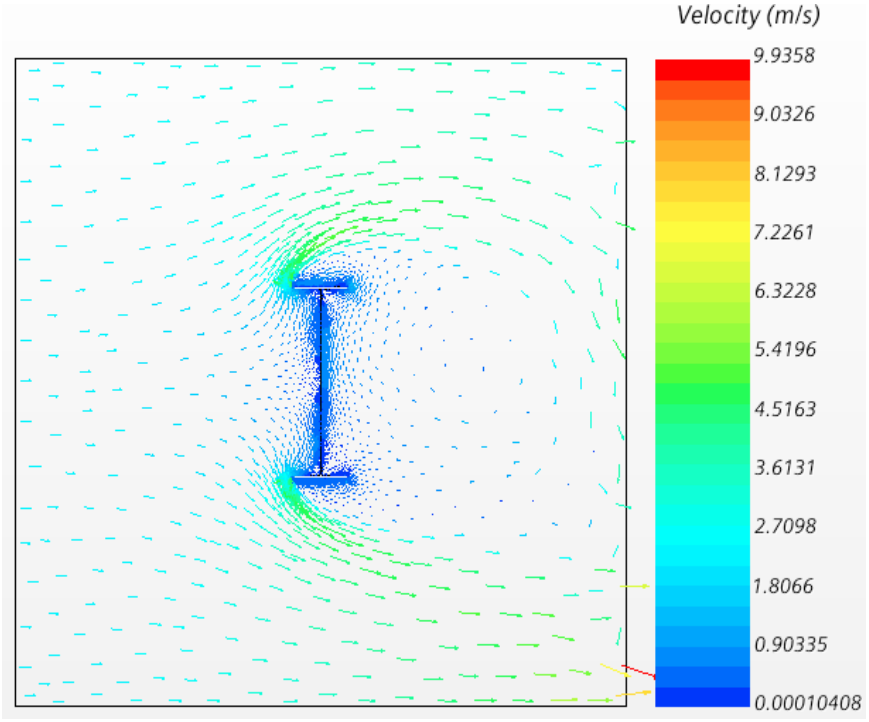

(a) Simulation Time = 1500 s

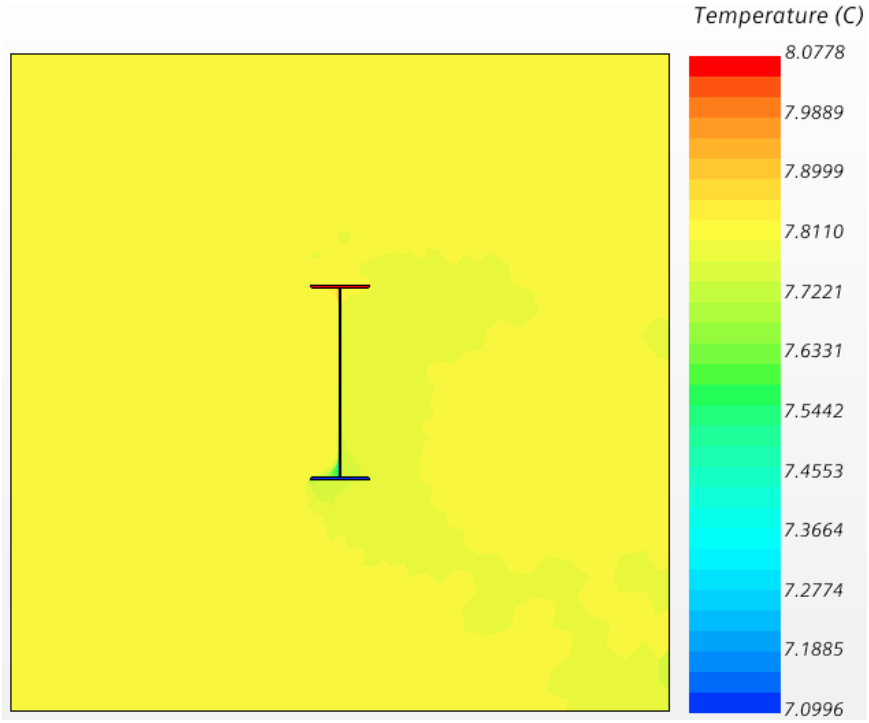

(b) Simulation Time = 1500 s

Fig. 6.16 Simulation results of (a) wind speed, and (b) temperature distribution in the model

Chapter 7

Summary and Conclusions

This study deal with evaluation of corrosion environment of bridges for its prevention and maintenance. Previously, a method to evaluate dew condensation due to atmospheric temperature and relative humidity was developed using inverse distance weighting (IDW) and a weather research and forecasting (WRF) numerical weather prediction technique. However, the accuracy improvement for corrosion evaluation of bridges using IDW and WRF have not been investigated sufficiently. In this study, accuracy enhancement of IDW for different land topographies and its employment was discussed to achieve more accurate results. Thus, a quantitative investigation was conducted. Additionally, appropriate adaption points selection of IDW was discussed, and the optimum number of interpolation points for evaluation of corrosive environment was proposed. Further, the accuracy improvement of WRF for corrosion environment evaluation was investigated to obtain more precise results. In Japan, the WRF model used United States Geological Survey-based land- land use data, gave inaccurate results to a certain extend. Therefore, the land use data provided by the Geospatial Information Authority of Japan is used to improve the accuracy of WRF model. Lastly, a total evaluation system of corrosion environment of bridges was developed through WRF/IDW technique as a large scale environmental information approach to proceed the investigation of corrosion environment to a local scale on the bridge members using STAR-CCM+ Software program.

In chapter 2, the use and adaption of an IDW method was investigated to estimate the temperature and relative humidity for difference land topographies, and the optimum number of interpolation point for the accurate evaluation of a corrosive environment was proposed. In this study, the temperature and relative humidity data of three meteorological observatories, Osaka, Suwa, and Shizuoka were used to compare the result obtained from the IDW. We assumed the Osaka to represent flat land, Suwa for a mountainous area, and Shizuoka an area relatively close to the sea, to reflected influence of water. A quantitative investigation of the IDW was carried out for the above mentioned meteorological stations from four, three, and two of their own local surrounding meteorological observatories, respectively. The comparison results of IDW when applying four, three, and two interpolation points clearly shows that the accuracy of the IDW can be improved to a certain extend by using three points for both temperature and humidity for flat land. The higher accuracy of the IDW was achieved from two interpolation points for the mountainous and oceanic areas. Additionally, the investigation revealed that although a slight difference was shown, almost the same precision was achieved for both three and two points. Regarding, the land topographies, the highest accuracy was obtained for both temperature and humidity for flat land as compared to mountainous and

oceanic areas. The outcome of this investigation showed that the accuracy of IDW for flat land is almost two-times higher compare to mountainous and oceanic areas.

In chapter 3, the temperature and humidity of Sanbonmatsu and Ooeyousui bridges in the northeast and northwest of Aichi prefecture were measured using field observation, and their results were compared with Nagoya meteorological observatory (NMO). The investigation results shows that the change in behavior of the temperature and relative humidity in both bridges are extremely linked with rate of change in the NMO, but the temperature and humidity of both bridges are not quite the same as NMO. However, the results of Ooeyousui is approximately similar to NMO, because it located near to NMO as compare to Sanbonmatsu. Thus, the difference in temperature and humidity at three points (Ooeyousui, Sanbonmatsu, and NMO) increased as a distance increased, and it is difficult to obtain the temperature and humidity of the entire prefecture only from NMO, it is essential to evaluate the corrosion environment of each single point using IDW technique. In addition, the investigation outcome demonstrated a lower temperature and higher relative humidity at Sanbonmatsu as compared to Ooeyousui which indicates more dew condensation likely to occur at Sanbonmatsu, although both regions shows a similar corrosive environment. Further, an evaluation of dew condensation was carried out at both bridge using ACM senor, the investigation shows that dew can easily occur in the bridges, and more dew tends to occur at Sanbonmatsu bridge. Finally, the investigation outcome dew condensation when using IDW and field observation were quite similar, and both confirmed the dew at Ooeyousui bridge. Thus, it concluded that IDW can be effective and useful.

In chapter 4, an improvement of accuracy for the evaluation of dew condensation was carried out using WRF technique. In this study, the GSI and USGS land use data were employed into the model and their results were compared with the actual map. The comparison results shows that the default USGS land use data currently utilized in the WRF modeling system, classify most of the land use type as Mixed Shrubland/Grassland; and Cropland/Grassland Mosaic which is outdated. Indeed, the USGS partially misrepresents the land use in the analysis model, whereas the GSI data accurately reflects the development of structures, industrial /commercial, and forest as well as the distribution of cropland. It means, the GSI data takes into account the land surface change due to urbanization, and can be updated regularly. Additionally, a quantitatively investigation of dew condensation was conducted for both Aichi and Gifu prefecture. The results shows the WRF-USGS overestimate the frequency of dew condensation as compared to WRF-GSI for Aichi prefecture, because the frequency of dew reduced after applying WRF-GSI. However, in the case of Gifu both results of WRF-USGS and WRF-GSI have similar results. It is concluded, for evaluation of the corrosion environment of steel bridges with use of the WRF technique, for mountainous areas, USGS land use data can be used without any changes. However, for urban areas, urban areas the GSI land use data should be used.

In chapter 5, the relationship between girder temperature and atmospheric temperature was investigated, and a temperature modification factor was proposed to obtain the girder temperature from atmospheric temperature. Particularly, it is very important for the accurate evaluation of dew condensation

on the bridges based on the actual girder temperature rather than bridge construction points. The investigation was performed based on the winter season, and a mathematical relation were proposed which can be easily applied to obtain girder temperature from the atmospheric temperature. Further, a comparative investigation of temperature and relative humidity was carried out for Toyokuni bridge along with Nagoya and Shinshiro meteorological observatories to examine the weather condition around the bridge, and as a results the low temperature and high relative humidity was observed which indicates the possibility of occurrence dew. Moreover, the present investigation outcome revealed that dew can occur even when the girder temperature is higher than the dew point temperature, this can be due to fog, because the fog forms when the difference between temperature and dew point reach 2.5 ℃. This was the new phenomena that was observed at both Toyokuni and Sanbonmatsu bridges, and confirmed by field measurements. Finally, an evaluation dew condensation due to fog was proposed by using WRF technique, and the validity of the proposed method was confirmed by field measurements.

In chapter 6, a total evaluation system for corrosion environment was proposed through WRF/ IDW technique as large scale environmental information approach to proceed the investigation of corrosion environment to a locale scale on the bridge members using STAR-CCM+ program. In this study, the evaluation of dew condensation was carried out at Ooeyousui bridge using field measurement, WRF technique, and STAR-CCM+, respectively then their results were compared. The evaluation results by WRF clearly revealed that the WRF/IDW techniques are very useful and effective to evaluate the corrosion environment of steel bridge at global scale (around the bridge), and there is no need for further investigation. However, this technique did not provide the sufficient information about the bridge members locally. On the other hand, the investigation revealed that the STAR-CCM+ can easily evaluate dew condensation locally in each part of the flange and girder. It can show simultaneously the dry, dry-dew and dew case, and more specifically determine the critical parts of flange where the tendency of dew condensation is significantly high. Hence, it is concluded for the evaluation of corrosion environment at global scale (around the bridge), the WRF/IDW is sufficient. If more detailed information of dew condensation is needed in structural members of bridge, the local investigation should be conducted using STAR-CCM+ Software.

Author's Research Activities

Journal papers with reviewing

Rasoli. Z., Nagata, K., Miyawaki, Y. and Kitahara, T., (2019), "Study on evaluation of corrosion environment on steel bridges using inverse distance weighting method", Journal of Structural Engineering, JSCE, Vol.65A, pp. 479-491.

Rasoli, Z., Nagata, K., Kitahara, T. and Sugiura, K., (2020), "Improvement of accuracy for the evaluation of corrosion environment on steel bridges using WRF technique", Journal of Structural Engineering, JSCE, Vol.66A, pp. 452-465.

Miwa, N., Nagata, K. and Rasoli, Z., (2021), "Evaluation of dew condensation on steel girder by inverse distance weighting method considering elevation difference", Journal of Structural Engineering, JSCE, Vol.67A (Accepted).

Conference and Symposium papers

Rasoli, Z., Nagata, K. and Kitahara, T.,(2018), " Monitoring of corrosive environment focusing on dew condensation in steel bridge", Proceeding of the Sixth International Symposium on Life-Cycle Civil Engineering, IALCCE, pp. 1175-1182.

Rasoli, Z., Nagata, K. and Miyawaki, Y., (2018), "Study on evaluation of corrosion environment using inverse distance weighting", Proceedings of the Thirty-First KKHTCNN Symposium on Civil Engineering, CD-ROM.

Rasoli, Z., Nagata, K. and Kitahara, T., (2019), "Corrosion environment of steel bridges using inverse distance weighting method", Proceeding of the 29th European Safety and Reliability Conference, ESREL, pp. 530-537.

Rasoli, Z., Nagata, K., Kitahara, T. and Sugiura, K., (2019), "Study on improvement of WRF accuracy for the evaluation of dew condensation on steel bridge", Proceeding of the Thirty-Second KKHTCNN Symposium on Civil Engineering, CD-ROM.